



UC-40

EGG-1183-1532

Technical Report No. L-1046  
15 October 1971

# EFFECTS OF RADIATION ON PHOTOGRAPHIC FILM

A STUDY

By

D. M. Dutton

Approved for Publication:

*V D Hedges*

MASTER

NOTICE

This report contains information of a preliminary nature and was prepared primarily for internal use at the originating installation. It is subject to revision or correction and therefore does not represent a final report. It is passed to the recipient in confidence and should not be abstracted or further disclosed without the approval of the originating installation, DTI Extension, Oak Ridge.

This Document is  
UNCLASSIFIED

NOTICE

This report was prepared as an account of work sponsored by the United States Government. Neither the United States nor the United States Atomic Energy Commission, nor any of their employees, nor any of their contractors, subcontractors, or their employees, makes any warranty, express or implied, or assumes any legal liability or responsibility for the accuracy, completeness or usefulness of any information, apparatus, product or process disclosed, or represents that its use would not infringe privately owned rights.

DISTRIBUTION OF THIS DOCUMENT UNLIMITED

DISTRIBUTION OF THIS DOCUMENT UNLIMITED  
TO ALL OFFICES AND AEC CONTRACTORS

## **DISCLAIMER**

**This report was prepared as an account of work sponsored by an agency of the United States Government. Neither the United States Government nor any agency thereof, nor any of their employees, makes any warranty, express or implied, or assumes any legal liability or responsibility for the accuracy, completeness, or usefulness of any information, apparatus, product, or process disclosed, or represents that its use would not infringe privately owned rights. Reference herein to any specific commercial product, process, or service by trade name, trademark, manufacturer, or otherwise does not necessarily constitute or imply its endorsement, recommendation, or favoring by the United States Government or any agency thereof. The views and opinions of authors expressed herein do not necessarily state or reflect those of the United States Government or any agency thereof.**

---

## **DISCLAIMER**

**Portions of this document may be illegible in electronic image products. Images are produced from the best available original document.**

## ABSTRACT

This study of the effects of radiation on photographic film is related to the Nevada Test Site's underground nuclear testing program, which has been active since implementation of the Limited Test Ban Treaty of 1963.

Residual radioactivity, which has accidentally been released on several tests, adversely affects the photographic film used in test data acquisition. The report defines this problem in terms of radiation-caused image degradation, radiation/matter interactions, types of radiation released by accidental venting, and the photographic effects of gamma and x-radiation.

This report also documents techniques and experimental findings that may be useful in recovering information from radiation-fogged film. Techniques discussed include processing methods, shielding, image enhancement techniques, and operational handling of potentially irradiated film.

## CONTENTS

	<u>Page</u>
ABSTRACT	ii
1. INTRODUCTION	1
2. DEGRADATION OF LIGHT IMAGES BY RADIATION FOGGING	2
2.1 Response of Film to Radiation	2
2.2 Darkening and Film Reading Error	3
2.3 The Sensitometric Effects of Non-Image-Forming Radiation	3
2.4 Granularity	4
2.5 Image Spreading-Modulation Transfer Function (MTF)- Resolving Power	7
3. INTERACTION OF FOGGING RADIATIONS WITH MATTER	9
3.1 X-Rays and Gamma Rays	9
3.2 Narrow-Beam Attenuation of Monochromatic Gamma or X-Ray Photons	10
3.3 Ionization Units	13
4. ACCIDENTAL RELEASES OF RADIOACTIVITY	15
4.1 Types of Releases	15
4.2 Explosion Phenomenology, Gas Formation and Fractionation	16
4.3 Energy Spectrum Affecting Photographic Materials	16
4.4 Empirical Evidence Supporting the Low-Energy Fogging Spectrum Hypothesis	17
5. PHOTOGRAPHIC ACTION OF X-RAYS AND GAMMA RAYS	21
5.1 Release of Electrons by Photon Absorption	21
5.2 Dissipation of Electron Energy	22
5.3 Distribution of the Latent Image	23
5.3.1 Latent Image Dispersion	23
5.3.2 Location of Latent Images	28
5.3.3 Chemical Sensitization and Its Effect on Latent Image Distribution	31
5.4 The Density/Exposure Relationship	35
5.5 X-Ray Spectral Sensitivity	39
5.6 Environmental Factors Affecting Sensitivity and Latent Image Fading	46

## CONTENTS (cont)

	<u>Page</u>
6. APPROACHES TO SOLUTION OF THE IRRADIATED FILM PROBLEM . . . . .	49
7. SOLUTION OF THE IRRADIATED FILM PROBLEM -	
TECHNIQUES AND EXPERIMENTAL FINDINGS . . . . .	58
7.1 Unconventional Processes . . . . .	58
7.2 Silver Halide Emulsion Preparation . . . . .	59
7.3 Environmental Conditions . . . . .	61
7.4 Shielding . . . . .	62
7.5 Erasing Fog's Latent Image . . . . .	63
7.6 Development Conditions Favoring Recovery . . . . .	65
7.6.1 In Situ Processing . . . . .	65
7.6.2 Viscous Processing . . . . .	66
7.6.3 Reversal Processing - Intensification . . . . .	66
7.6.4 Developer Characteristics . . . . .	68
7.6.5 Surface Latent Image Development . . . . .	68
7.6.6 Antifoggants . . . . .	71
7.6.7 Dye-Coupled Development and Rehalogenation . . . . .	73
7.6.8 Low-Contrast Development . . . . .	74
8. PHOTOGRAPHIC IMAGE ENHANCEMENT . . . . .	77
8.1 High-Contrast Printing . . . . .	77
8.2 An Optical Approach . . . . .	79
8.3 A Computer Approach . . . . .	82
8.4 Applications of Image Enhancement to Radiation-Fogged Film . . . . .	83
9. OPERATIONAL HANDLING OF POTENTIALLY RADIATION-FOGGED FILMS . . . . .	85
9.1 Pre-Event . . . . .	85
9.1.1 Selection of Film and Chemical Process . . . . .	85
9.1.2 Shielding . . . . .	86
9.1.3 Processing and Exposure Techniques . . . . .	86
9.1.4 Radiation Check Films . . . . .	86
9.2 Post-Event . . . . .	87
9.3 Image Enhancement . . . . .	88
REFERENCES . . . . .	89

## ILLUSTRATIONS

<u>Figure</u>	<u>Page</u>
2-1 Typical film-to-radiation response curve (D log E or H&D) . . . . .	2
2-2 Film reading error (PFR-2) versus density . . . . .	3
2-3 Characteristic curves of Kodak Super-XX Pan (developed 8 min. in Kodak DK-50 at 20° C) as affected by increasing amounts of hard x-radiation . . . . .	4
2-4 Film granularity versus density . . . . .	5
2-5 Granularity power spectrum as a function of diffuse density . . . . .	6
2-6 Photomicrographs of films developed to equal densities . . . . .	7
2-7 Power spectra for two films exposed with light (a and b) and x-rays (a' and b') . . . . .	8
3-1 Conversion curve, wavelength (Å) to voltage V (keV) . . . . .	11
3-2 Setup for measuring narrow-beam attenuation coefficient . . . . .	12
3-3 Conversion curve (approximate) relating photon energy to photons/cm <sup>2</sup> R and ergs/cm <sup>2</sup> R . . . . .	14
4-1 Shot film showing silhouette of x-irradiated Riteway holder . . . . .	18
4-2 Cross-section of Riteway 4 x 5 graphic film holder (3:1 magnification) . . . . .	18
4-3 Honeycomb layer of dissected Riteway 4 x 5 graphic film holder . . . . .	19
5-1 Mass-absorption of silver bromide as a function of wavelength (Å) . . . . .	21
5-2 Energy distribution of secondary electrons produced in polyethylene by primary electrons (65 keV and 1 Mev) . . . . .	23
5-3 Energy loss rate and range of electrons in pure silver bromide . . . . .	24
5-4 Photomicrograph of approximately 300-keV electron track in a nuclear track emulsion . . . . .	25
5-5 Grains exposed to alpha particles . . . . .	26
5-6 Grains exposed to x-rays . . . . .	27

## ILLUSTRATIONS (cont)

<u>Figure</u>		<u>Page</u>
5-7	Grains exposed to tungsten light, 1/100-second exposure time . . . . .	28
5-8	Grains exposed to low-intensity light, 40-hour exposure time . . . . .	29
5-9	Herschel effect (and reversal) after exposure to x-rays at temperature of liquid nitrogen . . . . .	30
5-10	Relative sensitivity at $D = 0.50$ for internal development for various ripening times . . . . .	32
5-11	Sensitivity at $D = 0.50$ for surface development for various ripening times . . . . .	33
5-12	Relative sensitivity at $D = 0.50$ for total development for various ripening times . . . . .	34
5-13	Relative surface/internal sensitivity ratio at $D = 0.50$ for various ripening times . . . . .	35
5-14	Relative sensitivity at $D = 0.50$ for post-fixation physical development for various ripening times . . . . .	36
5-15	Comparison of density-exposure curves for light and x-rays for a typical emulsion . . . . .	38
5-16	Schematic of an x-ray fluorescence sensitometer . . . . .	40
5-17	Spectral sensitivities of Kodak No-Screen and Type K x-ray films (incident roentgens versus wavelength) . . . . .	40
5-18	Spectral sensitivities of a front emulsion of Kodak No-Screen and Type K x-ray films (incident ergs/cm <sup>2</sup> versus wavelength) . . . . .	41
5-19	Spectral sensitivities of a front emulsion of Kodak No-Screen and Type K x-ray films (ergs absorbed/cm <sup>2</sup> versus wavelength) . . . . .	42
5-20	Spectral sensitivities of a front emulsion of Kodak No-Screen and Type K x-ray films (quanta absorbed/cm <sup>2</sup> versus wavelength) . . . . .	43
5-21	Absorbed energy required to produce $D = 1.5$ above fog (ergs/cm <sup>2</sup> versus wavelength) . . . . .	44

## ILLUSTRATIONS (cont)

<u>Figure</u>		<u>Page</u>
5-22	Response of film relative to air versus photon energy at normal, 1/2, 1/10, and 1/20 silver bromide content	45
5-23	Calculated response of G5 emulsions (Greening's formulation) as a function of silver bromide content	46
6-1	Possible solutions of the radiation-fogged film problem	50
6-2	Data retrieval - film processing techniques	51
6-3	Data retrieval - film storage considerations	52
6-4	Data retrieval - image enhancement techniques	53
6-5	Radiation hardening techniques - special emulsions	54
6-6	Signal intensification - film handling	55
6-7	Radiation hardening techniques - rapid access	56
6-8	Signal intensification - alpha system improvement	56
7-1	Photomicrographs (2500 magnification) of microtomed cross-sections of Kodak 7222 films exposed to produce a density of 1.0	66
7-2	Eastman Kodak 3404, D-19 process	70
7-3	Comparison of absolute speeds at 10 R of three films processed in DK-60A and extended range developers	75
7-4	Comparison of absolute speeds at 50 R of three films processed in DK-60A and extended range developers	76
8-1	Calculating a gamma correction curve	78
8-2	An optical spatial filter	80
8-3	A coherent processing system	80
8-4	Typical spatial filter functions	81
8-5	Essential components of a digital enhancement system	82
8-6	Comparison of unenhanced and enhanced x-ray images of a skull	84

## 1. INTRODUCTION

The United States Government has conducted underground nuclear tests at the Nevada Test Site (NTS) since the signing of the Limited Test Ban Treaty of 1963, which prohibits release of radiation beyond national borders. The test devices are deeply buried in underground shafts or tunnels designed so that, within reasonable limits, no radiation is released to atmosphere. However, accidental release of residual radioactivity to atmosphere has occurred on several of these tests.

Certain applications of nuclear test diagnostics at NTS involve the use of silver halide photographic materials for data recording. Following detonation and signal recording but prior to conventional processing, these films may be exposed to ionizing radiations. Such incidents, while infrequent, have been a persistent problem.

Compared to control films, light images on silver halide materials conventionally processed after exposure to high-energy radiation typically exhibit lower contrast, lower speed, lower dynamic range, and a higher noise level. These deficiencies interfere with the satisfactory recovery of data and may result in complete loss of the film record. Minimizing the effects of radiation fogging would enable recovery of more information, at a higher level of confidence, from accidentally irradiated film.

Much of the research into the radiation fogged film problem has had limited usefulness, either because the techniques used were not documented or were documented so that the overall parameters were not specified and results could not be duplicated. The net effect has been that most instances of radiation-fogged film have required lengthy and costly custom research.

The purposes of this report are to:

1. Describe the degradation of light images by radiation fogging.
2. Explain the interaction of fogging radiation and matter; e.g., absorption, scattering, shielding, and ionization.
3. Describe accidental venting and the types of radiation released.
4. Explain the photographic effects of radiation as related to the properties of silver halide photographic materials, subsequent chemical processing, degree of radiation sensitivity, and the formation of latent images.
5. Summarize documented experimental procedures for recovering information from radiation-fogged films.

## 2. DEGRADATION OF LIGHT IMAGES BY RADIATION FOGGING

As stated in Section 1, light images on silver halide materials conventionally processed after exposure to high-energy radiation typically (compared to control films) exhibit lower contrast, lower speed, lower dynamic range, and higher noise. The darkened image is also difficult to read in many instances. These deficiencies interfere with the satisfactory recovery of data and may result in a complete loss of the film record.

### 2.1 RESPONSE OF FILM TO RADIATION

A typical response curve is shown in Figure 2-1, where density is the log of the reciprocal of the transmittance. Exposures are expressed as log exposures because density is proportional to log exposure in the straight line region, B. The toe, A, is the region of minimal exposure and increasing slope. High-energy stepped exposures exhibit less toe than do light radiation exposures, and may be exponentially shaped. Segment C, the shoulder, is the region of maximum exposure and decreasing slope.

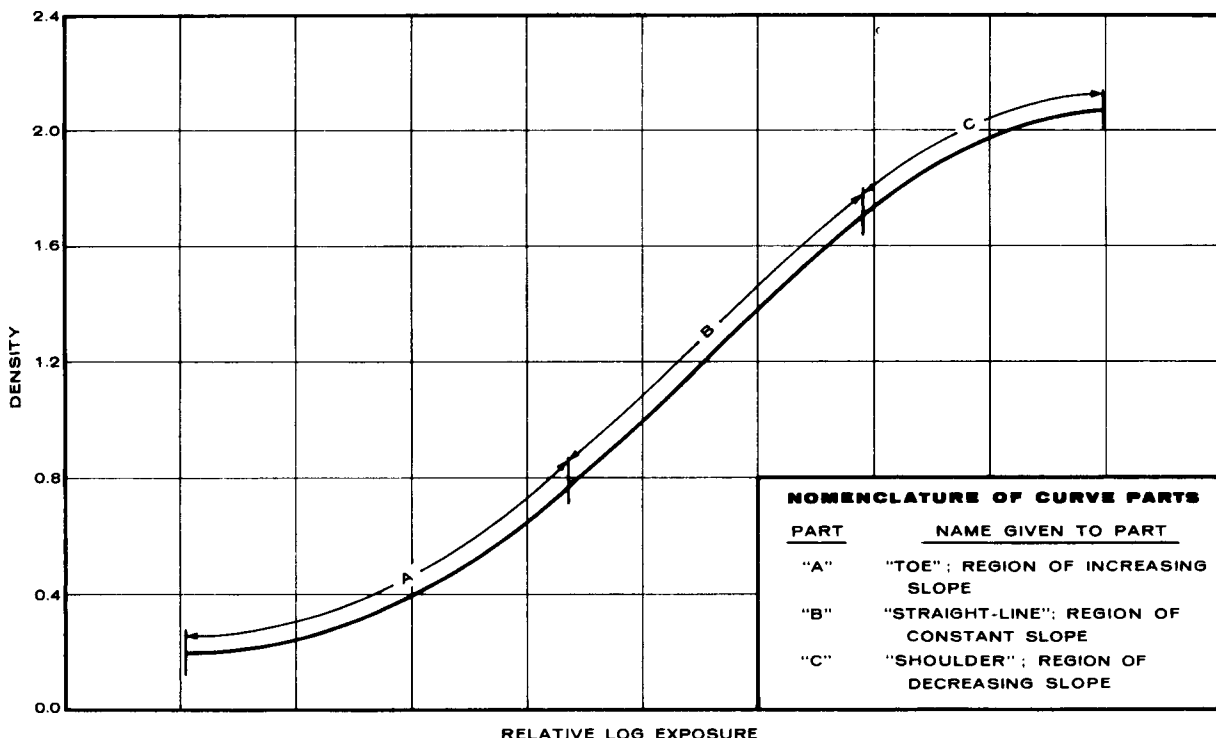


Figure 2-1. Typical film-to-radiation response curve (D log E or H&D).

## 2.2 DARKENING AND FILM READING ERROR

A fogged record (negative) appears to have darkened. A darkened record is not desirable because of reading errors caused by noise and non-linearities introduced into high-density reading areas by either visual or electronic film readers. The reading error as a function of background density for the Programmable Film Reader (PFR-2) is shown in Figure 2-2. The standard deviation of 400 points estimated to lie on the centerline of a strip 60 micrometers wide were plotted after modification of the optical system to improve the efficiency of use of light.

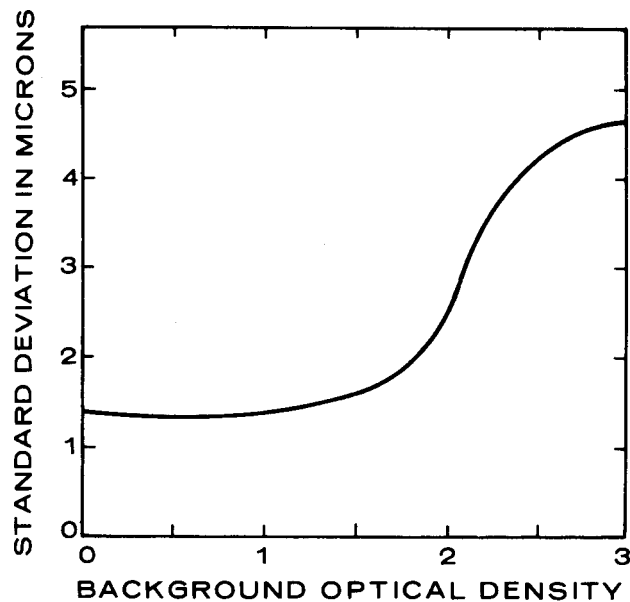


Figure 2-2. Film reading error (PFR-2) versus density.<sup>(1)</sup>

## 2.3 THE SENSITOMETRIC EFFECTS OF NON-IMAGE-FORMING RADIATION

A second effect of a non-image-forming exposure is loss of contrast in the threshold regions. The low densities in the toe are increased most, the high densities considerably less, and the maximum density very slightly. This loss in speed and contrast is analogous to a loss in signal level, since density differences in the film are the signal. These intensity distortions are illustrated for 1,000-kV x-ray fogging on Kodak Super-XX Pan film in Figure 2-3.<sup>(2)</sup>

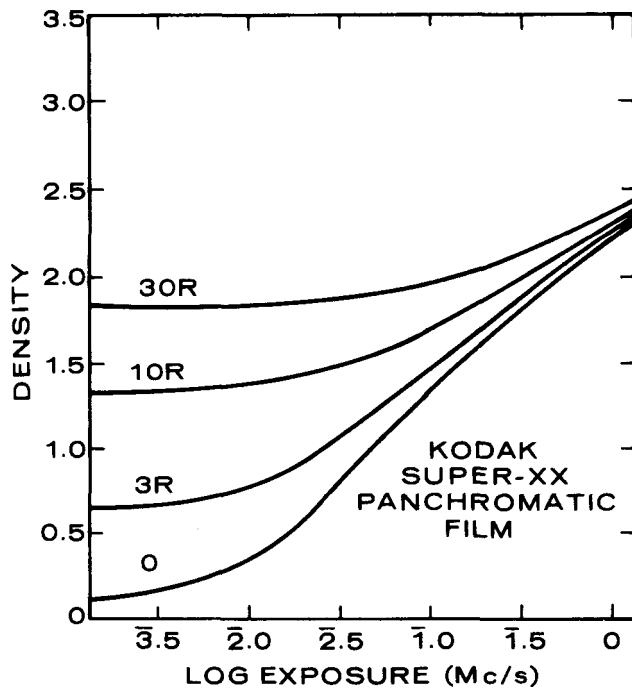


Figure 2-3. Characteristic curves of Kodak Super-XX Pan (developed 8 min. in Kodak DK-50 at 20°C) as affected by increasing amounts of hard x-radiation.<sup>(2)</sup>

Color shifts also produce sensitometric effects. Conventional color films consist of three or more layers of silver halide with segregated sensitivity to blue, green, and red light. These layers are specially processed to yield images in concentrations of yellow, magenta, and cyan dyes respectively. The speeds of the three layers are balanced to produce a gray or neutral image when exposed to a specified kind of white light. If the three layers do not have the same high-energy radiation sensitivity, the effects discussed above occur to varying degrees in the three layers and color balance shifts occur.

#### 2.4 GRANULARITY

A third effect of radiation fogging is an increase in the granularity or noise level in the developed images. Granularity,<sup>(3)</sup> a property of the microstructure of the photographic image, limits the confidence with which the level of exposure and location of an exposure incident upon a small area of a photographic emulsion can be determined. In the case of light exposures, the energy of many photons must be absorbed to render a grain developable; granularity is caused by the discrete nature of the silver halide particles themselves.

Granularity is a function of density, as illustrated for light exposures in Figure 2-4. <sup>(4)</sup>

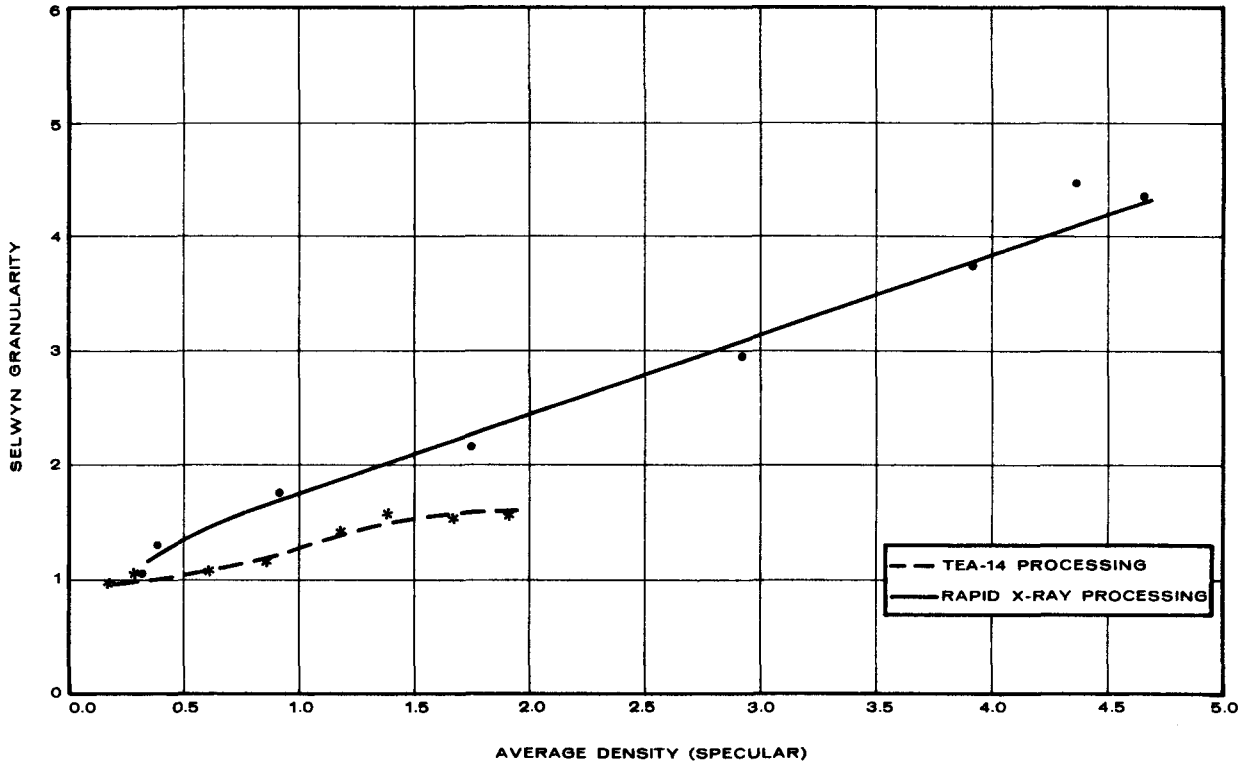


Figure 2-4. Film granularity versus density. <sup>(4)</sup>

While Selwyn or rms granularity defines the amplitude of the noise, a more complete description of the noise is obtained through power spectrum\* analysis. A power spectrum, the most complete analysis of noise possible, expresses density patterns as two-dimensional functions of spatial frequency. In physical terms, the noise power spectrum is a representation of noise broken down into its component frequencies while the rms value is an integral of the power spectrum. The power spectrum of granularity, also a function of density, is illustrated in Figure 2-5. <sup>(5)</sup>

---

\*Power spectra are sometimes called Wiener spectra.

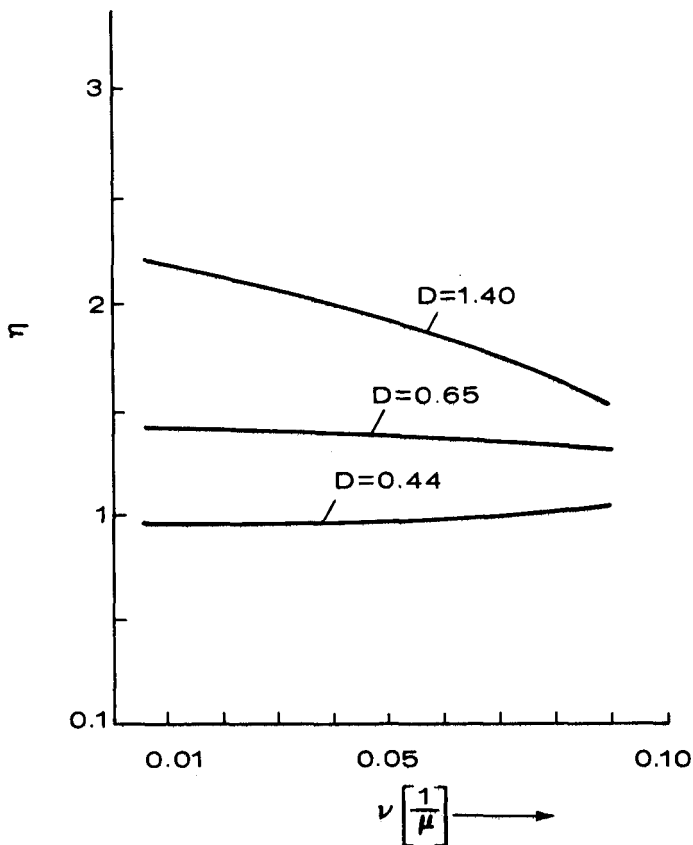


Figure 2-5. Granularity power spectrum as a function of diffuse density. <sup>(5)</sup>

At a constant density level, granularity is greater for high-energy exposures than for light exposures. This is illustrated in Figure 2-6. <sup>(6)</sup>

In contrast to light exposures, high-energy exposures do not require multiple photon absorption. In fact, absorption of one high-energy photon can make developable adjacent grains as well as the primary grain (see Section 5). The most important factor is the discrete nature of the quantum noise manifested as silver aggregates. The power spectrum of a high-energy exposure is thus approximately equal to the sum of the power spectra of the individual grains and the aggregates. At high frequencies, the values are about the same as for light exposures because in this region the fluctuations are caused by the individual grains; i. e., the large aggregates affect noise amplitude primarily at lower frequencies.

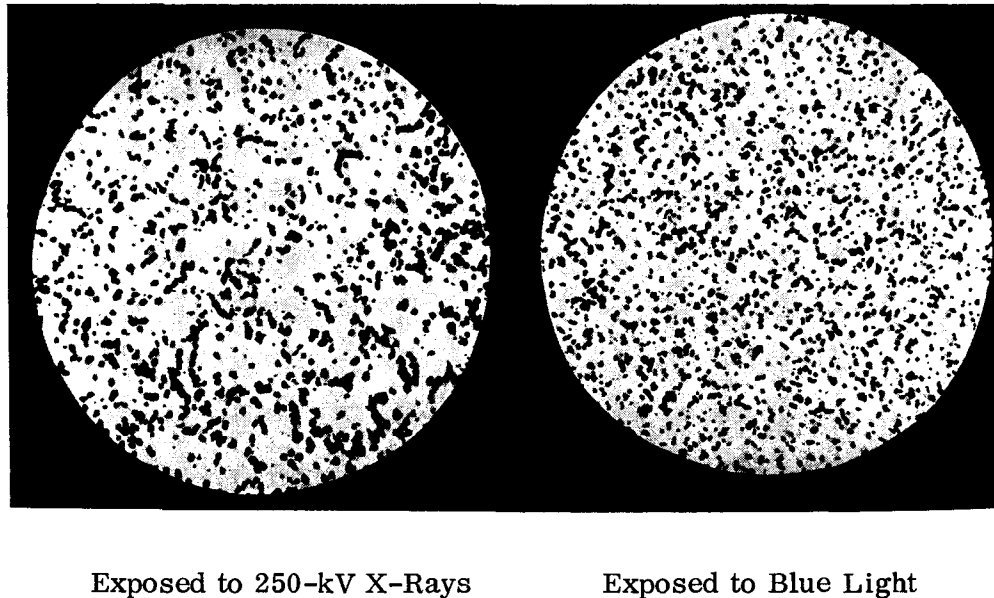


Figure 2-6. Photomicrographs of films developed to equal densities. <sup>(6)</sup>

Power spectra for exposures to all high-energy radiations approximate the configuration shown in Figure 2-7.

## 2.5 IMAGE SPREADING-MODULATION TRANSFER FUNCTION (MTF)-RESOLVING POWER

Radiation fogging cannot affect the spreading of light in an emulsion. However, since the image-forming exposure and fogging exposures are additive and the sensitometric response is non-linear, the spread function and MTF are degraded. The increase in granularity (noise) and decrease in microcontrast (signal) make difficult the distinguishing of detail (signal) at the reading stage. Darkening may also contribute to reading difficulties. These factors contribute to a loss in resolving power and other image quality factors.

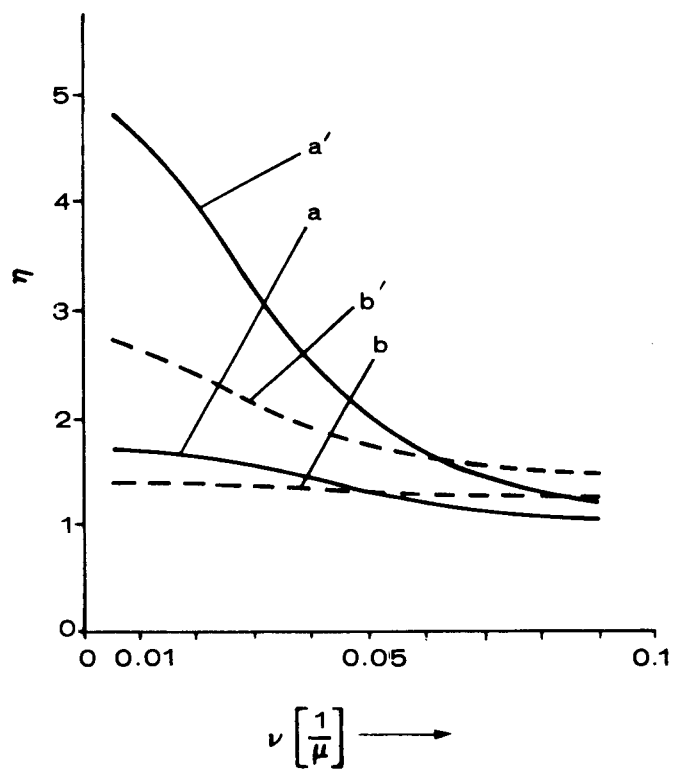


Figure 2-7. Power spectra for two films exposed with light (a and b) and x-rays (a' and b').<sup>(5)</sup>

### 3. INTERACTION OF FOGGING RADIATIONS WITH MATTER

Types of radiation/matter interactions discussed in this section include absorption, scattering, shielding, and ionization.

Alpha particles,  $\alpha$ , the nuclei of helium atoms,  ${}_2\text{He}^4$ , have a net charge of +2. Beta particles,  $\beta^-$ , are high-speed electrons with a charge of -1. Gamma rays or x-rays are photons and have no charge.

On an equal energy basis, alpha particles are less penetrating than beta particles and both are much less penetrating than photons. The range of 3-MeV alpha particles in air is  $\approx$  1.6 cm and that of 3-MeV beta particles is  $\approx$  1,300 cm, while the range of 3-MeV photons is many kilometers. These ranges roughly correspond to the stopping power of a sheet of paper, a few millimeters of aluminum, and a few centimeters of lead, respectively.

Except if alpha emitters are allowed to enter the camera station and camera proper, betas and photons are assumed to be solely responsible for radiation-fogged film. Exterior beta and soft photon fogging can be eliminated by modest shielding; a neutron exposure problem is not anticipated. Therefore, assuming the presence of modest shielding, harder photons would be the sole source of radiation fogging.

#### NOTE

The remainder of this report will concentrate on interactions of photons with matter and recovery of images irradiated by accidental venting.

#### 3.1 X-RAYS AND GAMMA RAYS

There is no difference between x-rays and gamma rays of an equivalent wavelength; however, it is the convention to distinguish between them on the basis of origin. Gamma rays originate in the unstable radioactive nuclei. X-rays are produced by interactions of high-speed electrons with matter outside the nucleus. Characteristic x-rays are emitted when an electron drops from a higher to a lower energy state, or may be generated by electron capture. Bremsstrahlung or continuous x-rays are emitted when high-speed electrons travel near atomic nuclei and are subjected to deflections by the nuclei's coulomb field. The change in the velocity of the electron field is manifested in the emission of a quanta of radiation. Since the electrons lose their energy in a random manner, a broad continuous spectrum of x-rays is emitted with the energy of the electrons becoming the limiting short wavelength of that spectrum. Since beta particles are high-speed electrons, Bremsstrahlung x-rays can be generated by interaction of beta particles with matter.

X-ray or gamma ray energy is expressed in terms of photons, with energy values given in keV or MeV. These energies are monochromatic or nearly so. The expressions kV and kVp specify the peak voltage across the generating apparatus rather than electron voltage of the photons proper. This peak voltage relates to spectral distribution only in that the maximum potential defines the upper limits of photon energy.

High-energy photons are frequently described in terms of wavelength rather than energy. The conversion formulas are:

$$V \text{ (keV)} = \frac{12.41}{\lambda \text{ (\AA)}} \quad \text{and} \quad \lambda \text{ (\AA)} = \frac{12.41}{V \text{ (keV)}}$$

$$\text{or} \quad V \text{ (MeV)} = \frac{0.01241}{\lambda \text{ (\AA)}} \quad \text{and} \quad \lambda \text{ (\AA)} = \frac{0.01241}{V \text{ (MeV)}}$$

A wavelength-to-voltage conversion curve is plotted in Figure 3-1.

### 3.2 NARROW-BEAM ATTENUATION OF MONOCHROMATIC GAMMA OR X-RAY PHOTONS

The total probability of a photon of a given wavelength ( $\lambda$ ) interacting in some way while passing through a layer of matter can be studied using the setup shown in Figure 3-2. The collimated beam of monochromatic photons penetrates the absorber, and undeflected and unabsorbed photons reach the broad-bandwidth detector. The attenuation of the intensity ( $I$ ) received by the detector is a function of the combined probabilities of outright absorption, deflection, and reflection. If a narrow-bandwidth detector tuned to the wavelength of the source is used, the evaluation excludes secondary photon radiation produced by interactions in the absorber. The resulting energy absorption coefficients are therefore much lower than their sister mass absorption coefficients.

Lambert's law of absorption states that each layer of equal thickness ( $d$ ) absorbs an equal fraction of the radiation traversing it. Expressed as the exponential law of attenuation,  $p$  is the probability of radiation traversing an absorber of thickness ( $d$ ) without being absorbed outright, reflected, or deflected and  $\mu$  is the absorption coefficient or probability of interaction per unit thickness (usually, 1 cm):

$$p = e^{-\mu d}$$

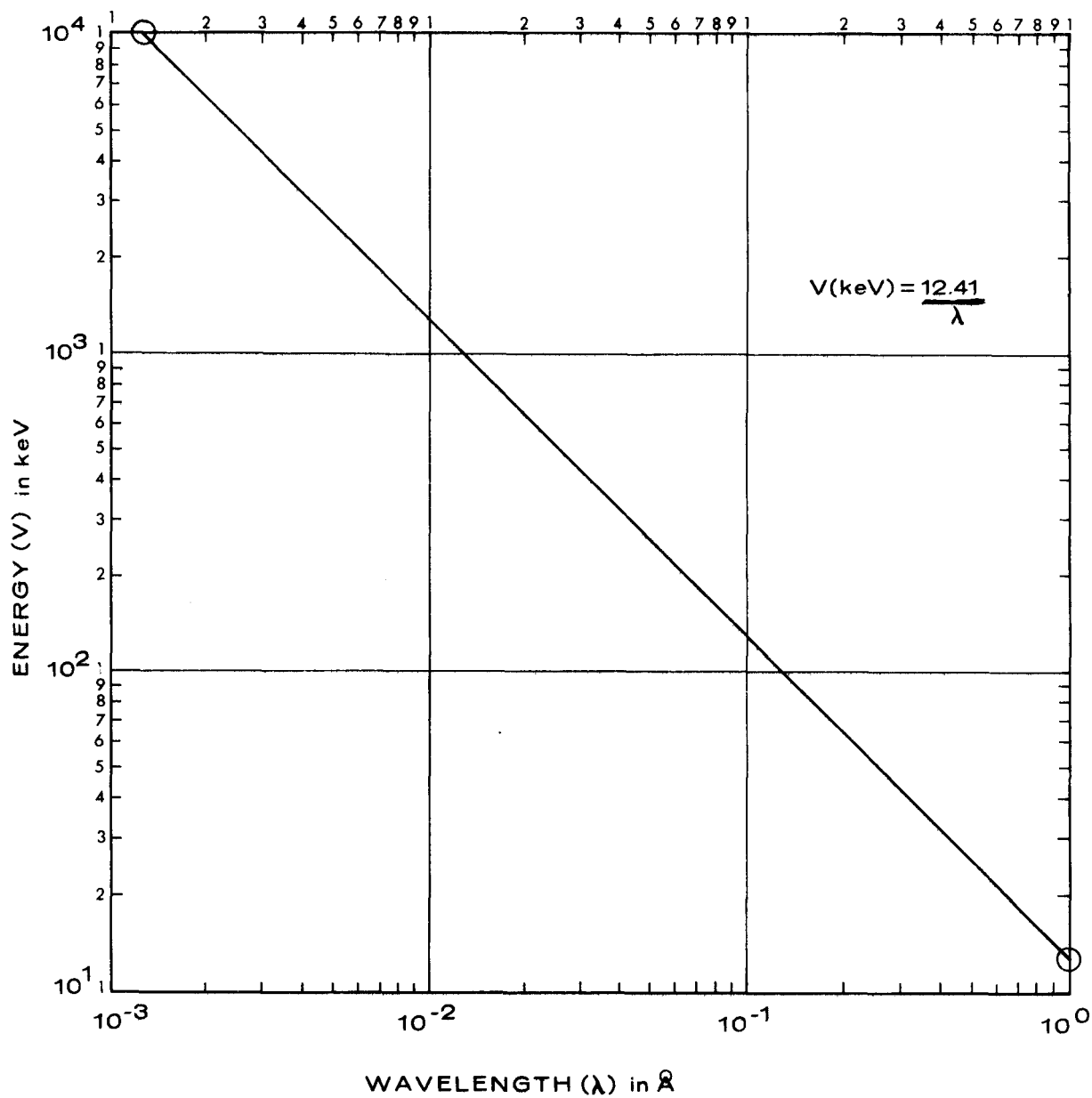


Figure 3-1. Conversion curve, wavelength ( $\text{\AA}$ ) to voltage V (keV).

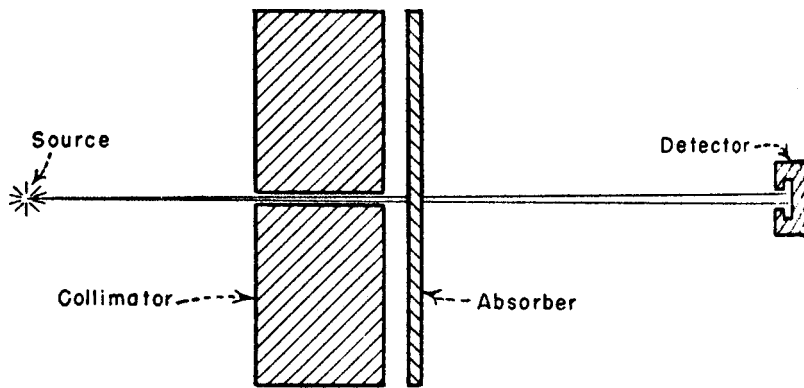


Figure 3-2. Setup for measuring narrow-beam attenuation coefficient.

The intensity ( $I$ ), after passing through a thickness ( $d$ ) the absorption coefficient of which is  $\mu$ , is related therefore to the original intensity ( $I_0$ ) by:

$$I = I_0 e^{-\mu d}$$

An index independent of the phase or physical state of the absorber, the mass absorption coefficient, is given by  $\mu/\rho$  where  $\rho$  is the density. The unit of the mass absorption coefficient is  $\text{cm}^2/\text{g}$ ,  $\text{cm}^2\text{g}^{-1}$ , or  $(\text{g}/\text{cm}^2)^{-1}$ , which represents the fraction absorbed in a  $1\text{ cm}^2$  area in a 1-gram layer of mass.

The half-value layer is that thickness ( $d_h$ ) of material, with absorption coefficient  $\mu$  for a given wavelength, which reduces incident flux by a factor of 2.

$$I/I_0 = 1/2 = e^{-\mu d_h}$$

$$\log 2 = \mu d_h \log e$$

$$d_h = (\ln 2)/\mu = 0.693/\mu$$

Tables of mass absorption coefficients for gamma and x-rays are frequently encountered in the literature. The values of the coefficients over a range of wavelengths can be seen to change markedly. For example, the mass absorption coefficient of aluminum is  $\approx 500.0$  at  $10.0\text{ \AA}$  (1.2 keV),  $14.0$  at  $1.0\text{ \AA}$  (12 keV),  $0.16$  at  $0.1\text{ \AA}$  (120 keV), and  $0.06$  at  $0.01\text{ \AA}$  (1.2 MeV). If one assumes a  $\rho$  of  $2.7\text{ g/cm}^3$

for a 1-mm aluminum absorber, this absorber will be nearly opaque to 10.0 Å radiation but nearly transparent to 0.01 Å radiation. This property of selective absorption or filtration is caused by the changing probabilities of photon interactions with matter as a function of wavelength. The longer wavelength or "softer" gamma or x-rays are most likely to interact with the absorber and are therefore the least penetrating.

Filtration or preferential attenuation of longer wavelengths is not the only process that changes a beam's spectral composition. The absorption or scattering of a given photon may produce secondary radiations of longer wavelength.

### 3.3 IONIZATION UNITS

Ionization units include the roentgen, curie, and rad.

The roentgen (R) is that quantity of gamma or x-radiation that will produce one electrostatic unit ( $1 \text{ esu} = 3.33 \times 10^{-10} \text{ coulomb}$ ) of ions in 1 ml of air at standard temperature and pressure (STP). The roentgen, then, is a unit of quantity of ionization in air and does not specify the quality ( $h\nu$ ) or intensity ( $I$ ) of gamma or x-radiation.

The roentgen is not necessarily a suitable index for studies involving film exposed to various x-ray wavelengths because in the range of wavelengths of 0.50 to 0.01 Å, the variation in the mass absorption of air is only about one tenth that of silver halide. However, absorption laws can be used to calculate the incident energy equivalent to a roentgen at any wavelength. Based on data from Herz,<sup>(7a)</sup> the approximate conversion curve in Figure 3-3 relates incident exposure to roentgens.

The curie (Ci) is a measure of the activity or rate of transformation of a radioactive material. One curie is equal to  $3.7 \times 10^{10}$  disintegrations per second.

The rad is the unit of absorbed dose and is equal to 100 ergs per gram of absorbing material.

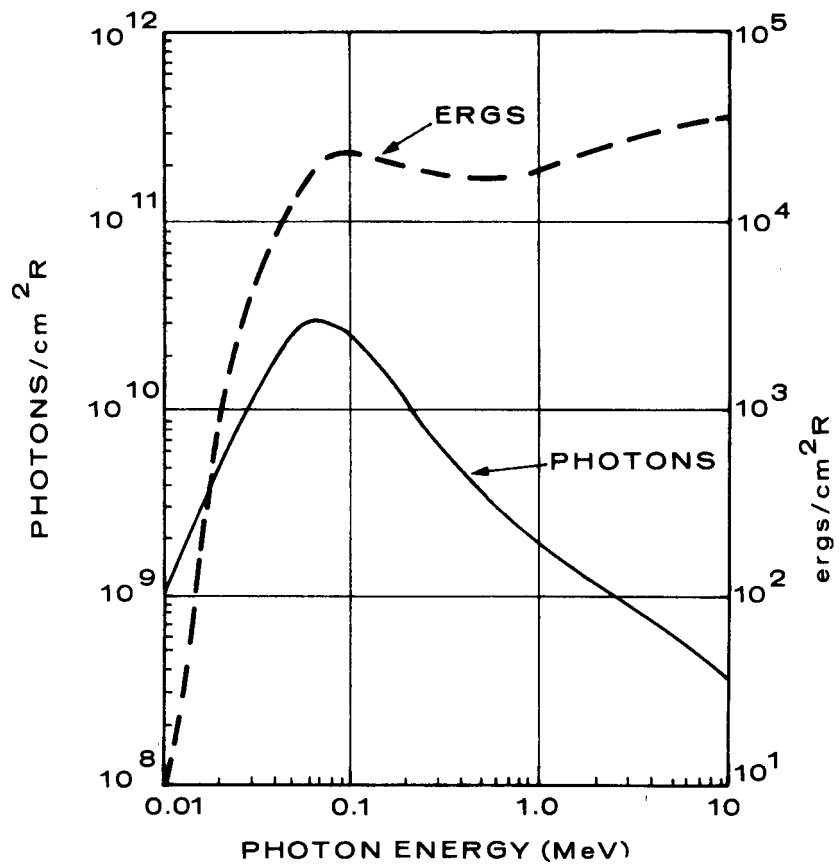


Figure 3-3. Conversion curve (approximate) relating photon energy to photons/cm<sup>2</sup> R and ergs/cm<sup>2</sup> R.

## 4. ACCIDENTAL RELEASES OF RADIOACTIVITY

The following discussion of accidental venting and radionuclide spectra is based on unclassified AEC and University of California documents available to the public through the National Technical Information Service. These documents are identified in the References.

### 4.1 TYPES OF RELEASES

A substantial body of theoretical and practical knowledge and experience has been acquired from the more than 200 underground tests that the AEC has conducted.<sup>(8a)</sup> Except for excavation events, device burial is sufficiently deep to make release of radioactivity improbable.

Releases occurring in the current underground testing program can be defined as follows: 1) the expected explosive release of both gaseous and particulate materials from a relatively shallow-buried nuclear excavation experiment; 2) massive release of both gaseous and particulate materials from a relatively deeply buried experiment at or very shortly after the time of detonation; and 3) seepage of predominantly gaseous materials from a relatively deeply buried physics or weapons experiment, occurring after the detonation.<sup>(9a)(10a, 10b)(11a)</sup>

In a "prompt" dynamic release, the material may be transported by kinetic energy through the test emplacement, detonation-produced fractures, or a pre-existing fracture, all of which extend to the ground surface.<sup>(8b)(9b)</sup> This type of venting, which has occurred on a few low-yield events less often than seepage, releases radioactivity of at most a few percent of that formed underground.<sup>(9a)</sup> Massive dynamic releases can occur only within a few minutes after detonation because underground temperatures and pressures decline very rapidly. The condensation of condensable gases, process of chimney formation, cavity collapse, and the quenching of moisture within cavity gases reduce the driving pressure within the cavity and minimize the possibility of any dynamic venting, even through a relatively direct path.<sup>(8c)</sup>

Seepage of radioactivity may occur by percolation of gases following their injection into fractures during the dynamic phase of cavity growth or dispersal by diffusion.<sup>(11a)</sup> Seepage, when it infrequently occurs, commences from as early as a few minutes to as late as many hours or a few days after detonation.<sup>(9a)</sup> The amount of radioactivity released by a given seepage is a very small fraction of that formed underground.<sup>(9a)</sup>

## 4.2 EXPLOSION PHENOMENOLOGY, GAS FORMATION AND FRACTIONATION

To understand the radiological differences between "prompt" dynamic ventings and slow seepages, it is necessary to briefly discuss those processes that contribute to differences in the energy spectrum of these two categories of release.

Following detonation, much of the radioactive material becomes permanently embedded in the cavity when the rock vapor condenses and solidifies.<sup>(8a)</sup> Radio-nuclides can be categorized as either volatile or refractory. The volatile materials have low vaporization temperatures and low melting points, while the refractory materials have high vaporization temperatures and high melting points. The refractory materials condense out rapidly as the cavity temperature and pressure lower, while the volatile materials are gaseous even at standard temperature and pressure.<sup>(9a)</sup> Consequently, the underground puddle of condensed and resolidifying rock becomes enriched with refractory fission products. Noncondensable gases remain and can be injected into fractures during the dynamic phase of cavity growth; subsequently, these gases may collect in voids formed from chimney collapses and diffuse through chimney rubble or through the surrounding material to the surface.<sup>(8c)(9b)(11b)</sup> Fractionation, then, makes the observed ratios of nuclides in radiochemical samples different from the ratios produced by the device.<sup>(12a)</sup> The degree to which fractionation occurs will play a major role in determining the energy spectrum of the irradiation.

## 4.3 ENERGY SPECTRUM AFFECTING PHOTOGRAPHIC MATERIALS

Initial gamma and neutron radiation can be excluded from consideration because of their absorption in the underground medium. Only residual radiation from the device and the neutron-activated environment need be considered. Fission products have been the predominant source of radiation in inadvertent ventings.<sup>(9a)</sup> Fission-product spectra and yields are a function of the fissioning nucleus and the energy spectrum of the initiating neutrons. Estimates of fission-product production have been discussed by Weaver, Bolles, and Fleming.<sup>(13-16)</sup>

If the release is dynamic, as in the case of stemming or closure failure, a wide spectrum of radionuclides from weapon residues, fission and fusion fragments, and activated elements may be released. If the release is not dynamic, many of these elements either condense out or are removed by absorption or chemical reaction. Inert elements are generally not removed by absorption or chemical reaction; both inert elements and the halogens have low boiling points and are not readily condensed out.

For prompt dynamic venting, the radiation spectrum would be expected to be similar to the initial energy spectrum of fallout.<sup>(16)</sup> Glasstone<sup>(12b)</sup> has indicated that for a typical (0-1 minute after detonation) gamma ray spectrum, over 70% of the gamma ray photons have energies of 0.75 MeV or less. The approximately 6.5-MeV nitrogen capture gamma rays for air bursts were included in this estimate and supposedly contributed a major part of the total observed energy.<sup>(12b, 12c)</sup> If these 6.5-MeV components are neglected, the expected spectrum would shift considerably toward the lower energies.

Considerable fractionation has been observed in seepage type releases. Refractory elements condense out underground and the chimney material acts as a filter so that the greater portion of those gases reaching the surface are inert. Under standard conditions, numerous isotopes apply.<sup>(8b-8d)(9c)(11c-11e)(17, 18)(19a-19e)</sup>

#### 4.4 EMPIRICAL EVIDENCE SUPPORTING THE LOW-ENERGY FOGGING SPECTRUM HYPOTHESIS

Fogging patterns on film due to film holder construction or use of lead foil tape indicate that a significant fraction of the radiation effecting the fogging is contributed by soft gamma or x-rays and/or hard beta particles. It must also be remembered that silver halide photographic materials are tens and sometimes hundreds of times more sensitive to components in the 1.0-0.1-Å region than in the less than 0.02-Å region. Consequently, in an exposure to a mixture of wavelengths, heavy weight is given to the softer components.

On some events where releases have occurred, a honeycomb fogging pattern caused by film holder construction (see Figure 4-1) has been observed on the processed film. Figure 4-1 has been burned in directly from the duplicate of an original shot film. The original film, which was located in the front of a film holder, shows a distinct shielding pattern. The density of the original film's shielded areas is approximately 0.2 less than the 2.9-3.0 density of the unshielded background. The Kodak Royal Pan original was developed for four minutes at 90° F in Kodak Rapid X-Ray Developer. The Riteway holder construction consists of a bakelite darkslide, sheet of film, sheet of 0.032-cm aluminum, honeycomb of 0.127-cm aluminum, sheet of 0.032-cm aluminum, sheet of film, and a bakelite darkslide. A cross-section of this holder without film or darkslides is shown in Figure 4-2, and the honeycomb layer is shown in Figure 4-3.

#### NOTE

Use of the Riteway type holder has been discontinued; a solid plenum holder is now used.

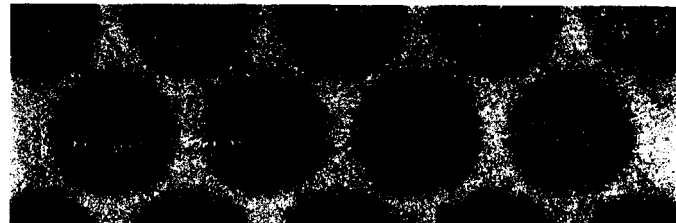


Figure 4-1. Shot film showing silhouette of x-irradiated Riteway holder.

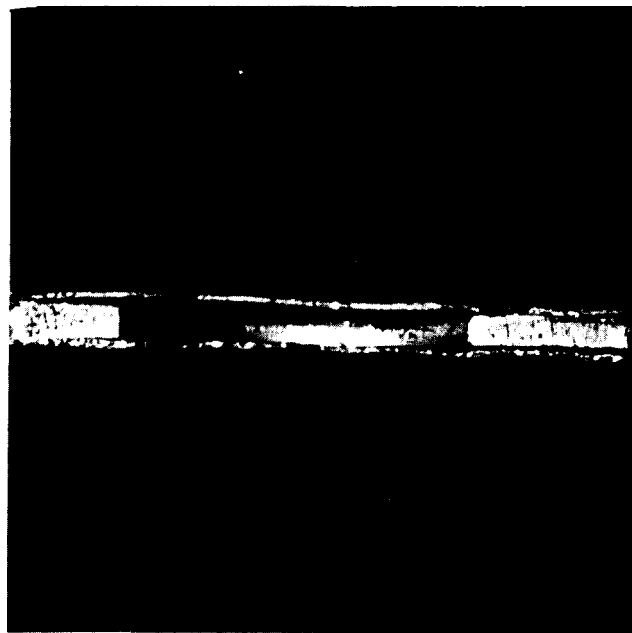


Figure 4-2. Cross-section of Riteway 4 x 5 graphic film holder (3:1 magnification).

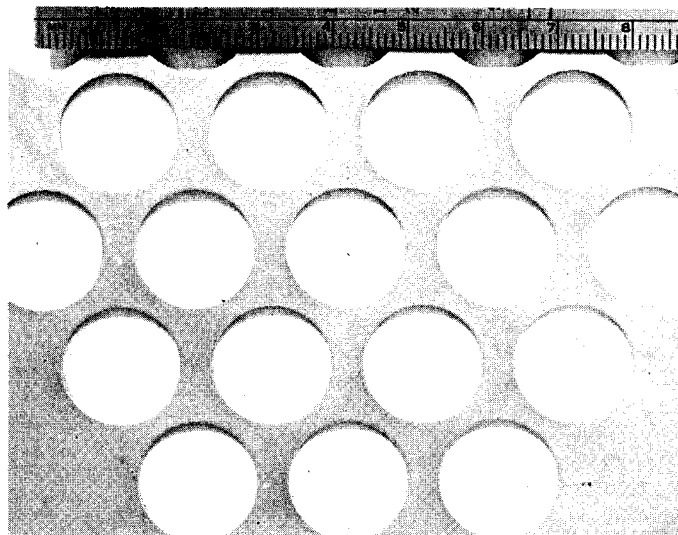


Figure 4-3. Honeycomb layer of dissected Riteway 4 x 5 graphic film holder.

Lead foil tape is used on some film holders that occasionally have been irradiated in field use. Borden Mystik Tape No. 7430 is typical. This lead foil is approximately 0.0114 cm thick, and one layer has a mass of 120 mg/cm<sup>2</sup>. The analysis of the alloy is 98% lead, 1% antimony, and 1% tin.<sup>(20)</sup> The small but significant density difference observed on processed irradiated film where the strips of tape have been overlapped is additional evidence supporting the low-energy spectrum hypothesis.

Radiation specialists at the Nevada Test Site have provided additional information about the energy spectrum of radiation releases.<sup>(16)(21)</sup> A reasonably large percentage of the radiation detected above ground after a seepage release is of the less than 250-keV type. Post-shot core samples and drillback have strong components in the less than 100-keV range. Scattering of primary photons by local materials hardens the spectrum of the primaries and also results in dislocations in orbital electrons in local materials and the secondary emission of K and L x-rays from these stimulated materials. These secondaries have much longer wavelengths than their stimulating primaries; i.e., less than 100 keV down to a few keV.

Again, the shielding provided by the film holder and camera is adequate to eliminate any alphas except for alpha emitters entering the camera proper. No neutron exposure is expected except for the very small amount emitted by  $^{89}\text{Br}$  and  $^{137}\text{I}$ .

## Conclusions

1. The photon and particle spectrum can vary considerably depending upon the device, type of release, and other conditions and variables.
2. The types of release can be divided into two categories; prompt dynamic release and seepage or gaseous diffusion release. Inert and volatile isotopes predominate in the gaseous diffusion release.
3. For prompt dynamic releases, the photon fogging spectrum peaks at less than 750 keV.
4. For gaseous diffusion releases, the photon fogging spectrum peaks at some lower energy and longer wavelength.
5. Fogging by betas may occur with either type of release, but could be eliminated by modest shielding.
6. An alpha or neutron problem is unlikely.
7. Fogging by soft gammas could be significantly reduced by modest shielding.

### NOTE

The device emplacement, safety precautions, radionuclide spectrum, and extent and character of the venting problem are summarized in six unclassified AEC documents. (8e, 9d, 10c, 11f, 19f, 22)

## 5. PHOTOGRAPHIC ACTION OF X-RAYS AND GAMMA RAYS

### 5.1 RELEASE OF ELECTRONS BY PHOTON ABSORPTION

The absorption of x-rays in silver bromide as a function of wavelength is shown in Figure 5-1. <sup>(7b)</sup> While photon absorption by gelatin, base, and halides other than bromide in film cannot be neglected, silver bromide is the prime ingredient for the release of photoelectrons. The exposing action of high-energy photons does not originate directly from the absorption of the photons but rather from the action of primary electrons emitted by the absorption process.

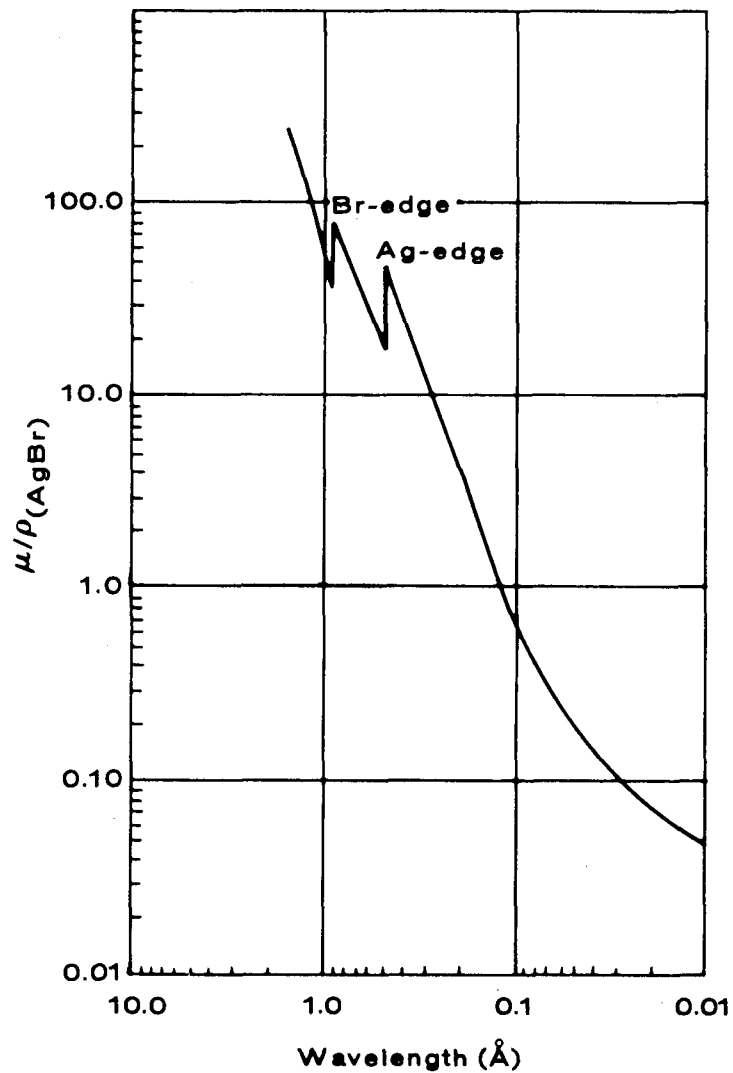


Figure 5-1. Mass-absorption of silver bromide as a function of wavelength (Å). <sup>(7b)</sup>

High-energy photons with wavelengths longer than approximately 0.01  $\text{\AA}$  are absorbed primarily through photoelectric absorption and Compton scattering. Pair-production is the predominant mode of absorption for shorter wavelength photons. The primary electrons released, which have considerable kinetic energy and are capable of traveling a significant distance, may fog many grains along this track.

## 5.2 DISSIPATION OF ELECTRON ENERGY

The high-velocity primary electrons release their energy to silver halide by mechanisms such as direct ion-pair production and formation of knock-on electrons.<sup>(23a)</sup> These mechanisms cause ionization events, liberating electrons into the conduction band of the silver halide. The amount of energy released to a crystal in a given step, which will largely determine the efficiency and latent image distribution caused by the ionizing radiation, will depend on the range-energy relationships for an electron of that given velocity.

Longer wavelength x-rays produce electrons with high specific ionizations and short ranges that give up their energy in a series of large steps. Shorter wavelength x-rays generate photoelectrons with lower specific ionizations and longer ranges, and energy loss is small over the greater part of their path.

The number of secondary electrons of all energy levels is much higher if they are released by a high-energy primary electron or photon than by a low-energy one, but high-energy primaries produce a spectrum in which the low-energy secondaries are relatively higher than for the low-energy primaries. These high- or low-energy secondaries are respectively responsible for the inefficient and massive overexposure or the more nearly efficient and more nearly optimum exposure of individual crystals. The electron slowing-down spectrum or secondary electron spectrum is shown in Figure 5-2 for 65-keV and 1.3-MeV primary electrons traversing polyethylene, which has electron stopping characteristics similar to those of gelatin.<sup>(24)</sup> The range of an average primary can be estimated from the integral under these curves.

Figure 5-3 shows that the range of secondary photoelectrons in pure silver bromide increases rapidly with increasing energy and that the rate of energy loss decreases rapidly with increasing energy.<sup>(25)</sup> Consequently, the electron has its highest ionization per unit length of path near the end of its path. Figure 5-4 demonstrates that the largest number of grains are fogged near the end of an electron track.<sup>(7c)</sup> The scattering observed is typical. The probability of scattering increases as the electron slows. The darkening caused by x-ray exposure results from the superimposition of many such tracks in the emulsion.

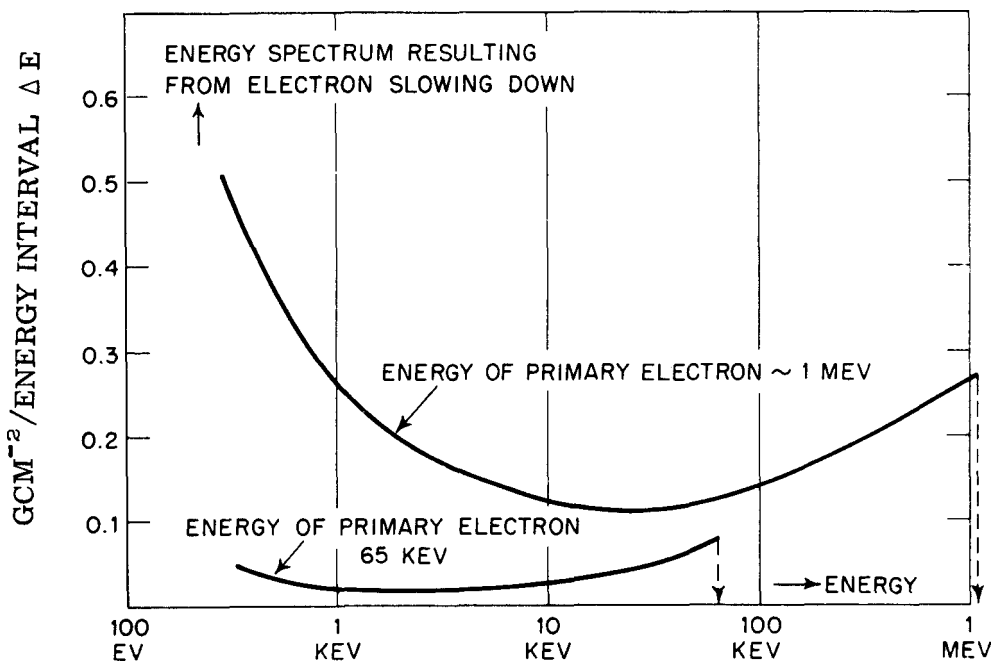


Figure 5-2. Energy distribution of secondary electrons produced in polyethylene by primary electrons (65 keV and 1 MeV).<sup>(24)</sup>

### 5.3 DISTRIBUTION OF THE LATENT IMAGE

The conduction electrons initiated through the interactions of electrons with silver halide can travel through the conduction band of the silver halide if their energy is greater than about 6 eV.<sup>(26)</sup> Conduction electrons can become trapped at specific sites and can reduce silver ions to form silver aggregates at these points, which may act as latent images or development centers.

#### 5.3.1 Latent Image Dispersion

The latent image formed by a normal photographic exposure has never been directly observed. Hamm and Comer<sup>(27)</sup> described amplification and specimen preparation techniques that make it possible to resolve the enlarged latent images with an electron microscope. Through use of these techniques, Hoerlin and Hamm<sup>(28)</sup> studied the latent images from exposures made with alpha particles, x-rays, light of optimum intensity, and light of very low intensity. Their work is discussed extensively in the following pages. The observations of the structural details of latent images must be made with some caution because

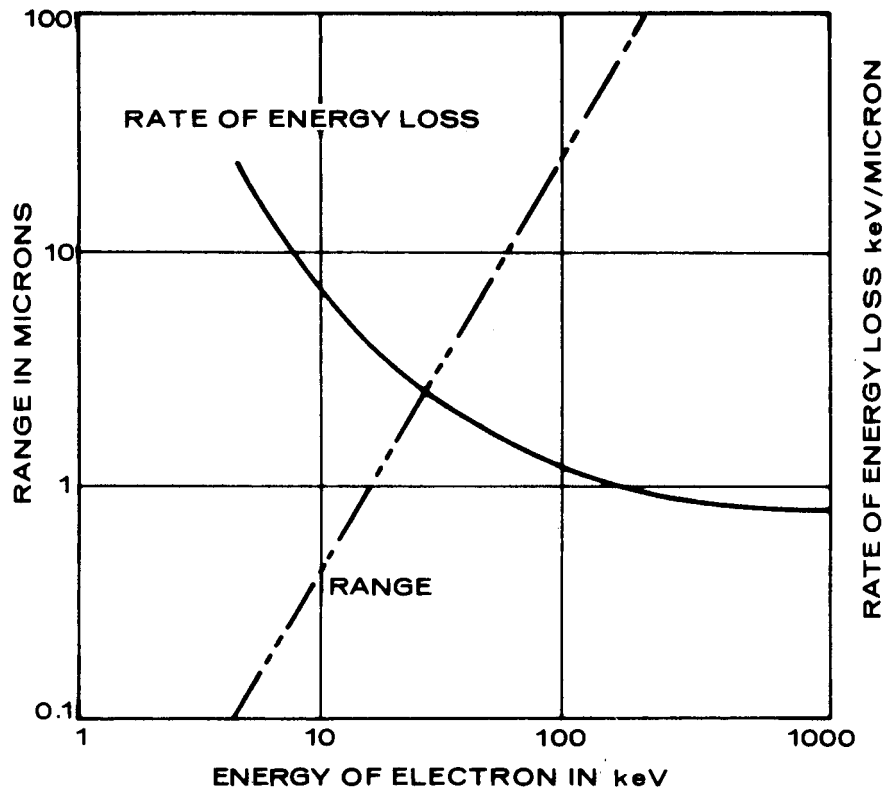


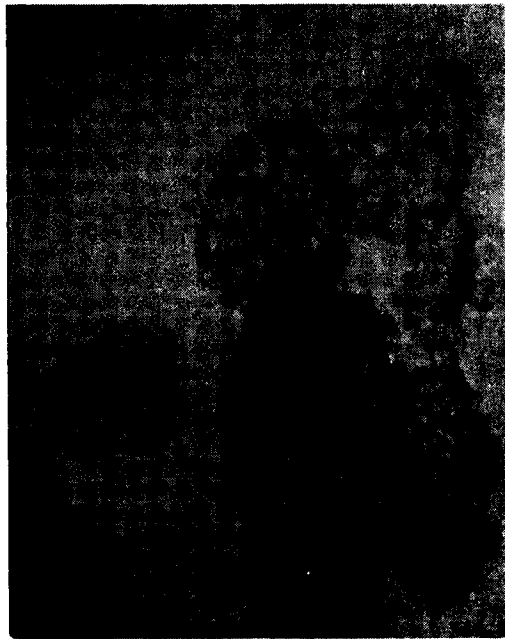
Figure 5-3. Energy loss rate and range of electrons in pure silver bromide. <sup>(25)</sup>

partial development and gold latensification amplification techniques are likely to be influenced by diffusion and latent image development. The alpha particle exposures were made with a polonium source producing approximately 5.3-MeV particles. Theoretical calculations indicated that 15 grains would be hit per particle with an average exposure of 360,000 eV. If 6 eV is necessary to raise an electron to the conduction band, the average exposure would be 60,000 electrons per grain for the passage of one particle. In spite of recombination, one would expect a relatively dense electron cloud to be produced throughout the grain with all sizes of traps becoming filled and operative. The latent image is therefore probably highly dispersed and individual latent images small.

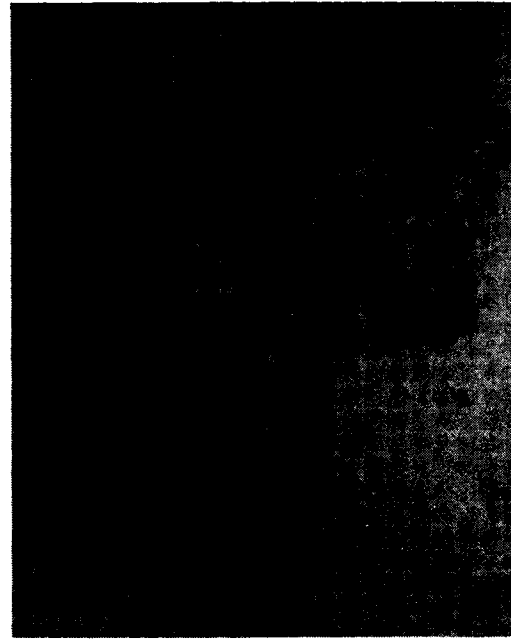


Figure 5-4. Photomicrograph of approximately 300-keV electron track in a nuclear track emulsion. <sup>(7c)</sup>

The foregoing was confirmed by the electron micrographs. Figure 5-5 (A and B) shows the gold-latensified latent image of typical alpha particle exposures. The grains exhibit large patches of dispersed latent images. These densely populated areas probably correspond to the entrance, path, and exit sites of the alpha particles. As is shown in Figure 5-5(C), some grains exhibit no latent images or display them only in fog centers. Two of these grains show the finely dispersed latent image of alpha particles, and two (fewer and larger specks) are chemical fog grains. <sup>(28)</sup>



(A) 21,600 Magnification



(B) 39,200 Magnification

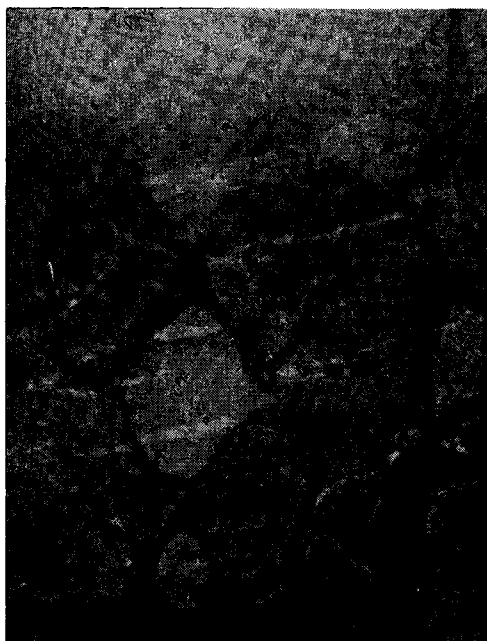


(C) 30,400 Magnification

Figure 5-5. Grains exposed to alpha particles.<sup>(28)</sup>

The x-ray exposures were made with a slightly filtered 65-kVp source. Range and energy loss data indicate that each hit grain receives approximately 10 keV per hit; i.e., about 1500 conduction electrons are produced per hit. Again, theory indicated that a large number of small latent images would appear. This was verified, as shown in Figure 5-6. The centers are larger but fewer than those produced by alpha particles, as expected because of the lower ionizing power of the x-rays. The irregular pattern shown is probably due to multiple hits. The electron track shown in Figure 5-6(A), which occurred in about 5% of the examples, is probably the track of a photoelectron making a grazing hit across the face of the crystal.<sup>(28)</sup>

The optimum intensity light exposures were for an exposure time of 1/100 second. The latent images were found to be larger and fewer in number and more uniformly distributed than those initiated by alpha particles or x-rays, as shown in Figure 5-7.

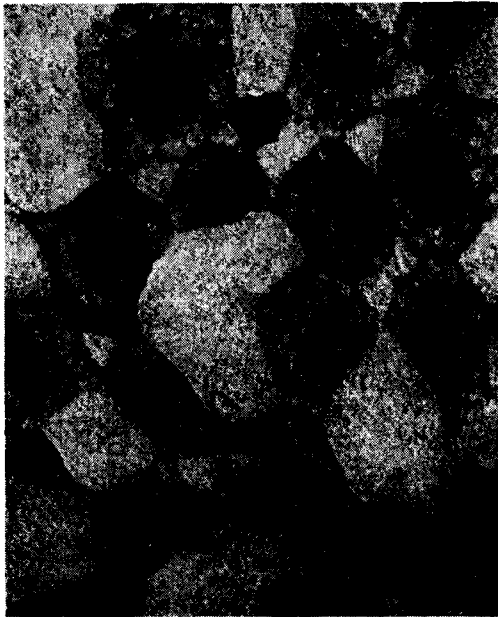


(A) 24,800 Magnification



(B) 17,600 Magnification

Figure 5-6. Grains exposed to x-rays.<sup>(28)</sup>



(A) 13,600 Magnification



(B) 25,600 Magnification

Figure 5-7. Grains exposed to tungsten light, 1/100-second exposure time. <sup>(28)</sup>

With a low-intensity light exposure time of 40 hours, photoelectrons form stable sites only in the deepest traps. Because these traps grow with subsequent injection of electrons, aggregation would be expected to be confined to a very few centers. This is confirmed in the typical examples shown in Figure 5-8, where over 90% of the grains were found to have one to three large gold specks.

Hoerlin and Hamm concluded that for a fast chemically-sensitized emulsion, different types of exposure produce the latent image characteristics expected through application of the Gurney-Mott theory; <sup>(23b)</sup> viz., alpha particles and x-rays were found to produce a very large number of finely dispersed centers, light of optimum intensity and 1/100-second duration produced a small number of centers, and low-intensity light exposures of 40 hours duration produced even fewer specks.

### 5.3.2 Location of Latent Images

Hoerlin and Hamm's micrographs (see Paragraph 5.3.1) indicate that light exposures may be more surface in character than those of high-energy radiation. Although these results are difficult to interpret due to the three-dimensional character of the grain and the two-dimensional character of electron



(A) 32,800 Magnification



(B) 18,400 Magnification

Figure 5-8. Grains exposed to low-intensity light, 40-hour exposure time. <sup>(28)</sup>

microscopy, additional evidence based on other methods of chemical evaluation is nearly conclusive in support of this hypothesis.

The Herschel effect may take place with exposed, unprocessed film when infrared photons are absorbed by the metallic silver comprising a latent image. The photoelectric effect causes a photoelectron to be released into the conduction band of the silver halide, oxidizing the atom of silver to the ionic state and erasing part of the original exposure. Kornfeld's work with a slow narrow grain size distribution emulsion revealed a marked Herschel effect for both light and x-ray exposures, which implies that latent images are surface in character.<sup>(29)</sup> This appeared to be confirmed by development in total and internal latent image developers. Kornfeld explained this result by assuming that internal silver atoms were present but too finely distributed to be developable. A reversal of the Herschel effect at high densities after an x-ray exposure at the temperature of liquid nitrogen, as shown in Figure 5-9, is evidence for the presence of internal silver. Figure 5-9's film was developed in a high solvent level developer (D-19) for four minutes at 20°C.

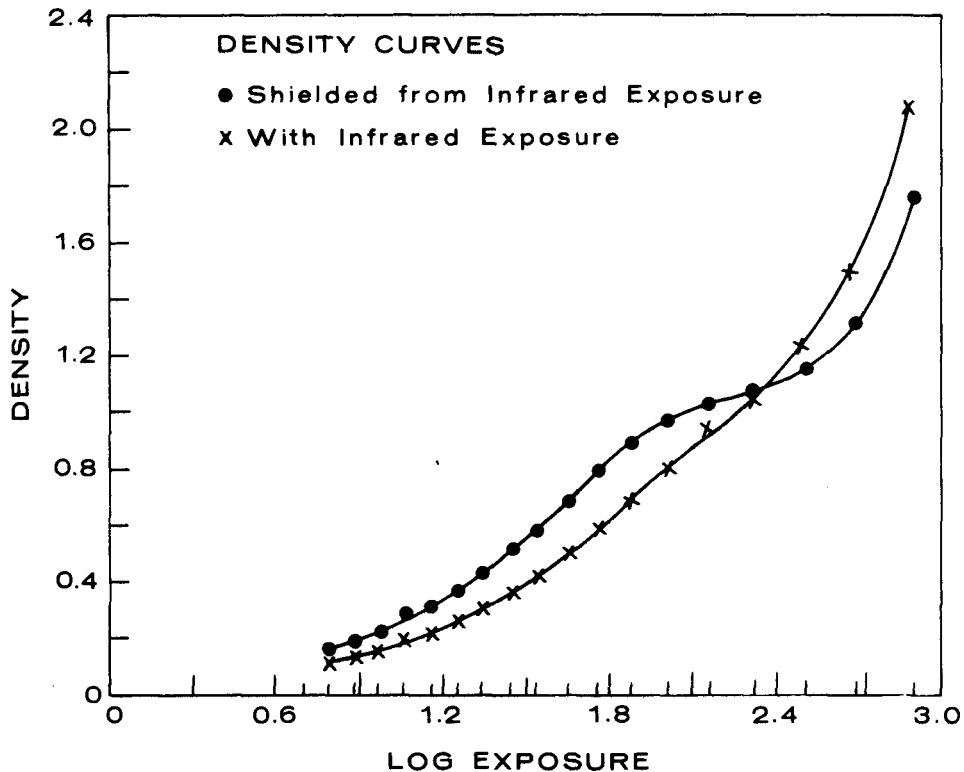


Figure 5-9. Herschel effect (and reversal) after exposure to x-rays at temperature of liquid nitrogen.<sup>(29)</sup>

While the terms "surface" and "internal" latent image suggest the physical location of development centers in a silver halide grain, the practical application of the concept does not lie in determining the location of the latent image but rather in determining the response of the emulsion to a surface developer or an internal development sequence.

Solvents dissolving silver halide expose otherwise inaccessible internal latent images to developing action. Typical silver halide solvents include the thiosulfates, thiocyanates, cyanides, sulfites, alkali halides, certain amines, organic and inorganic ammonias, and water. Alkali halides such as potassium

iodide promote internal development by replacing bromide in the crystal with iodide, thereby cracking the grain or promoting recrystallization. A developer containing little or no silver halide solvent is termed a surface latent image developer, while a developer containing a substantial amount of solvent is a total latent image developer. To promote true internal development, any surface latent image silver must be destroyed by treatment in a solution containing an oxidizing agent such as chromium trioxide, acid-ferricyanide, or acid-dichromate.<sup>(30)</sup> When a total latent image developer is used after this prebleaching treatment, the sequence is termed internal development.

Several researchers have used these techniques to distinguish surface from internal latent images for high-energy exposures. Their results indicate that high-energy exposures produce latent images that are more or less uniformly distributed throughout the grain.<sup>(24)(31-35)</sup>

### 5.3.3 Chemical Sensitization and Its Effect on Latent Image Distribution

The latent image distribution of an exposed emulsion is strongly affected by the manufacturing process. After-ripening consists of holding the washed and melted emulsion at approximately 50°C for perhaps an hour. Small, carefully-controlled amounts of impurities called sensitizers are added, which are adsorbed on and absorbed in the silver halide crystals. After-ripening and chemical sensitization are known to be more effective in increasing light and short wavelength x-ray sensitivity than long wavelength x-ray sensitivity. Sulfur, gold, and iodide sensitization probably increase surface sensitivity by forming trapping sites and crystal deformations. Introduction of thallium salts in the emulsion may increase short wavelength x-ray sensitivity and decrease light sensitivity. Sensitization with lead salts has been reported to both increase<sup>(23c)</sup> and decrease<sup>(25)(35)</sup> x-ray sensitivity. Tomoda also reports a hypersensitization of light sensitivity and densensitization of x-ray sensitivity through silver salt treatment.<sup>(35)</sup> Mercury vapor, a hypersensitizer or latensifier for light, has been reported to cause partial destruction of alpha particle latent images in nuclear track emulsions.<sup>(36a)</sup> The fact that the spectral sensitivity of emulsions is affected by chemical sensitization is itself an indication that latent image distribution is affected. Danguy, Hautot, and Sauvenier, Klein, and Nepela and Nitka found similar results in distribution of latent image as a function of x-ray wavelength and chemical sensitization.<sup>(23c)</sup>

The data of Nepela and Nitka,<sup>(24)</sup> which clearly demonstrate these effects, are summarized on the following pages. Their approach was to measure latent image distribution as a function of chemical ripening. Since sensitivity center formation is a function of ripening time, Nepela and Nitka prepared silver bromo-iodide emulsions with various ripening times and exposed them to high- and low-intensity light, filtered 65- and 250-kVp x-rays, and  $^{60}\text{Co}$  gamma rays.

Surface development and physical development were applied to confirm the hypothesis that chemical ripening improves the surface sensitivity of silver halides. Chemical ripening time was found to strongly influence light sensitivity and barely affect x-ray sensitivity for surface development. Chemical ripening time influenced x-ray and gamma ray sensitivity more for total and internal development. Their results are summarized in Figures 5-10 through 5-14, which are taken from the referenced article.<sup>(24)</sup>

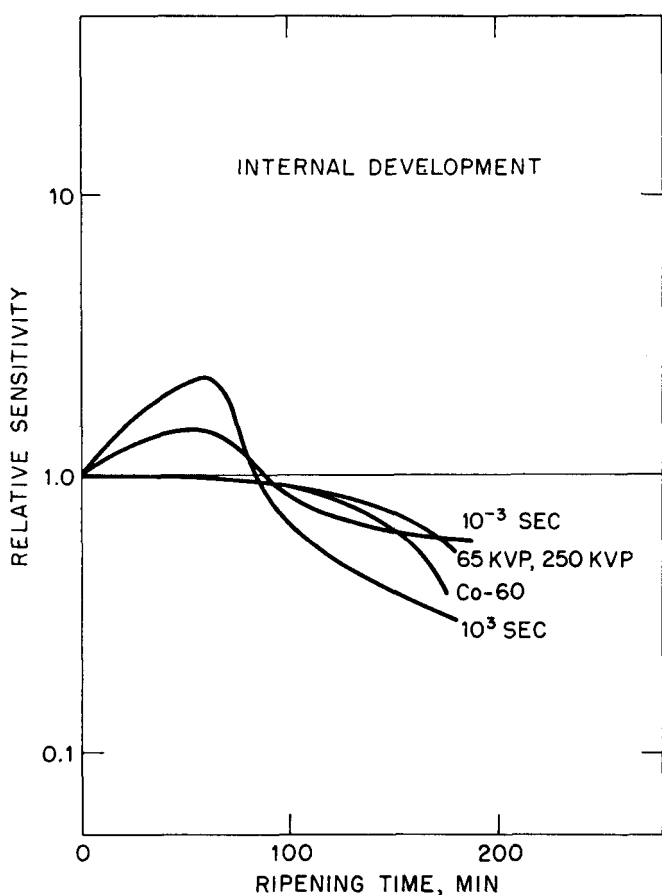


Figure 5-10. Relative sensitivity at  $D = 0.50$  for internal development for various ripening times.<sup>(24)</sup>

For physical development, which is indicative of the quantity of latent image nuclei formed during exposure, a general speed increase with progressive ripening was observed for all types of exposures, particularly for x-ray and gamma ray exposures. Figure 5-14 indicates that irrespective of radiation energy, the number of sensitivity centers increases for each ripening stage and that x-rays and gamma rays produce more nuclei per crystal than does high-intensity light.

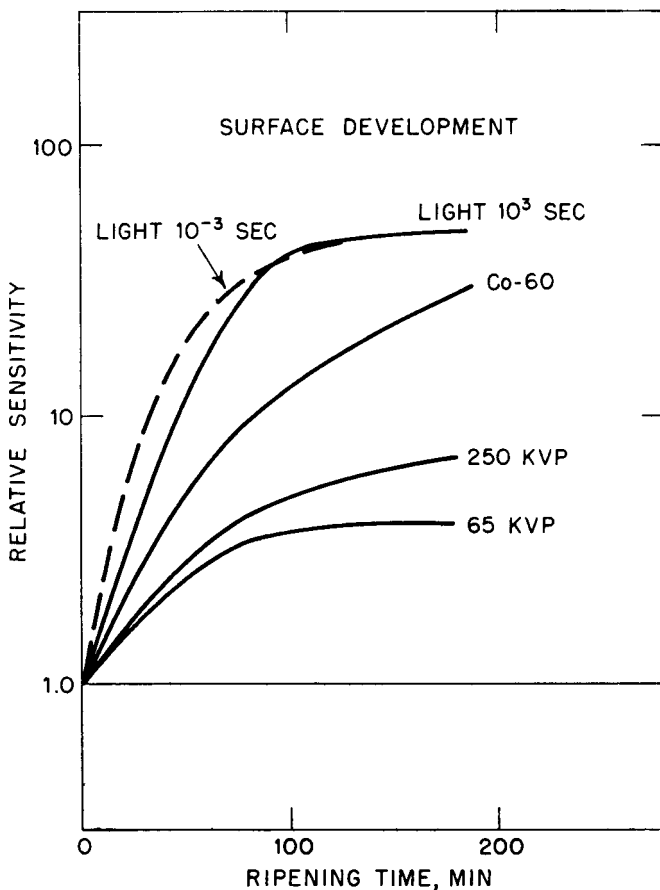


Figure 5-11. Sensitivity at  $D = 0.50$  for surface development for various ripening times. <sup>(24)</sup>

Pre-exposure chemical bleaching of samples of a commercial x-ray film exposed to light, x-rays, and gamma rays resulted in greater speed losses for light exposures ( $1.2 \log E$  loss) than for  $^{27}\text{Co}^{60}$  ( $0.45 \log E$  loss) or x-ray ( $0.1 \log E$  loss) exposures compared to untreated controls. This demonstrates the greater participation of surface sensitivity centers in high-intensity light exposures than the gamma ray and x-ray exposures.

This data clearly demonstrates that chemical ripening contributes markedly to high-intensity light sensitivity, contributes moderately to  $^{27}\text{Co}^{60}$  gamma ray sensitivity, and is relatively unimportant for longer wavelength x-rays. The data also indicates that in high-intensity light exposures latent images are primarily surface in character, and that the latent images become progressively less surface in nature as high-energy wavelength increases. This data is in agreement with Nam, <sup>(37)</sup> who prepared simple emulsions with both high and low internal-to-external sensitivity site ratios.

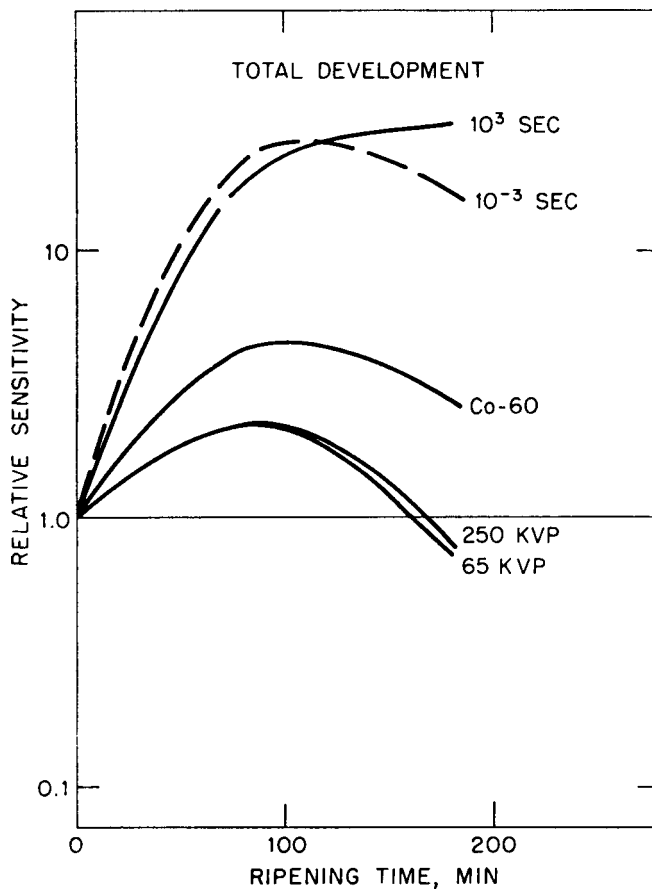


Figure 5-12. Relative sensitivity at  $D = 0.50$  for total development for various ripening times. <sup>(24)</sup>

#### Explanation of Results

Longer wavelength x-rays produce electrons with high specific ionizations and short ranges that give up their kinetic energy in a series of large steps, resulting in the formation of many latent image nuclei in an affected crystal. Thus, many internal image nuclei are formed around sensitivity centers not affected by chemical sensitizers. Shorter wavelength x-rays generate photoelectrons with lower specific ionization, longer range, and smaller energy loss over the greatest part of their path. Surface sensitivity centers require fewer silver atoms to become stable or developable. These smaller energy losses result in fewer latent image centers that are primarily surface in nature.

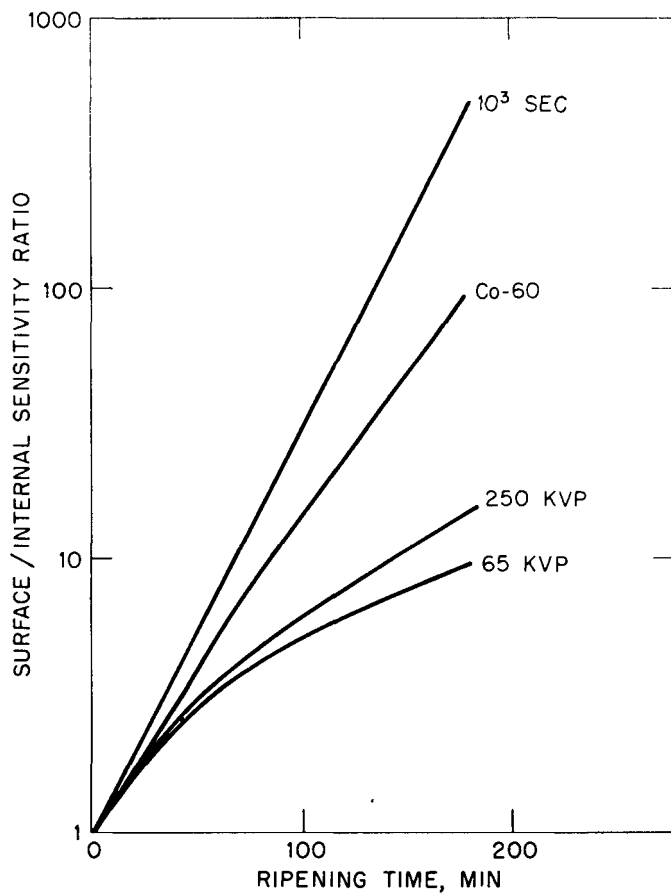


Figure 5-13. Relative surface/internal sensitivity ratio at  $D = 0.50$  for various ripening times.<sup>(24)</sup>

The number of secondary electrons of all energy levels is much higher if they are released by a high-energy rather than a low-energy primary electron or photon, but high-energy primaries produce a spectrum in which the low-energy secondaries are higher in energy relative to the low-energy primaries. These high or low-energy secondaries are respectively responsible for the inefficient and massive overexposure or the more nearly efficient and more nearly optimum exposure of individual crystals.

#### 5.4 THE DENSITY/EXPOSURE RELATIONSHIP

The interaction of a high-energy photon or particle with matter produces a primary electron, which in turn produces the secondary electrons (secondaries) responsible for photographic action.<sup>(24)</sup> Figure 5-2 illustrates the secondary/

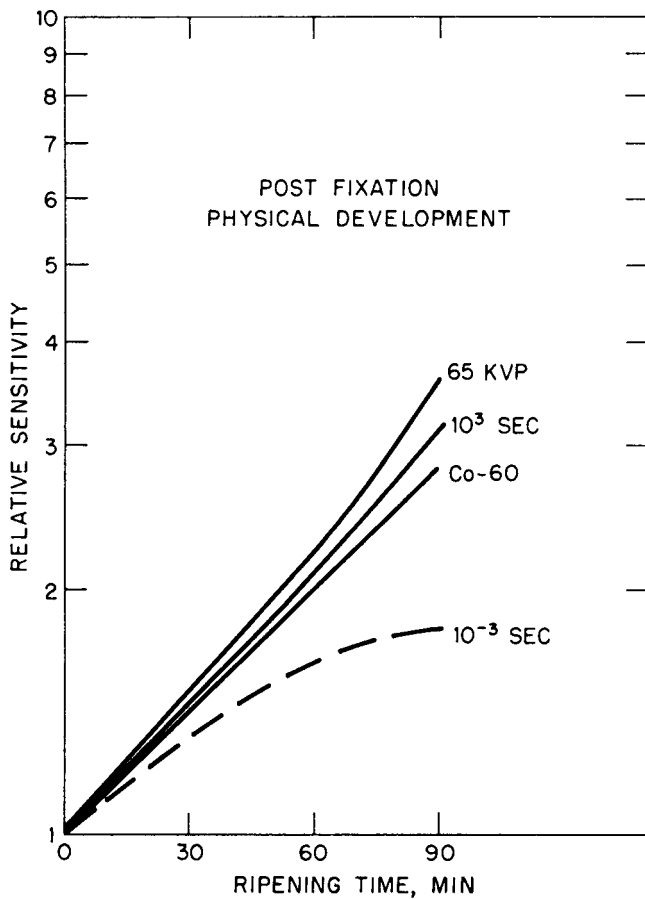


Figure 5-14. Relative sensitivity at  $D = 0.50$  for post-fixation physical development for various ripening times.<sup>(24)</sup>

primary electron slowdown spectrum for 1-MeV and 65-keV primaries in polyethylene.<sup>(24)</sup> Figure 5-3 shows the rate of energy loss and electron range in silver bromide.<sup>(25)</sup> The rate of energy loss for the secondaries,  $dE/dx$  (keV/micron), is approximately 0.9 keV/micron at 1 MeV and several hundred keV/micron for 1 keV. However, the average energy loss in keV/micron for electrons in a photographic emulsion is, due to the emulsion's gelatin content, slightly lower than indicated in Figure 5-3.<sup>(7d)</sup>

The energy required for the liberation of an electron from the silver halides is about 6 eV,<sup>(26)</sup> consequently, the average number of electrons liberated in one hit of a 1.0-micron diameter crystal would be on the order of several hundred to several thousand conduction electrons. The energy of a visible light photon is a few eV; the photon's absorption results in the liberation of only one conduction electron. Studies have indicated that 5 to 10 conduction electrons must normally be liberated

to render a grain developable.<sup>(23d)</sup> Therefore, one hit will be adequate to form a developable latent image in electron exposures and several hits will be necessary for light exposures.

The general shape of the characteristic curve can be derived theoretically for the one-hit case and the multiple-hit case.<sup>(7e)</sup> If the number of grains made developable by absorption of one electron is constant for all electrons during exposure, the number of developable grains is proportional to exposure. If density is proportional to numbers of developed grains, as is the case in conventional processing, one-hit density is proportional to exposure and the D log E characteristic is exponential but limited by saturation effects. In the case of light exposures (multiple hits), the number of grains made developable by absorption of one photon is not constant for all photons during exposure and the number of developable grains is not proportional to exposure. Threshold effects produce a toe, and a shoulder results from saturation effects. Light characteristic curves frequently have an approximately linear D log E configuration over some range.

These calculated responses, which have been experimentally verified by several researchers for conventional development, are illustrated in Figure 5-15.<sup>(7f)</sup>

Given the photographic response curves for any two types of radiation, it is possible to predict the D log E curve for them when exposures are successive. The results of successive exposures to radiations of different photon energies (200-kV x-rays and 1.25-MeV  $^{27}\text{Co}^{60}$  gamma rays), to high-energy photons and light, and to light and infrared, show that after some initial transition phenomena the shape of the D log E curve is essentially the same as that of the second type of exposure administered alone.<sup>(38)</sup>

As determined in the light and high-energy photon studies by Ehrlich and McLaughlin,<sup>(38)</sup> there is a transition between the D log E curve for high-energy photons and light for both surface and internal development using Dupont Type 502. Surface as well as internal latent images were observed to be eventually dominated by the second exposure if it was of sufficient intensity. With surface development, there is an initial desensitization, especially for transitions from the higher densities of the ascending branches and from the solarization regions. With internal development, observed regions of initial sensitization sometimes seem to complement those regions of initial desensitization for surface development. These findings were summarized as follows:

"1. If the exposure administered first, produces a density in the ascending branch, lying below the maximum density that can be produced by the type of radiation used for the second exposure, then the second exposure causes an increase in optical density, roughly up to that maximum density after an initial transitional effect, the exposure required for a given density change along the mixed-exposure curve is the same as along the characteristic curve corresponding to the second exposure administered alone.

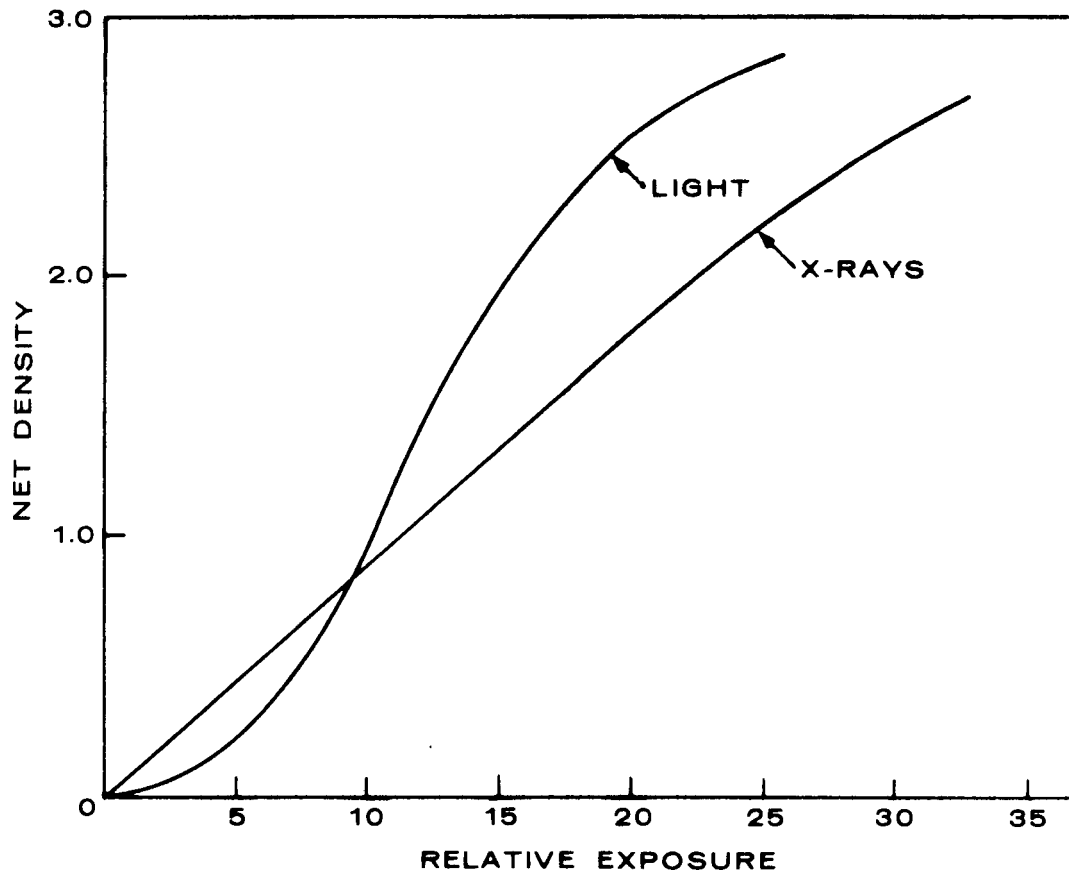


Figure 5-15. Comparison of density-exposure curves for light and x-rays for a typical emulsion. (<sup>71</sup>)

2. If the density attained with this first exposure, lies in the solarization branch, but still below the maximum density attainable with the second type of exposure, the transition toward the characteristic curve for the second exposure in general does not lead up to the maximum density corresponding to the second exposure before the solarization branch sets in.

3. If the exposure administered first, produces a density that lies above the maximum density characteristic for the type of radiation used for the second exposure, the second exposure, after an initial transitional effect, causes a decrease in density; beyond the transition region, the exposure required for a given density change along the downward mixed-exposure branch is essentially the same as along the solarization branch of the characteristic curve corresponding to the second exposure.

4. When the surface latent image experiences a transitional desensitization effect, a corresponding transitional sensitization effect occurs in the internal image. In the case of the surface image, the initial densensitization by the first type of exposure becomes more pronounced for mixed-exposure curves beginning at the shoulder or in the solarization branch of the curve characteristic for the first exposure.<sup>(38)</sup>

### 5.5 X-RAY SPECTRAL SENSITIVITY

Variation in sensitivity as a function of x-ray wavelength is probably typical for large grain size emulsions, given total development. Seemann<sup>(39)</sup> determined the spectral sensitivities of Kodak No-Screen and Kodak Industrial Type K x-ray films in the region between 0.2 and 2.5 Å (60 to 4.8 keV) using a filtered K fluorescence sensitometer (see Figure 5-16). Figures 5-17 through 5-20 variously illustrate the relation between wavelength and the dosage required to produce a net density of 1.0 above fog.

Data by Gunther and Tittel<sup>(40)</sup> are included in Figure 5-20 for comparison. Their results are the number of quanta absorbed per silver atom freed (photolized) by the radiations.

#### NOTE

Because the roentgen is tied to the ionization of air, it may mistakenly be believed that film has peak sensitivity at about 0.30 Å (40 keV). Hamilton<sup>(23e)</sup> points out that in discussions of photographic response, it is more meaningful physically to express sensitivity in terms of ergs/cm<sup>2</sup>. It is conventional in radiometry and sensitometry to express the sensitivity of a sensor in terms of incident energy per unit area necessary to elicit a given response.

Figure 5-18 indicates that sensitivity drops sharply as wavelength shortens. This change is due predominantly to the change in the absorption coefficient of the silver halides. The sharp changes in incident sensitivity at approximately 0.50 and 0.90 Å are due to the abrupt changes in the absorption coefficients of silver and halide respectively at those wavelengths or K edges. Spectral sensitivity expressed in terms of ergs absorbed per unit area indicates the photographic efficiency as a function of wavelength. Seemann's data<sup>(39)</sup> indicating decreasing efficiency with decreasing wavelength disagrees with Hoerlin's (see Figure 5-21),<sup>(6)</sup> which indicates increasing efficiency with decreasing wavelength.

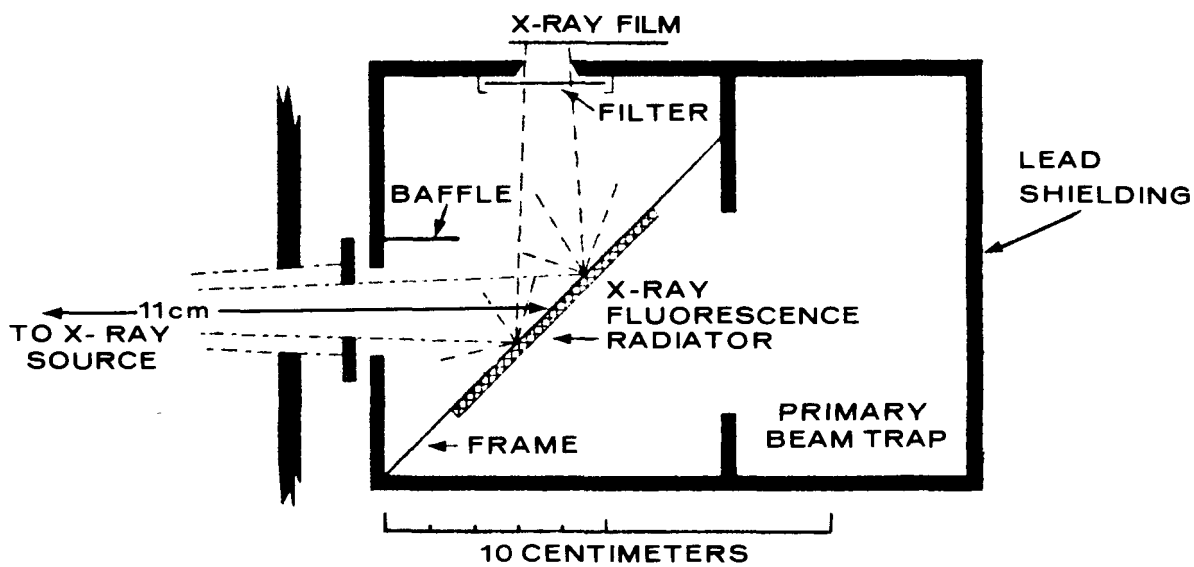


Figure 5-16. Schematic of an x-ray fluorescence sensitometer. <sup>(39)</sup>

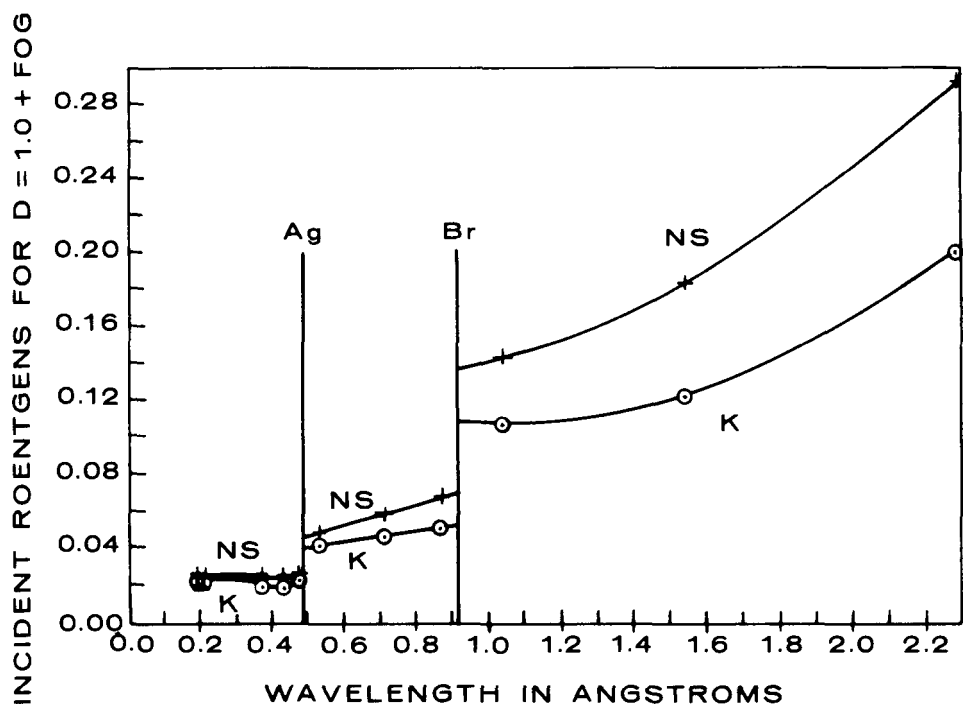


Figure 5-17. Spectral sensitivities of Kodak No-Screen and Type K x-ray films (incident roentgens versus wavelength). <sup>(39)</sup>

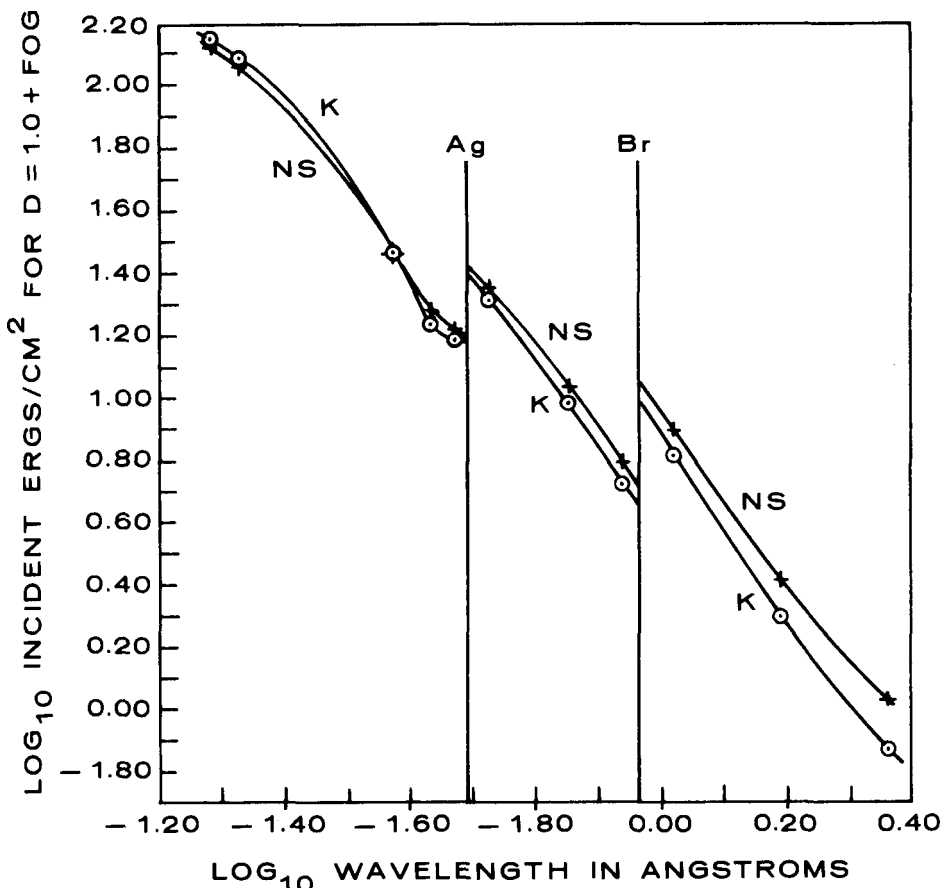


Figure 5-18. Spectral sensitivities of a front emulsion of Kodak No-Screen and Type K x-ray films (incident ergs/cm<sup>2</sup> versus wavelength). <sup>(39)</sup>

The curve based on Smith's data<sup>(41)</sup> is similar to Seemann's.<sup>(39)</sup> Smith<sup>(42)</sup> maintains that the differences in these curves' shapes result from the consideration of different factors in computing absorbed dose. Thus while there is general agreement that incident exposure efficiency decreases with decreasing wavelength, opinions diverge regarding absorbed dose.

It is the consensus of the literature that the quantum efficiency of the photographic process does increase with decreasing wavelength of the primary radiation. Plotting spectral sensitivity in terms of number of photons absorbed expresses this, but neglects Planck's law and therefore ignores the fact that the energy of a photon is inversely proportional to wavelength.

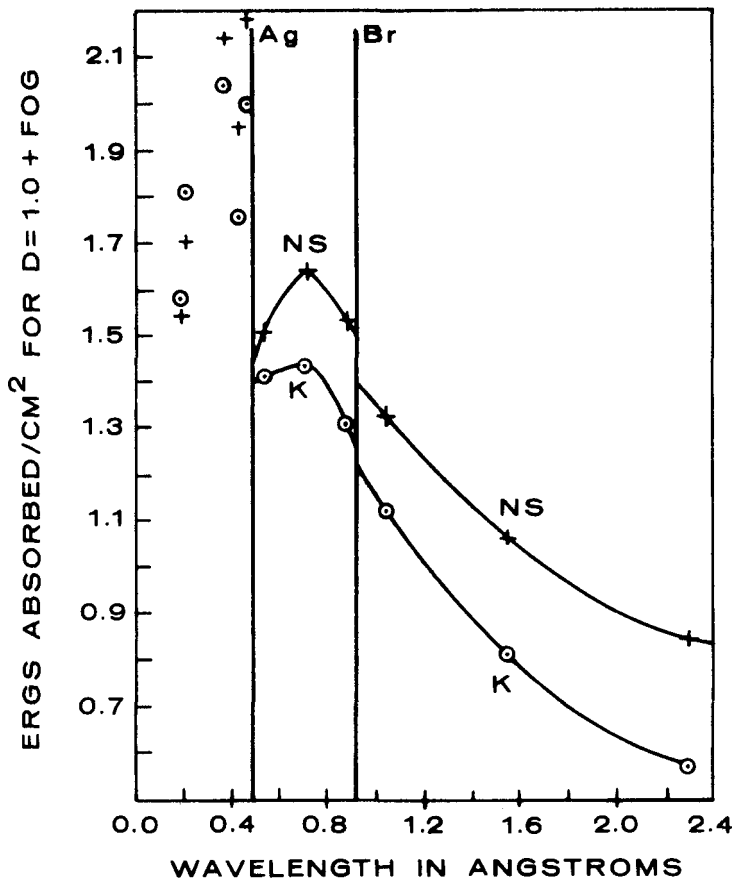


Figure 5-19. Spectral sensitivities of a front emulsion of Kodak No-Screen and Type K x-ray films (ergs absorbed/cm<sup>2</sup> versus wavelength).<sup>(39)</sup>

Hamilton,<sup>(23e)</sup> Herz,<sup>(78)</sup> Hoerlin,<sup>(6)(25)</sup> Greening,<sup>(43)</sup> Nepela and Nitka,<sup>(24)</sup> and others have discussed the mechanism of high-energy latent image formation and quantum efficiency in both theoretical and empirical terms. A high-energy primary electron or photon produces a secondary spectrum in which low-energy secondaries are proportionally higher relative to the spectrum produced by a medium- or low-energy primary. High-energy secondaries less efficiently expose the grains through massive overexposure.

A number of emulsion making and processing variables may affect the spectral sensitivity of an emulsion. Feigenbaum (Corney and Clear)<sup>(44)</sup> has indicated that gelatin-to-silver halide ratio has an insignificant effect on sensitivity. Hoerlin<sup>(25)</sup> found that short wavelength x-ray sensitivity was not significantly affected by silver halide-to-gelatin ratio for an adjusted coating thickness yielding

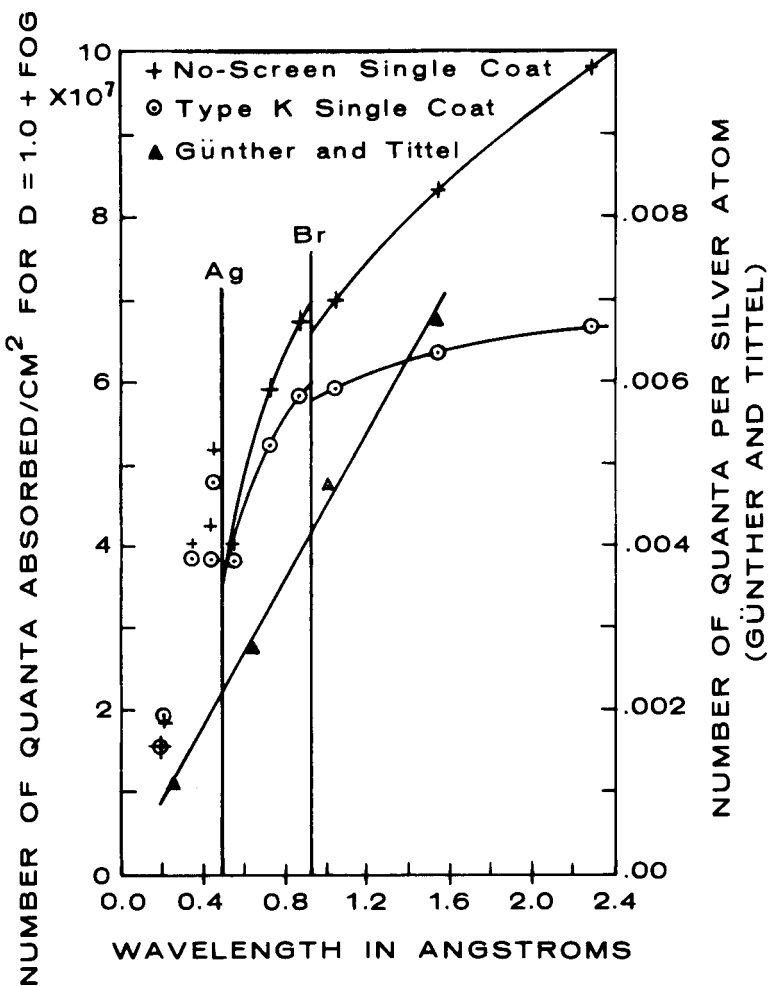


Figure 5-20. Spectral sensitivities of a front emulsion of Kodak No-Screen and Type K x-ray films (quanta absorbed/cm<sup>2</sup> versus wavelength).<sup>(39)</sup>

equivalent amounts of silver halide per cm<sup>2</sup>. Chhabra<sup>(45)</sup> found that long wavelength sensitivity was sharply reduced in emulsions with 1/10 and 1/20 normal silver bromide while shorter wavelength response was negligibly affected. Chhabra's response of Ilford G5 emulsion as a function of photon energy and silver halide content (see Figure 5-22) are in fair agreement with the expected responses shown in Figure 5-23.<sup>(45)</sup>

#### NOTE

The dashed curve in Figure 5-22 gives the ratio of film response (normal and 1/10 normal silver bromide content) as a function of photon energy.

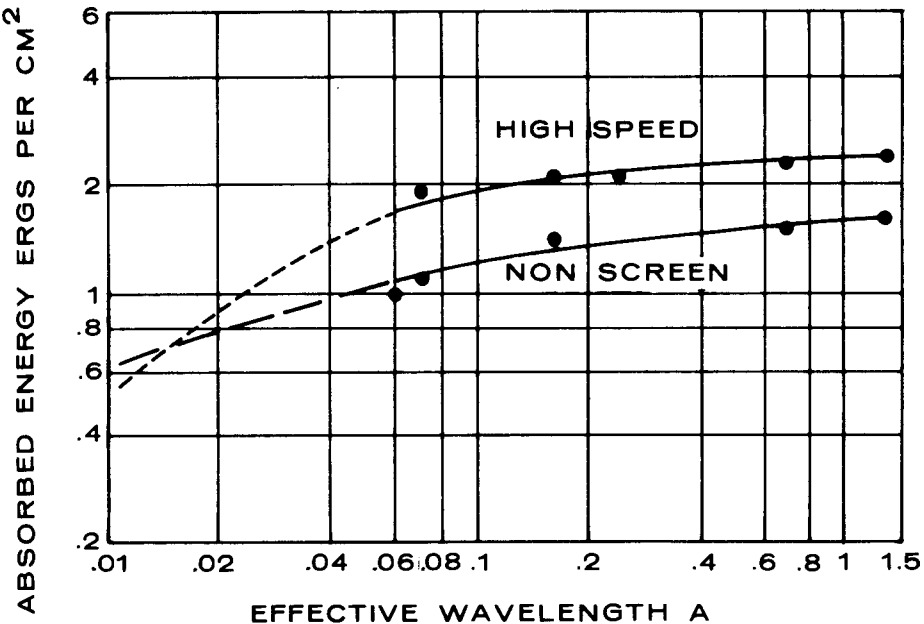


Figure 5-21. Absorbed energy required to produce  $D = 1.5$  above fog (ergs/cm<sup>2</sup> versus wavelength).<sup>(6)</sup>

Both the calculated and experimental results indicate that the gelatin-to-silver bromide ratio has a significant effect only on the lower photon energies' sensitivity (less than 150 keV) through the range of concentration tested (normal to 1/20th normal). The calculated results were obtained using formulas described by Greening.<sup>(43)</sup> These calculations assume that the photographic effect is proportional to the energy absorbed by the silver bromide in the emulsion and include factors for fluorescent x-rays emitted by silver bromide not utilized by the emulsion, energy lost through secondary electrons leaving the emulsion, energy lost by the grains to the gelatin, and energy gained by the silver bromide through secondary electrons produced in the gelatin.

After-ripening and sulfur and gold chemical sensitization are more effective in increasing light and short wavelength x-ray sensitivity than long wavelength x-ray sensitivity.<sup>(23c)(24, 25)</sup> Lead and cadmium give nearly equal sensitivity increases to light and low- and high-energy x-rays.<sup>(23c)</sup> Thallium behaves similarly to lead,<sup>(23c)</sup> but Hoerlin<sup>(25)</sup> and Tomoda<sup>(35)</sup> reported losses in light sensitivity for thallium additives. Sulfur, gold, and iodide additions probably increase surface sensitivity by forming trapping sites for electrons and crystal deformations, while

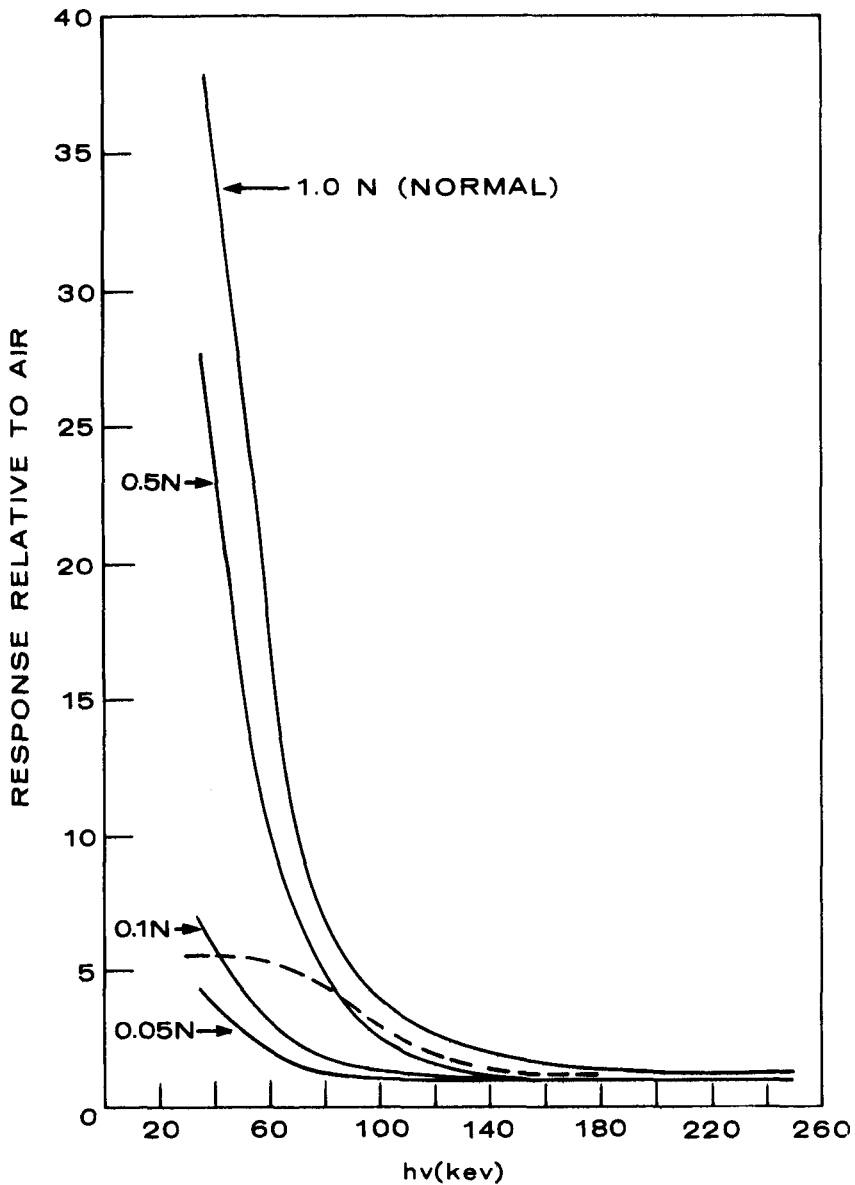


Figure 5-22. Response of film relative to air versus photon energy at normal,  $1/2$ ,  $1/10$ , and  $1/20$  silver bromide content. <sup>(45)</sup>

lead, cadmium, and thallium appear to provide traps for positive holes. <sup>(23c)(25)</sup> (Paragraph 5.3 may be consulted regarding the effects of ripening and chemical sensitization and the effect of development location on spectral sensitivity.)

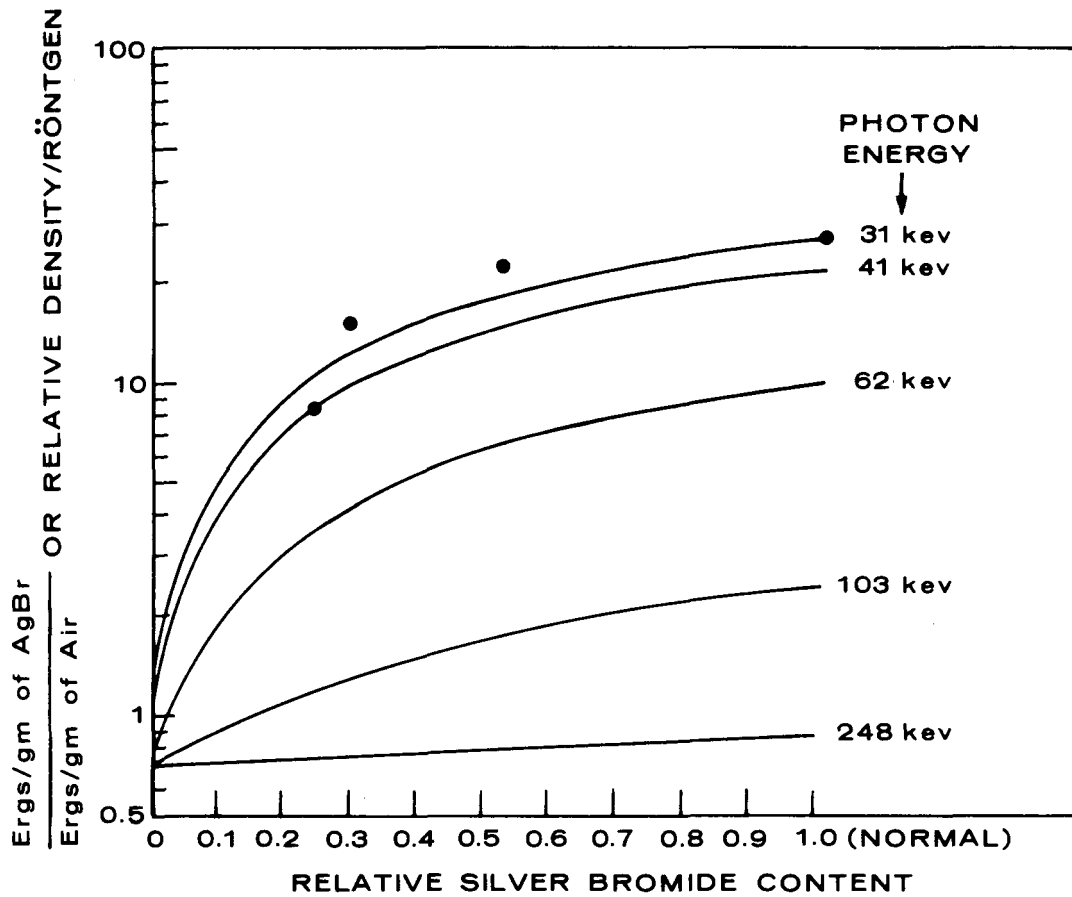


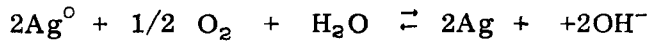
Figure 5-23. Calculated response of G5 emulsions (Greening's formulation) as a function of silver bromide content. <sup>(45)</sup>

Shaffer<sup>(46)</sup> reports that a photosolubilized lith type film processed conventionally exhibited a light characteristic curve similar in shape and slightly slower than that of the same untreated emulsions, while the 1.25-MeV characteristic curve exhibited a markedly lower slope and speed than that of the same emulsion untreated.

## 5.6 ENVIRONMENTAL FACTORS AFFECTING SENSITIVITY AND LATENT IMAGE FADING

The environment of an emulsion prior to exposure, during exposure, and during post-exposure storage may affect its sensitivity. Important environmental factors include temperature, pressure, moisture, and oxygen, which seem to interact with each other and the nature of the exposure in a complicated manner. The quality of the radiation and, in the case of light the duration of the exposure, are also important.

James' summary of the literature on environmental effects concentrates on light exposures.<sup>(47)</sup> Hamilton<sup>(23f)</sup> and Herz<sup>(7h)</sup> have prepared brief reviews concentrating on the effects of high-energy exposures. Other researchers have also discussed environmental effects, particularly in connection with film badge dosimetry and nuclear track emulsions. Faraggi and Albouy,<sup>(45)</sup> who found that latent image fading was largely due to oxygen and water vapor in the environment of the emulsion, surmised that the following reaction was taking place:



The ionic mechanism of latent image formation becomes more efficient as temperature increases.<sup>(23g)</sup> Trapping efficiency or the stability of latent image centers decreases with increasing temperature,<sup>(23h)</sup> and latent image fading is accelerated by increasing temperature. The reciprocity curve for light exposures shifts to the left with increasing temperature.<sup>(23i)</sup> Spectral sensitization and desensitization are temperature-dependent in a complicated manner.<sup>(47)</sup> Berg and Mendelsohn<sup>(49)</sup> found that at 4° K, x-ray sensitivity was relatively less reduced than light sensitivity. This contrasts with the findings of Falla<sup>(50)</sup> that some emulsions may lose more internal sensitivity than surface sensitivity. Brodsky and Kathren<sup>(51)</sup> found that x-ray sensitivity increases with temperature for high-humidity environments, but is independent of temperature for 0% humidity environments over the range of 300 to 330° K.

Several investigators have found that light sensitivity decreases with increasing pressure.<sup>(47)</sup> Yagoda<sup>(36b)</sup> reports that the gamma ray sensitivity of nuclear track emulsions increases with increasing pressure. James<sup>(47)</sup> claims that interpretation of results is difficult due to interference by oxygen and moisture, pressure due to gelatin, and changes in the silver bromide optical absorption spectrum with pressure.

Low-intensity reciprocity failure can be minimized by evacuating emulsions before and during exposure. The presence of oxygen in gelatin is critical for dye desensitization. Latent image-fading of light-, x-ray-, and alpha-initiated latent images is accelerated by water vapor and oxygen.

McLaughlin and Ehrlich<sup>(52)</sup> found that coarser-grained emulsions tend to fade less than finer grained emulsions; other investigators have observed no such effect.<sup>(53-55)</sup> The presence of halogen acceptors tends to minimize fading.<sup>(52)</sup> High pAg emulsions and emulsions with low silver bromide concentration may exhibit more pronounced fading, and the presence of sensitizing or desensitizing dyes may hasten fading.<sup>(36c)</sup> Some studies indicate that fading is greatest for a particular level of high-energy exposures and is less for exposures above or below that level.<sup>(53, 54)</sup> One study indicated that fading increases with the size of the development center.<sup>(52)</sup> It is generally conceded that along a single track in a

nuclear emulsion, more fading occurs at the beginning of the track (low specific ionization) than at the end (high specific ionization). Using 80-kVp x-rays and 1.25-MeV gammas, Herz<sup>(7b)</sup> found fading rate to be a function of wavelength over storage periods of several months; other studies have confirmed this result.<sup>(65, 66)</sup> McLaughlin and Ehrlich<sup>(52)</sup> did not observe this effect, but storage periods in their studies did not exceed one week. There is evidence that surface latent images fade more rapidly than internal latent images,<sup>(23f)(63, 64)</sup> and that light latent images fade more rapidly than those of alpha and beta particles.<sup>(47)</sup> James<sup>(47)</sup> reports that during the early stages of fading of surface latent images formed by alpha and beta particles, the internal latent image initially increased, reached a maximum, then decreased. Latent images formed by light showed a continuous decrease for both surface and internal latent images.<sup>(47)</sup>

#### NOTE

Many of the environmental experiments have been crossed experiments, involving humidity and temperature, in which the influence of water vapor and temperature were to be studied. However, in many cases the humidity input variable was relative humidity, which is a function of temperature, rather than absolute water vapor content. For example, if in mapping a response surface relative humidity were maintained constant while temperature was varied, water vapor content would not remain constant. These practices could distort the resulting data if not interpreted and reported properly.

Sensitivity and latent image fading are influenced by many emulsion making and environmental factors and their interactions. If the fading rate is greater for light than for gamma radiation, environmental precautions to minimize fading should be taken if exposed film is not to be processed immediately. An environment consisting of low temperature, low water vapor, and low oxygen is indicated in this case. If the fading rate is found to be greater for gamma exposures than for light, storage in an environment that accelerates fading might be useful; i. e., the opposite environment might be indicated.

## 6. APPROACHES TO SOLUTION OF THE IRRADIATED FILM PROBLEM

Hansen, McCue, and Wyckoff<sup>(57)</sup> organized possible solutions to the radiation-fogged film problem into the flow diagram shown in Figures 6-1 through 6-8.

Adams<sup>(58)</sup> recommends the following methods for reducing the detrimental effects of space radiation on film:

### "I. INHIBIT FORMATION OF UNDESIRED LATENT IMAGE

- a). Bulk shielding
- b). Electric or Magnetic Shielding
- c). High Humidity Storage
- d). Film Manufacture in Space
- e). Film Processing in Space
- f). Low Temperature Storage
- g). Storage Under Influence of Electric Field
- h). Desensitize Internal Sites During Film Manufacture

### II. ERASURE OF UNDESIRED LATENT IMAGE

- a). Herschel Effect
- b). Oxidizing Agents
- c). High Humidity

### III. REJECT UNDESIRED LATENT IMAGE

- a). Minimize Internal Grain Sensitivity  
During Manufacture
- b). Selectively Process Optical Imagery
- c). Process Undesired Latent Image Before Optical  
Exposure, Reverse Process Afterwards."<sup>(58)</sup>

Anderson's proposed methods of reducing background radiation fogging by space radiation deal with in situ film manufacture, in situ film processing, low-temperature storage, high-humidity storage, and storage in electrical fields.<sup>(59)</sup> Proposed methods of erasing the undesired latent image included the Herschel effect, chemical oxidizing agents, and post-fogging storage in a high-humidity environment.

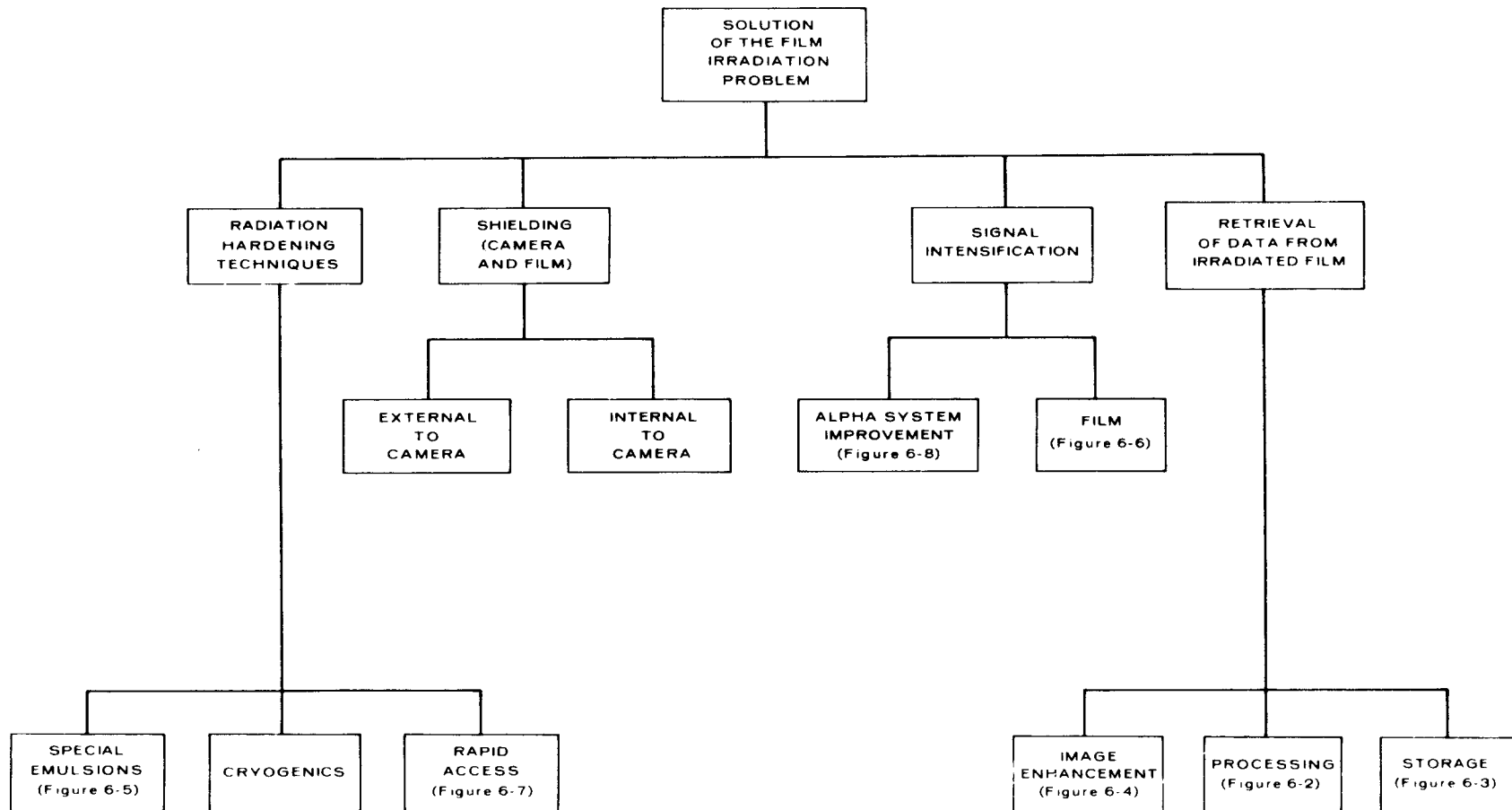


Figure 6-1. Possible solutions of the radiation-fogged film problem.

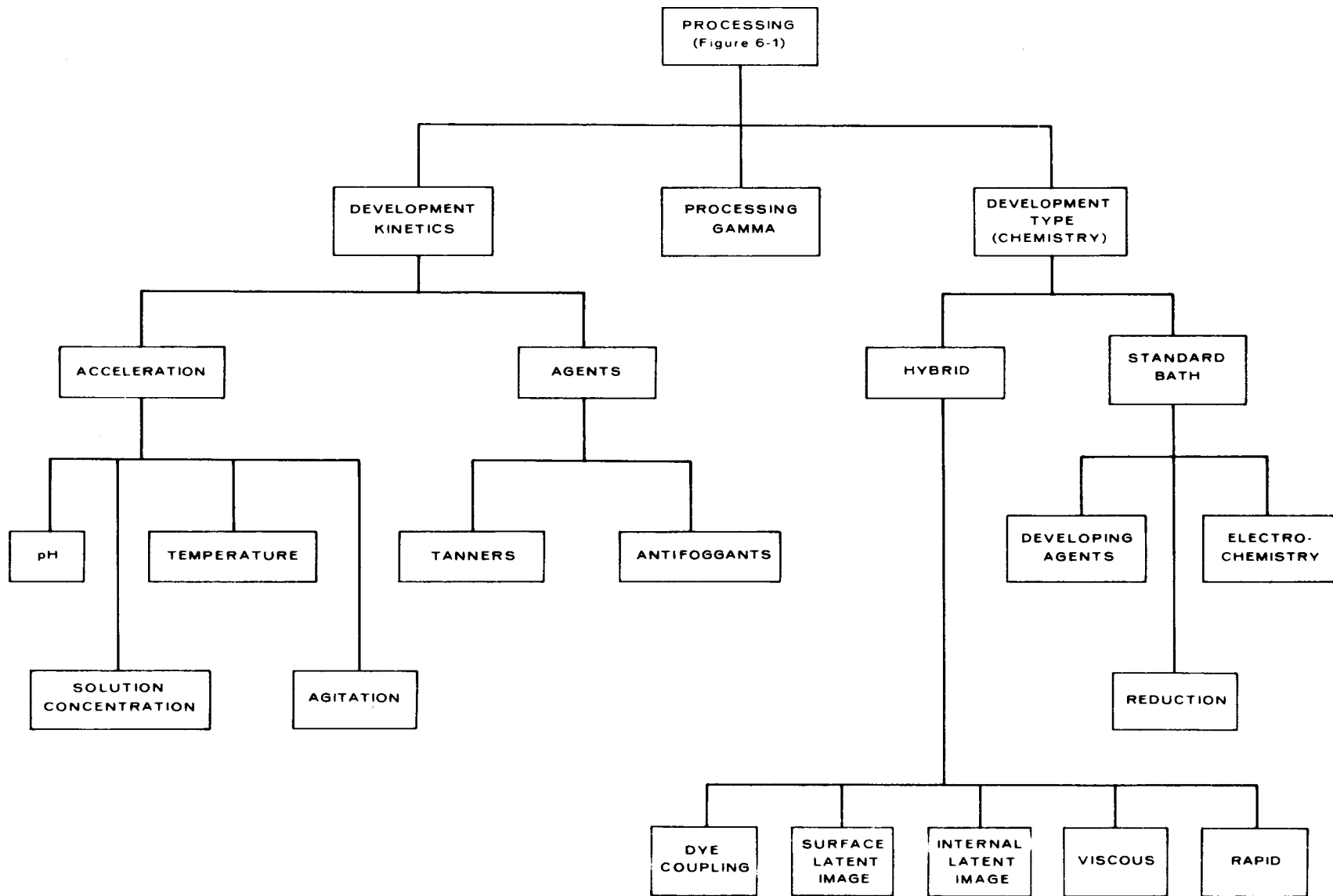


Figure 6-2. Data retrieval - film processing techniques.

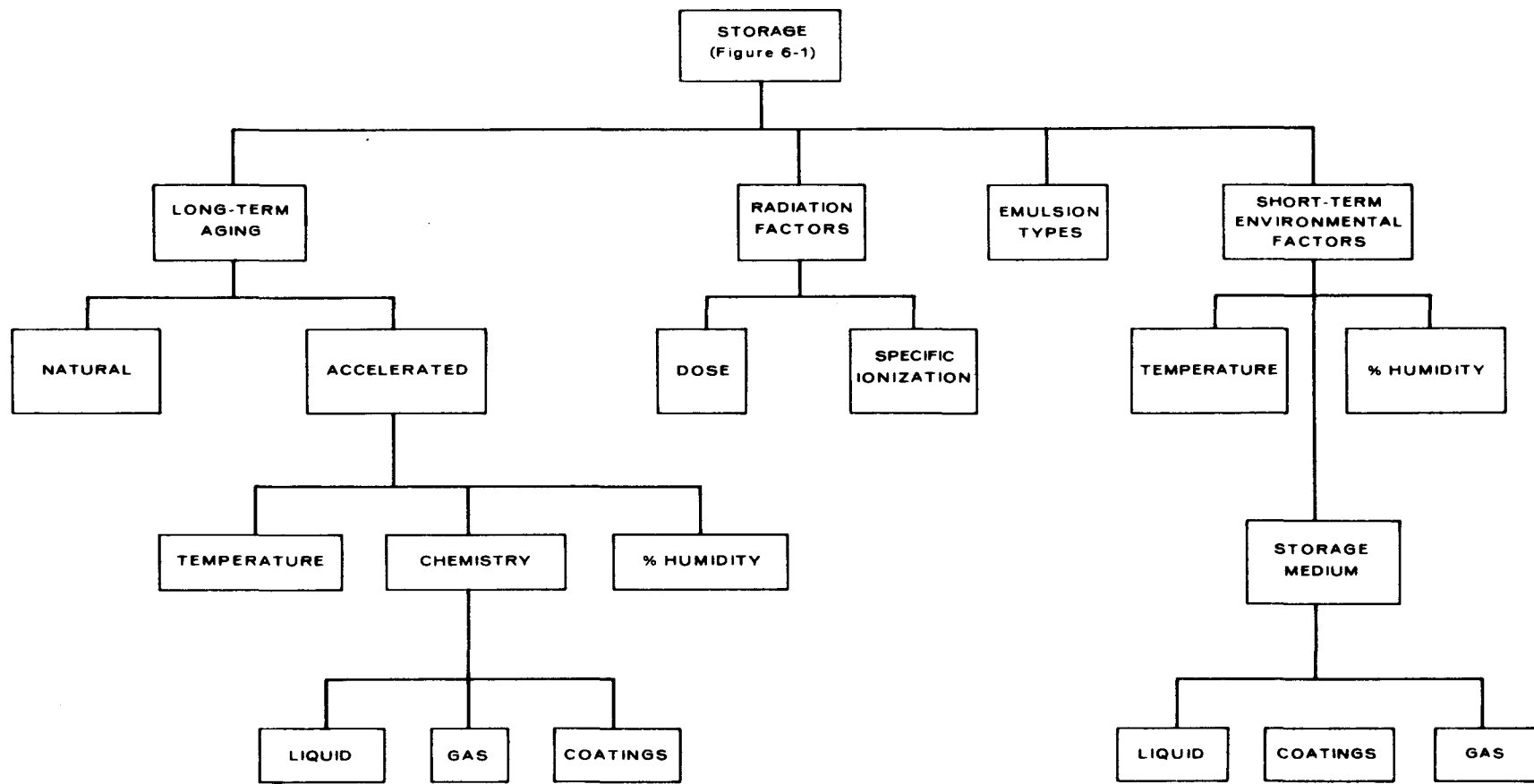


Figure 6-3. Data retrieval - film storage considerations.

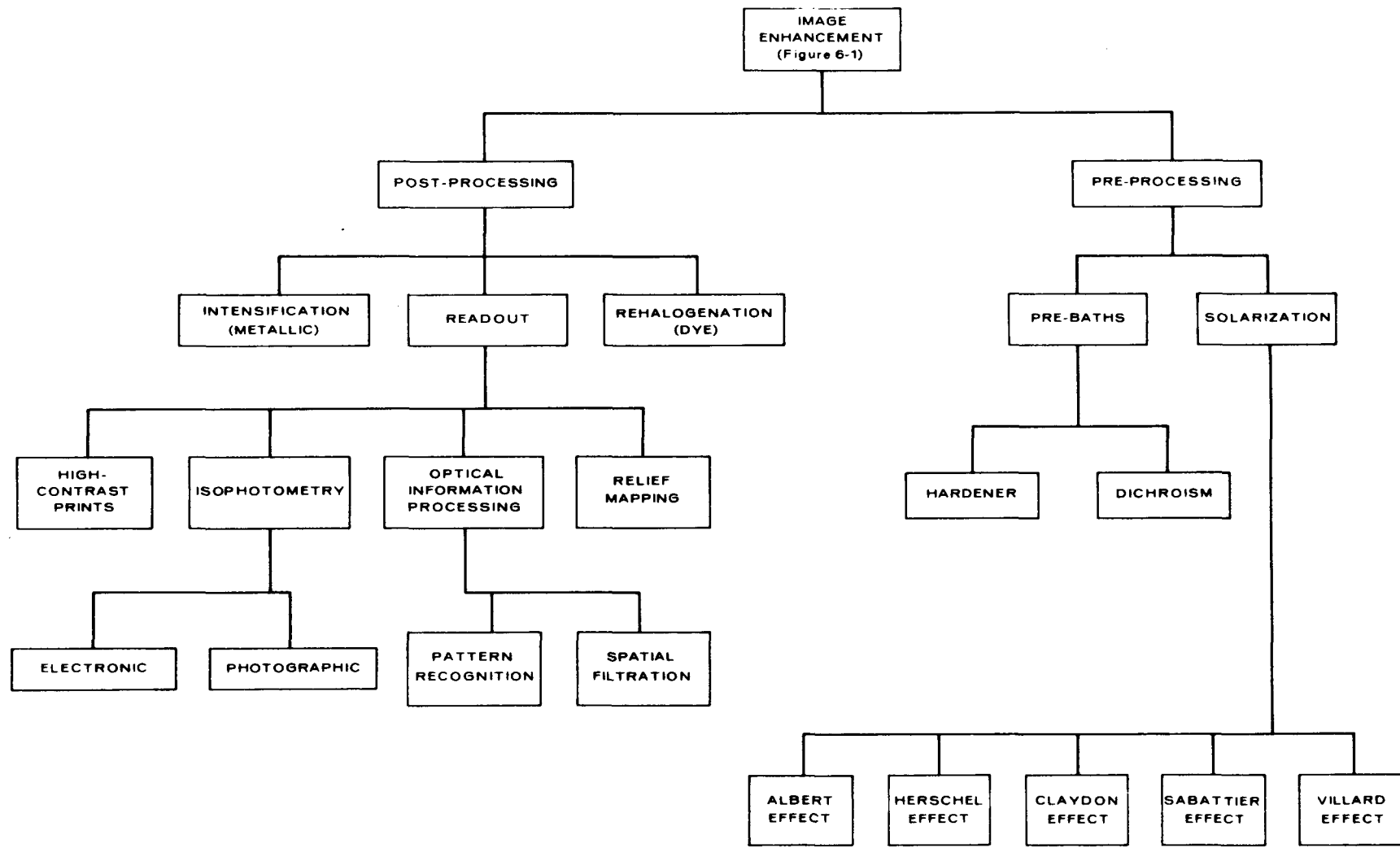


Figure 6-4. Data retrieval - image enhancement techniques.

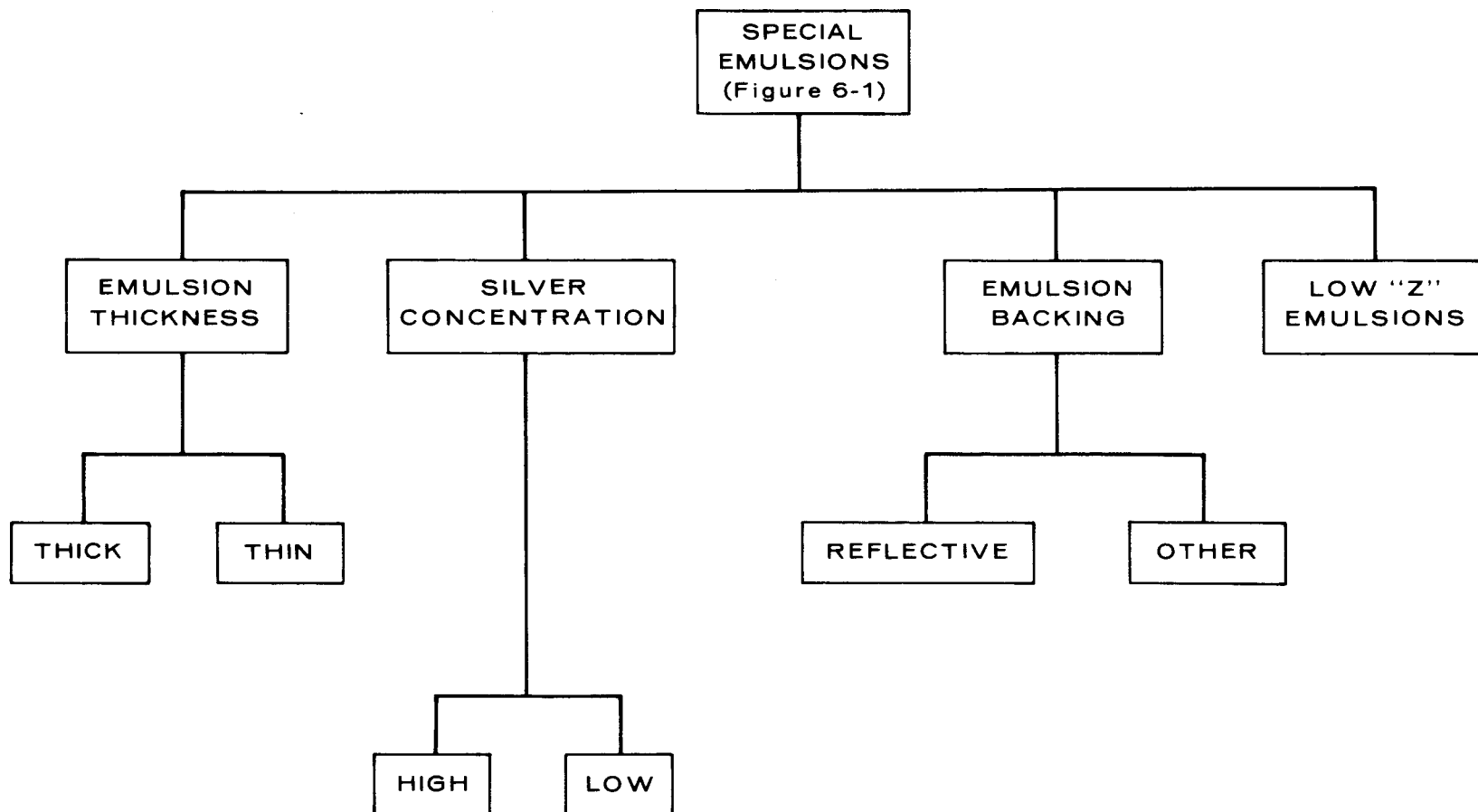


Figure 6-5. Radiation hardening techniques - special emulsions.

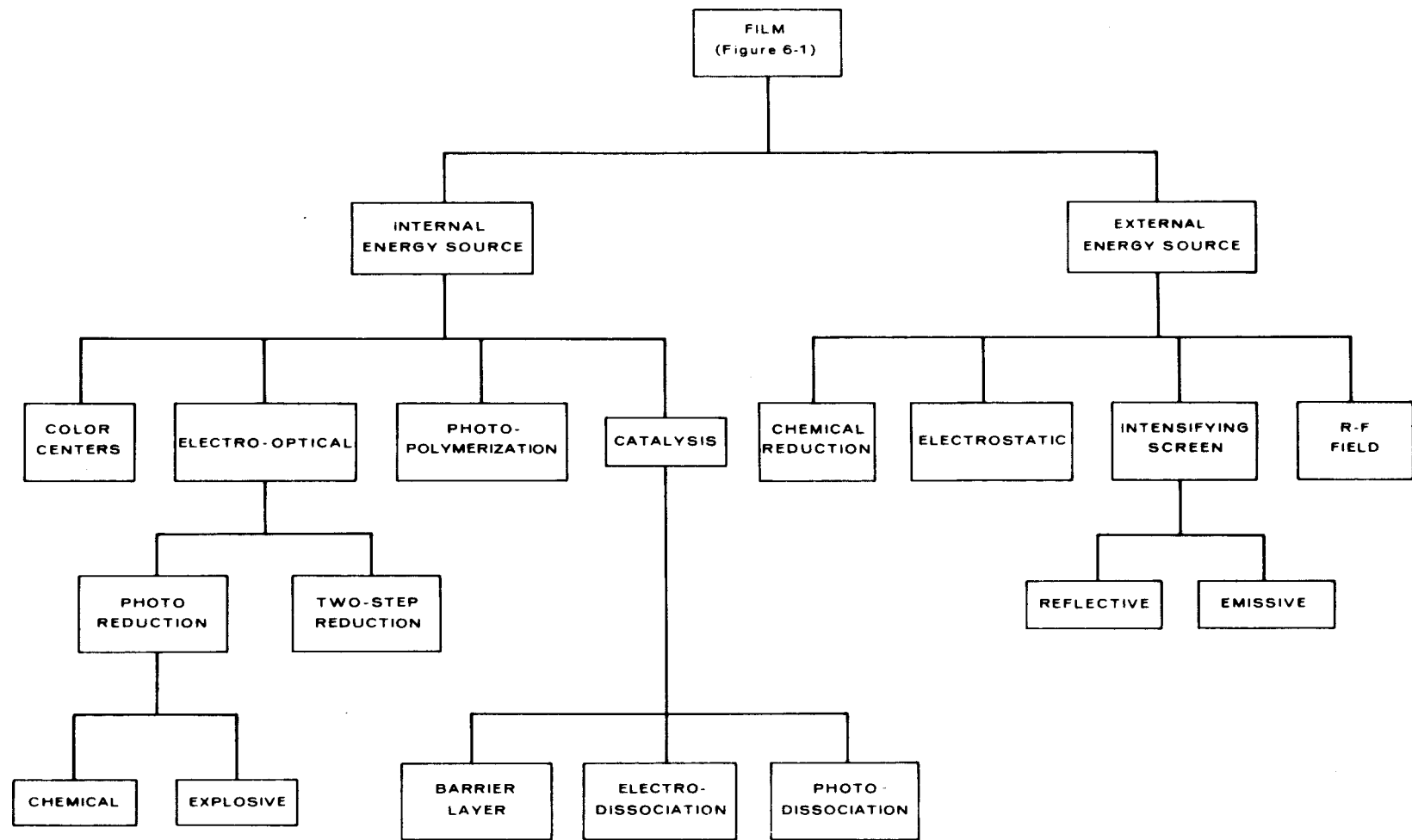


Figure 6-6. Signal intensification - film handling.

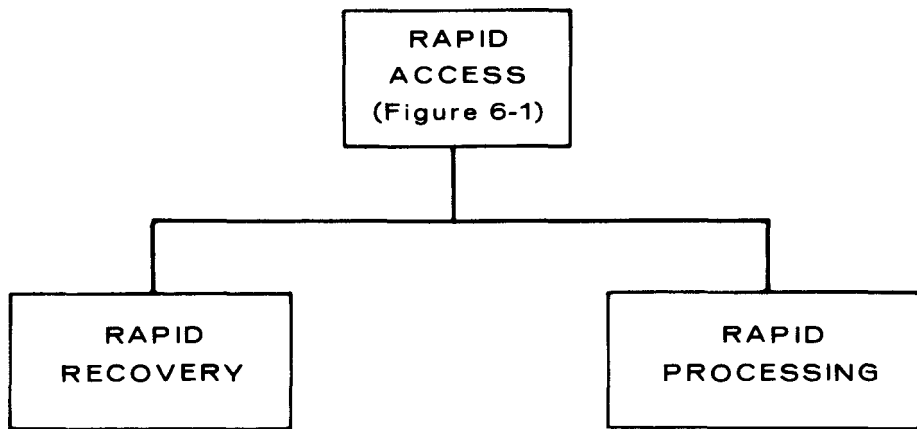


Figure 6-7. Radiation hardening techniques - rapid access.

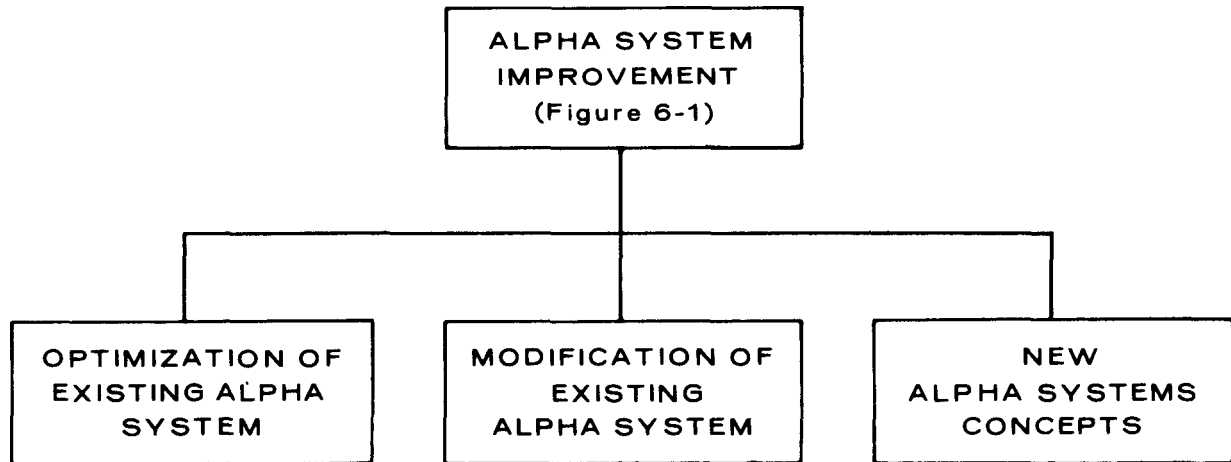


Figure 6-8. Signal intensification - alpha system improvement.

The ionizing spectrum of space radiation includes particles with mass and sometimes charge, as well as high-energy photons. Evidence discussed in Paragraphs 4.3 and 4.4 demonstrates that high-energy photons are the principal fogging radiations encountered in the current NTS testing program. Methods such as electrical or magnetic shielding are therefore not applicable for use at NTS.

Space radiations frequently fog film prior to the image-forming exposure. In NTS applications, the image-forming exposure occurs prior to radiation fogging. Consequently, such methods as in situ emulsion preparation and complete erasure of latent images after fogging are not applicable.

## 7. SOLUTION OF THE IRRADIATED FILM PROBLEM - TECHNIQUES AND EXPERIMENTAL FINDINGS

Conclusions drawn from the experiments described in many of the works referenced in this report may be criticized as inadequately founded or as reflecting subjective distortion. There is a lack of documentation and statistical method. For example, an estimate of variability, without which it is theoretically impossible to detect differences of magnitude, was seldom reported.

Current applications of information contained in this section are subject to unknown error because manufacturers constantly improve emulsions in subtle ways without informing the customer. Significant changes are sometimes flagged by the label "improved product" without change of the product's name. Consequently, findings based on the use of materials manufactured more than a few years ago may not be applicable to current products.

Manufacturers frequently designate sheet and roll films with identical names while coating their bases with different emulsions, and many of the emulsions used in the reviewed research are no longer manufactured. Manufacturer quality control is often based on monitoring those variables and limits known to affect the product's tolerable performance with normal use. Replication of the researcher's results for non-standard use may therefore be subject to unexpectedly wide product variability. Some of the films discussed are not applicable to present recording requirements, such as the high light speed necessary in fast-writing oscillography.

Paragraph 7.1 covers unconventional photography; silver halide photography is discussed in succeeding paragraphs.

### 7.1 UNCONVENTIONAL PROCESSES

Unconventional photographic processes are those not employing silver halide, such as xerography, photopolymerization, and free radical systems.

Hansen<sup>(60)</sup> has published a bibliography of articles (complete through 1969) on unconventional processes. Kosar<sup>(61)</sup> discusses many processes in some depth. In describing the liabilities of silver halide processes, Robillard<sup>(62)</sup> states that "...there are limitations which are difficult to overcome, such as the fogging of emulsions due to x-rays or nuclear radiations . . . ;" Robillard

then discusses a synthetic approach to the formulation of new photographic processes, with emphasis on systems in which sensitivity can be controlled by physical means (e.g., electric field, magnetic field, and heat). The systems discussed are variously based on catalysis, variation in dielectric constant of a phosphor under illumination, reduction of semiconductor oxides, and quenching of color centers. Examples of photographic results obtained with specific systems are given.

While the speed, resolution, and dynamic range of some unconventional systems are not as advanced as those of the best silver bromide emulsions, improved versions may be developed later. However, the unconventional systems are either relatively insensitive to radiation or their sensitivity can be turned off after exposure to light. Also, since the light speed of these systems is far too low for conventional oscillography, the systems appear unready for field use. Research is still active in these areas, but usually at a small dollar volume per specific system compared to that spent on conventional silver halide materials.

## 7.2 SILVER HALIDE EMULSION PREPARATION

The preparation of silver halide emulsions has been comprehensively discussed by several authors, including Herz<sup>(7)</sup> (Chapter 3), James and Higgins<sup>(63)</sup> (Chapter 2), and Berry and Loveland (Mees and James, Chapter 2).<sup>(23)</sup> Zelikman and Levi,<sup>(64)</sup> Croome and Clegg,<sup>(65)</sup> and Duffin<sup>(66)</sup> have also written on the subject.

Paragraphs 5.3 and 5.5 cite evidence indicating that in modern emulsions, most light-initiated latent images are located near the surface of the grain. Latent images initiated by harder photons (greater than 200 keV) are primarily surface in character as are those of light, while those of softer photons (less than 50 keV) produce relatively internal latent images. After-ripening and chemical sensitization, which principally affect surface sensitivity, are more effective in increasing light sensitivity than high-energy photo sensitivity.

Francis<sup>(67)</sup> and Plumadore<sup>(68)</sup> suggest that an emulsion combining Lippmann grains and high-speed large grains might be more resistant to radiation fogging, conjecturing that the Lippmann emulsion grains would act as traps to capture the secondary and recoil electrons. The difference in development rate of the two types of crystal would offer a means of separating the density contributed by the Lippmann grains. This approach would probably not be productive for two reasons: 1) Hoerlin's data<sup>(25)</sup> on range and energy loss

of electrons in pure silver bromide indicates that the amount of passive silver halide dispersed among active grains could be expected to affect the tail of the slow-down spectrum only (see Figures 5-2 and 5-3); and 2) Greening's formulas<sup>(43)</sup> indicate that the introduction of significant additional amounts of passive high atomic weight materials into the emulsion would cause more of the incident x-rays to be absorbed by the emulsion and converted into secondaries.

Plumadore<sup>(68)</sup> suggests that emulsion preparation techniques employed in Land's<sup>(69, 70)</sup> Solubilization by Incipient Development might be useful. Shaffer<sup>(46)</sup> reported that a photosolubilized lith type film processed conventionally exhibited greater losses in speed and slope for 1.25-MeV photons than for light, compared to untreated emulsions.

Greening<sup>(43)</sup> calculates that truly absorbed x-ray exposure could be reduced, and energy lost by grains to gelatin increased, by increasing both the amount of gelatin in an emulsion and the coating thickness at a constant amount of silver bromide per unit of area on the film base. In this case, light sensitivity would not be expected to change. Corney and Clear<sup>(44)</sup> discount the role of silver halide-to-gelatin ratio, but Chhabra's results<sup>(45)</sup> agree with Greening's calculations.

Tomoda<sup>(35)</sup> found that a silver salt solution pre-soak produced hypersensitization for light exposures and desensitization of approximately a factor of two for x-ray and gamma-ray exposures.

If it were known that a specific film was to be exposed to severe amounts of fogging radiation, the following manufacturing suggestions could be advanced:

1. Use chemical sensitizers in greater than normal amounts.
2. Extend after-ripening time.
3. Treat the emulsion in a silver salt pre-soak prior to exposure.
4. Use a photosolubilized emulsion.
5. Prepare the emulsion with about ten times the normal amount of gelatin, and coat the support with about five times the normal thickness of emulsion.
6. Place a light-reflective layer between the emulsion and the support.

These changes from normal emulsion-making would not be expected to adversely affect light sensitivity but should reduce x-ray sensitivity, probably by about ten times. However, there would be serious image quality trade-offs for the light exposure. Items 1, 2, and 3, which would be expected to substantially increase emulsion fog and affect the emulsion's stability, would probably require special low-humidity and low-temperature environmental precautions. Also, the emulsion would probably have to be exposed and developed within 48 or even 24 hours after hypersensitization (Item 3). Item 4 would probably reduce sensitivity to light, but Items 1, 2, and 3 might neutralize this effect. Items 5 and 6 would substantially degrade the modulation transfer and resolution of the system.

It is doubtful, then, that these modifications would be advisable in cases of less severe fogging, or when the likelihood of fogging is remote as in the current testing program at NTS.

### 7.3 ENVIRONMENTAL CONDITIONS

Paragraph 5.6 describes the role of environment during exposure and storage after exposure. Sensitivity and latent image fading are influenced by many emulsion-making environmental factors and their interactions. Hansen, McCue, and Wyckoff,<sup>(57)</sup> Adams,<sup>(58)</sup> and Anderson<sup>(59)</sup> suggest that x-ray sensitivity during fogging might be limited by a high-humidity or low-temperature environment, and that acceleration of latent image fading in a post-exposure environment might be beneficial. Paragraph 5.6 also explains that low-temperature storage, after light exposure but during fogging exposure, would have a significant effect. However, this approach seems no more feasible for field use than does in situ processing. Further, a post-exposure environment designed to accelerate latent image fading might not be beneficial. The literature indicates that fading increases with the size of the latent image,<sup>(52)</sup> that surface latent images fade more rapidly than internal latent images,<sup>(23f)</sup> (47) (53, 54) and that light latent images fade more rapidly than those of high-energy exposures.<sup>(23f)</sup> In spite of this evidence, latent image fading acceleration techniques may eventually prove useful. While there is widespread concern over fading in film badge dosimetry applications, this has not been the case with light radiometry applications.

Anderson<sup>(59)</sup> suggests that films stored in electric fields might exhibit less fogging. Films could be swept with alternating electric fields to reduce the probability of electrons combining with a silver ion to form a latent image silver atom. A second method would be to apply a constant electric field that would sweep silver ions and electrons to opposite ends of the crystal. The literature indicates that electric fields, applied concurrent to exposure, limit

sensitivity to relativistic particles but destroy previous light exposures. (71-73)  
It is therefore doubtful that this technique would be beneficial.

#### 7.4 SHIELDING

Shielding, even when limited to a few millimeters of lead, may significantly reduce fogging. The response of a photographic system on some part of the characteristic curve is proportional to the integral effect of dependent factors taken wavelength by wavelength. In spite of the large number of dependents, the problem can probably be reduced to about three factors. The relative net response on some part of the characteristic curve is approximately:

$$\gamma \cdot \int_{\lambda_1}^{\lambda_2} J_\lambda \cdot T_\lambda \cdot S_\lambda \cdot d\lambda$$

where

$\gamma$  is the slope of the  $D \log E$  characteristic over some part of the curve

$J_\lambda$  is the source energy distribution

$T_\lambda$  is the spectral transmittance distribution of filters and absorbing materials

$S_\lambda$  is the spectral sensitivity distribution of a specific emulsion stored and developed under specific conditions.

Minimization of  $T_\lambda$  for x-rays can be seen to be particularly important for those  $\lambda$  where  $J_\lambda$  and  $S_\lambda$  have high values. Paragraphs 4.3, 4.4, and 5.5 present evidence that  $J_\lambda$  and  $S_\lambda$  are greatest for wavelengths longer than 0.05 Å (240 or 120 keV). Shielding is particularly effective here, because this is not only where matter absorbs most completely but also where the energy spectrum and film sensitivity are greatest. On that part of the x-ray  $D \log E$  curve where the slope is greater than unity, a reduction in effective log exposure would result in a correspondingly larger reduction in background density.

Lockwood<sup>(74)</sup> has conducted preliminary tests of an armored film back with sensitometrically exposed Royal-X Pan film and DK-50 development. The results were not encouraging for 1.25-MeV fogging but noticeably improved for 101-keV fogging.

## 7.5 ERASING FOG'S LATENT IMAGE

Various methods of optical or chemical oxidation have been suggested for erasing background fog. These techniques are applied after exposure but before development.

Acceleration of latent image fading may erase background fog. However, there are indications that fading is more pronounced for surface latent images than for internal latent images; this would make the method unsuitable for erasure in the presence of light images (see Paragraph 5.6). <sup>(23)</sup> <sup>(53,54)</sup>

Hansen, McCue, and Wyckoff, <sup>(57)</sup> Adams, <sup>(58)</sup> Anderson, <sup>(59)</sup> Hoerlin, <sup>(75)</sup> and Goldstein and Sherman <sup>(76)</sup> indicate that the Herschel effect and other exposure effects might erase background fog. Most of the research has concentrated on the Herschel effect, which the Gurney-Mott theory of latent image formation can be used to explain. Metallic silver specks are optically oxidized by absorption of infrared photons and a subsequent injection of photoelectrons into the conduction band of the silver halide. The silver ion or hole left by the removal of the electron moves away, leaving the latent image smaller by one atom. The electrons then move through the conduction band until they fall back into normal positions, become trapped at impurity centers, or reduce sensitizing dyes. The rate of the reaction is normally so slow that low-intensity reciprocity failure minimizes the chance of those secondary traps becoming stable. The Herschel effect is the corresponding loss in developed density. A very intense bleaching or Herschel exposure will produce a forward or fogging effect, and bleaching decreases with increasing delay between the fogging and bleaching exposures. <sup>(77-80)</sup> Hoerlin, <sup>(75)</sup> Feigenbaum, <sup>(81)</sup> and Hansen, McCue, and Wyckoff <sup>(82a)</sup> reported failure to improve differentiation after Herschel exposures. Goldstein and Sherman <sup>(76)</sup> claim that erasing was more complete for light and alpha tracks. Kornfeld <sup>(29)</sup> states that latent images for light are three times more sensitive to Herschel erasure than those of x-rays. Hansen, McCue, and Wyckoff <sup>(82b)</sup> studied the literature on the Herschel, Clayden, Villard, and Albert effects and concluded that they would probably not be useful in solving the problem. In any case, most of the exposure effects have been achieved with primitive emulsions and are rarely experienced with modern emulsions. Even with primitive emulsions, these effects are reputedly difficult to achieve and control. In terms of present knowledge and photographic theory, these techniques would probably not contribute to recovery of irradiated film. Chapter 8 of Mees and James <sup>(23)</sup> gives a comprehensive account of exposure effects.

Certain oxidizing agents bleach latent images by oxidizing metallic silver. These chemicals include solutions of thorium nitrate ( $\text{Th}(\text{NO}_3)_4$ ), potassium permanganate ( $\text{KMnO}_4$ ), hydrogen peroxide ( $\text{H}_2\text{O}_2$ ), chromium

trioxide ( $\text{CrO}_3$ ), hydrochloric acid (HCl), sulfuric acid ( $\text{H}_2\text{SO}_4$ ), nitric acid ( $\text{HNO}_3$ ), formic acid ( $\text{HCOOH}$ ), acetic acid ( $\text{HC}_2\text{H}_3\text{O}_2$ ), mercuric chloride ( $\text{HgCl}_2$ ), and cupric sulfate ( $\text{CuSO}_4$ ).<sup>(36d)(83)</sup> Ackerman and Faissner<sup>(83)</sup> found that oxidizing treatments were more efficient in suppressing beta and gamma fog than alpha tracks. Yagoda<sup>(36d)</sup> reports that these treatments seem to have a smaller effect on protons than on other high-energy radiations or particles. Ackerman and Faissner<sup>(83)</sup> speculated that treatment with acid agents tended to suppress the smaller latent image centers more than large ones. If this is the case, these techniques might be useful in recovering irradiated light recordings. However, experience with internal developers indicates that oxidizing treatments destroy surface centers more vigorously than internal ones.

Francis<sup>(67)</sup> reported on bleaching experiments with the objective of selectively bleaching the latent image caused by radiation. One procedure consisted of 1) immersing 30 R fogged 4XN in a drop/L solution of 3-mercaptop-1, 2-propanediol, 2) immersing the film in DuPont 3B bleach and 3C clearing bath, and 3) processing in D-19. Background fog was eliminated at the expense of a 3.0 log E light speed loss. Hansen, McCue, and Wyckoff<sup>(82)</sup> reported on experiments utilizing bleaching solutions. Both mild hydrogen peroxide and strong, dichromate-sulfuric acid bleaching solutions demonstrated non-selective bleaching of light and high-energy radiation initiated latent images.

Feigenbaum<sup>(81)</sup> and Johnson<sup>(84)</sup> have reported improved recovery using Berry's "chemical solarization" method. This method attempts to control chemical solarization so that maximum solarization occurs at the same log E as the light exposure, thus pushing the trace density above background fog. The film is then developed in a developer that differentiates, to some degree, between a light and gamma exposure. Although results were not encouraging, it was reported as superior to all other methods investigated. No procedural details were given. Hansen, McCue, and Wyckoff<sup>(82c)</sup> reported difficulty in achieving the effect; their results were inconclusive. Their technique consisted of pre-bathing the film in a bath composed of five parts of a 5% sodium nitrite solution and one part of a 3% hydrogen peroxide solution. The film was continuously agitated in this solution for a given time, rinsed, and then still-developed for 30 minutes at 68° F. The soaking time and developer formulation were not specified. Films processed in this sequence normally exhibited several images. However, 40 R irradiated Royal-X Pan failed to demonstrate this effect. The technique was judged unsuccessful in recovering additional data from irradiated films. Johnson<sup>(85)</sup> indicates that the following two formulations were investigated:

1. Pre-bath: Soak film for 10 minutes at 68 - 70° F with agitation in a 5% solution of sodium nitrite ( $\text{NaNO}_2$ ).

Developer: 68 - 70° F for 50 minutes (no mention of agitation).

Hydroquinone	20 g
Sodium sulfite	20 g
Sodium carbonate	50 g
Sodium bisulfite 5% solution	300 ml
Formaldehyde	12.5 ml
Solution X (8g benzotriazole/	
300 ml H <sub>2</sub> O)	20 ml
H <sub>2</sub> O	1 L

2. Pre-bath: Soak film for 30 minutes at 68 - 70° F with no agitation in a 5% solution of hydrogen peroxide (H<sub>2</sub>O<sub>2</sub>).

Developer: 68 - 70° F for 50 minutes (no mention of agitation).

No other reference to Berry's chemical solarization was found in the literature, and the actual technique is difficult to define. For example, the choice of processing formula is unexpected: Johnson<sup>(85)</sup> refers to use of a negative type, moderate sulfite level formula rather than a reversal type formula. Solarized images developed in negative type developers exhibit reversal, therefore trace density would be expected to be below background if solarization occurred. The moderate solvent action of the developer would probably minimize the appearance of solarization and differentiation between fog and light image.

## 7.6 DEVELOPMENT CONDITIONS FAVORING RECOVERY

### 7.6.1 In Situ Processing

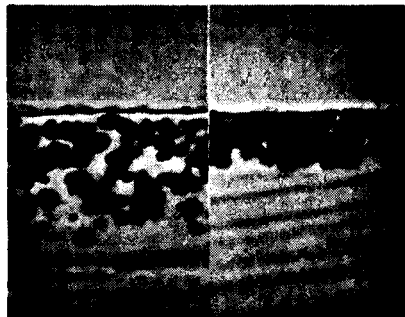
Immediate in situ monobath processing of light-exposed film prior to radiation fogging is an effective recovery method because processed films are insensitive to radiation. Smith<sup>(86)</sup> describes an in-camera processor for the Dynafax camera. Ebeltoft and Hatch<sup>(87)</sup> describe a device that on receipt of a signal from a remote control point automatically pulls exposed Type 40 Polaroid film through the processing cycle, waits the preset delay time and, advancing the roll one frame, separates the receiving sheet from the negative. The circuit is then reset, ready for another trigger pulse. The unit is designed to fit the back of an EG&G 850 or 850A oscilloscope camera. In theory, almost any black and white emulsion could be placed in the Polaroid packet proper; the film, if unfogged, could be processed conventionally. Meibaum and McKellar<sup>(88)</sup> designed and evaluated a rapid access processor that when attached to the back of an oscilloscope camera can be remotely

triggered to begin the processing of potentially irradiated film within 20 seconds after exposure. A spring-driven transport mechanism moves the film from the taking position to a processing position, where it is processed for 1.5 minutes at 120°F in Kodak MX-448-4 monobath. Sensitometric results with Kodak 2479 film compare favorably with the conventional processing of other high-speed materials used in NTS oscillography.

#### 7.6.2 Viscous Processing

Feigenbaum<sup>(81)</sup> and Hansen, McCue, and Wyckoff<sup>(89)</sup> speculated correctly that high-energy fogged crystals were equally distributed through the depth of the emulsion and that most light-fogged crystals were near the surface. The attenuation of light through an emulsion is significant; <sup>(23,1)</sup> attenuation of all but the softest x-rays is negligible. Their attempt to restrict processing to the emulsion's surface by using a high concentration developer with thickening agents failed to improve recovery. However, restricting development to the surface of an emulsion by viscous processing is feasible, as is illustrated in Figure 7-1. <sup>(90)</sup>

Left: D-96 Processing



Right: Kodak Viscomat  
Monobath Processing

Figure 7-1. Photomicrographs (2500 magnification) of microtomed cross-sections of Kodak 7222 films exposed to produce a density of 1.0.

#### 7.6.3 Reversal Processing - Intensification

Feigenbaum<sup>(81)</sup> found that little improvement resulted from attempts to reversally process irradiated film. Nepela and Nitka<sup>(91)</sup> report that using reversal materials and processing in conjunction with intensification could eliminate much of the effect of radiation fogging. A reduction in D<sub>max</sub> in the fogged and reversally processed films can be enhanced partly by intensification. Negative materials can probably be reversally developed to yield

a similar result. An optimum first developer was formulated, consisting of:

Calgon	2.0 g
Metol	2.4 g
Na <sub>2</sub> SO <sub>3</sub>	200.0 g
Hydroquinone	80.0 g
KBr	16.0 g
NaCNS	16.7 g
NaOH	80.0 g
H <sub>2</sub> O to make	4.0 L

A first developer in a reversal process often contains large amounts of silver halide solvents, which normally are necessary to maintain low fog levels in the processed film. In this case, their inclusion may have had a detrimental effect.

A developer with 50g/L sulfite, 4g/L bromide, and 4.2g/L thiocyanate would be expected to promote vigorous internal development. Differential development times and dilutions were recommended for various films, including:

<u>Negative Type</u>	<u>Developer</u>	<u>Recommended Development Time (minutes) at 68° F, with Continuous Agitation</u>
Ansco Supreme	Stock	9
Ansco Triple S Pan	Stock, Diluted 1:1	8
Ansco Isopan	Stock	8
Ansco All-Weather Pan	Stock, Diluted 3:1	6
E. K. Verichrome	Stock, Diluted 1:1	4
E. K. Plus X	Stock, Diluted 1:1	2
E. K. Panatomic X	Stock, Diluted 1:1	2
E. K. Royal Pan	Stock, Diluted 1:1	6

Chemical intensification recovery is limited because the desired characteristic curve cannot be restored by any known intensification technique. Intensification is usually proportional; fogging is subproportional in negative processed materials and superproportional in reversely processed materials.

#### 7.6.4 Developer Characteristics

Developer characteristics affecting recovery include developer activity, time and temperature factors, dilution, and type of developing agent.

Spear<sup>(92)</sup> reports that development time, temperature, and age of developer produced no difference in gamma fog density when developer activity was normalized to the control values. Feigenbaum<sup>(93)</sup> speculated that complete development would be desirable for radiated film because it would recover some of the contrast lost by fogging. Hoerlin<sup>(75)</sup> assumed that development activity was significant because of the shorter induction time for light exposures than high-energy exposures.

Experiments were conducted with developers over a range of developer activity. The results indicated that incomplete development by shortened development times or dilution may increase differentiation for gamma ray levels of up to 20 R on Kodak Tri-X-AR. The use of developers with "weak developing agents" was reported to increase differentiation, and an unspecified glycine developer was reported to give fair results.<sup>(75)</sup>

#### 7.6.5 Surface Latent Image Development

Although the terms "surface" and "internal" latent image suggest the physical location of development centers in a silver halide grain, the practical application of the concept lies in determining the response of the emulsion to a surface developer or internal developer rather than in determining the location of the latent image.

Internal development is more efficient in developers containing silver halide solvents or alkali halides. Solvents dissolving silver halide expose otherwise inaccessible internal latent images to developing action. Typical silver halide solvents include the thiosulfates, thiocyanates, cyanides, sulfites, alkali halides, certain amines, organic and inorganic ammonias, and water. Alkali halides such as potassium iodide promote internal development by replacing bromide in the crystal with iodide, thereby cracking the grain or promoting recrystallization.

## NOTE

When comparing in text the solvent action of various developers, it is productive in the case of silver halide solvents to compare ionic strengths rather than relative concentrations. Solvent action is also a function of processing time and temperature, and may be influenced by development accelerators or antifoggants. For empirical comparisons of solvent action, rates of solution should be determined. James and Vanselow<sup>(94)</sup> have studied these factors.

It should be possible, through experimentation, to design a developer promoting a high surface-to-internal speed ratio. If high-energy photons initiate latent images more internal than those of light, use of such a developer might be a successful approach to the irradiated film problem.

Evidence cited in Paragraph 5.3 indicates that latent image distribution is internal for soft x-rays and surface for light. As x-ray wavelength decreases, the distribution becomes more nearly surface in character. Hansen, McCue, and Wyckoff<sup>(82)</sup> found that the latent images of 1.25-MeV gamma rays were surface in character but not to the extent of those for light, explaining this phenomenon as the basis for lack of significant improvement in processing irradiated films using surface latent image developers.

Greater success might have been obtained with film fogged by longer wavelength gammas. Hoerlin<sup>(75)</sup> reported, without elaboration, that an absence of silver halide solvents increased differentiation. Feigenbaum<sup>(81)</sup> claimed that surface latent image developers produced intolerable losses in contrast and film speed. Nam<sup>(37)</sup> reported successfully rescuing Kodak 3404 irradiated to 320 R at 0.66 MeV; however, the irradiated samples exhibited a surface-to-internal speed ratio increase at least four times higher than unirradiated films. Nam explained that the effect was "...similar to hypersensitization by a pre-fogging technique," but his claim to successful recovery is questionable since the control developer D-19 produced higher speed with both irradiated and unirradiated samples of Kodak 3404. Although Nam did not so state, it may be assumed that the stepped light exposure followed radiation fogging, as was the case for his camera picture tests. The sensitometric responses for the non-irradiated and irradiated samples for both surface and D-19 development are shown in Figure 7-2.

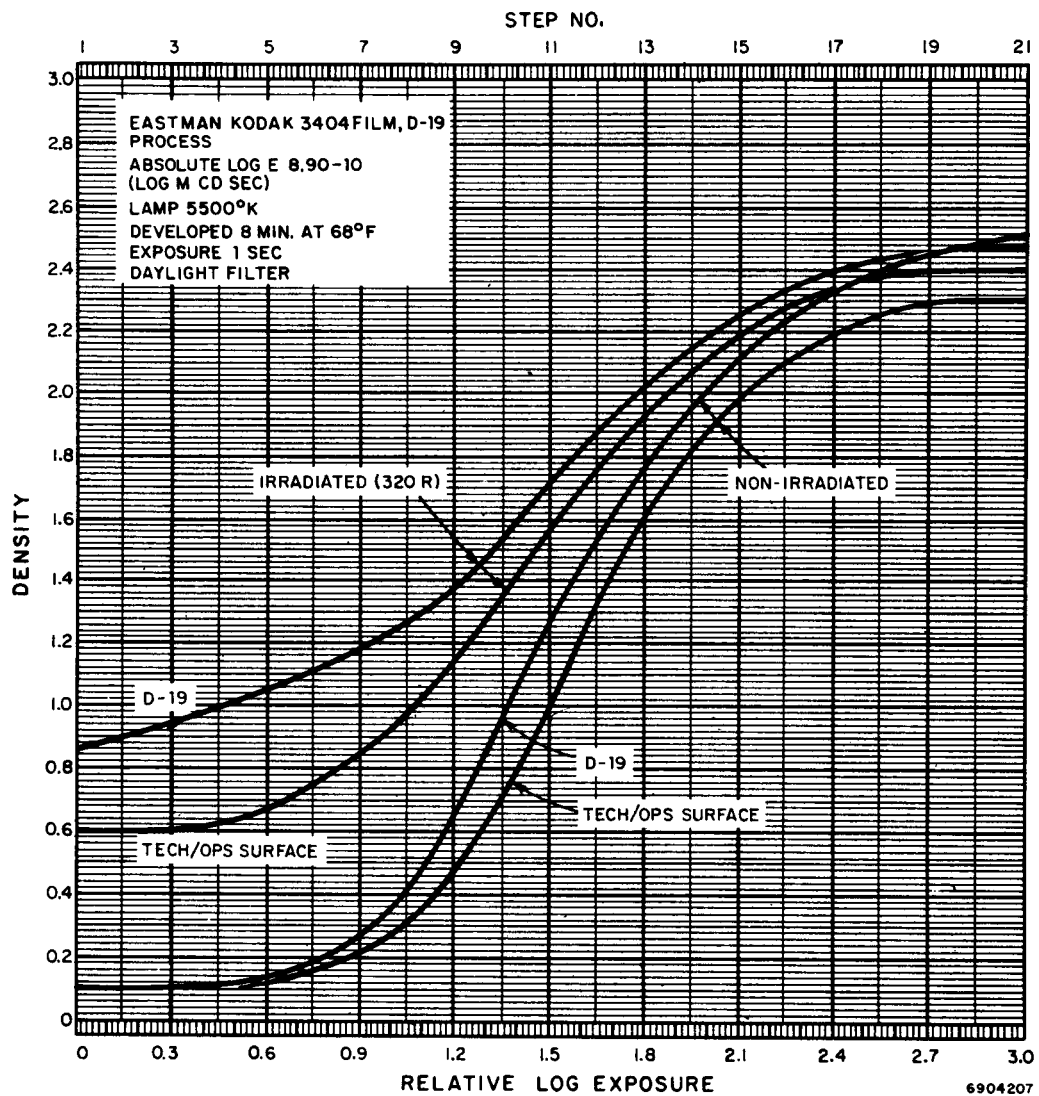


Figure 7-2. Eastman Kodak 3404, D-19 process. (37)

Nam's picture tests comparing the recovery of irradiated film processed in D-19 and Tech/Ops surface developer are inconclusive, because the comparison is of prints made under identical printing conditions rather than under optimum conditions for each negative. The Tech/Ops surface developer formula is shown below.

Metol	1.4 g
Ascorbic acid	3.3 g
KBr	1.0 g
Sodium metaborate	5.0 g
H <sub>2</sub> O to make	1.0 L

Adjust pH to 10.0 with NaOH

Development time 20 min.

Development temperature 20° C

Although the evidence is not conclusive, surface latent image development appears to be one of the more promising approaches to the irradiated film problem.

#### 7.6.6 Antifoggants

Hansen, McCue, and Wyckoff,<sup>(82)</sup> investigating the effect of adding benzotriazole to D-19 for Royal-X Pan fogged by 40 R, concluded that the sole benefit was a reduction in background density and that the additive suppressed both light and radiation sensitivity. Investigations of antifoggant additives by Shaffer<sup>(95)</sup> and Dutton<sup>(96)</sup> indicate that above some threshold, light film speed is a function of the concentration of antifoggant in the developer.

Hoerlin<sup>(75)</sup> assumed that organic development retarders might be more readily adsorbed on small silver nuclei than on larger ones, thus restraining the development of the smaller, presumably gamma-initiated latent images more than the larger ones. Benzotriazole, nitrobenzimidazole, and 1-phenyl-5-mercaptotetrazole (PMT) were used; the best results were obtained with benzotriazole.

Two formulas utilizing this technique were reported:

#### D-19X

D-19	1600 ml
Solution X	400 ml
5% Sodium bisulfite solution	200 ml

Solution X

Benzotriazole	8 g
Methanol	50 ml
H <sub>2</sub> O	350 ml

(Hoerlin's formula for solution X differs from that given by Johnson. <sup>(85)</sup>)  
Develop for 24 - 40 minutes at 68° F with intermittent agitation.

P-aminophenol Modification

P-aminophenol	7.5 g
Sodium sulfite	20 g
Sodium carbonate	50 g
Solution X	150 ml
H <sub>2</sub> O	1 L

Develop for 30 - 60 minutes at 68° F with intermittent agitation.

For 100 R fogged Tri-X-AR film, ten steps were claimed for D-19X compared to none for conventional processing and sixteen steps for unirradiated film. Feigenbaum <sup>(81)</sup> reports that the D-19X technique gave some good results when applied to recovery of event-related film. At 100 R., where formerly no recovery was possible, the technique proved effective with Royal-Pan and gave good results with Double-X and Plus-X at radiation levels in excess of 200 R. Feigenbaum did not provide any quantitative data or curve comparisons.

Wilson <sup>(97)</sup> found that a two-solution or split development technique called DM-12-G offered superior recovery of event-related Royal-X Pan and 2479 film. A 55° F solution temperature was used and development time was 17 minutes in solution A with agitation for the first minute only, followed by 2 minutes in solution B with agitation for the first 5 seconds only.

Formula for DM-12-G:

Solution A

Water	1 L
Hydroquinone	185 grains
Phenidone A	12 grains
Sodium sulfite, anhydrous	1 oz + 263 grains
Sodium carbonate, anhydrous	2 oz + 50 grains
Potassium bromide	31 grains
Benzotriazole	3 grains

Dilute with water stock solution A 1:7 before use; do not dilute stock solution B.

### Solution B

Water	1 L
Sodium hydroxide	50 grains

Base plus fog levels of approximately 0.9 were obtained compared to 1.6 to 1.8 for control fogged films.

Wyckoff<sup>(98)</sup> and Plumadore<sup>(99)</sup> speculate that developers saturated with antifoggants might be beneficial. Wyckoff's<sup>(98)</sup> latest irradiation recovery recommendation is to prepare a high Phenidone concentration developer by dissolving as much Phenidone B as possible in water, raising pH to 11 - 12, and using 1-ascorbic acid as an anti-oxidant with saturated amounts of 6-nitrobenzimidazole nitrate acting as an antifoggant.

The presence of organic antifoggants or restrainers in developers increases the activation energy necessary for development. The effectiveness of an antifoggant has been reported to be due to its: 1) affinity for  $\text{Ag}^+$  and the increasing of the pAg of the emulsion; 2) adsorption to the silver halide crystal, thereby forming salts of significantly lower solubility; and 3) forming of irreducible complexes around latent image centers.<sup>(23k)</sup> In the light of Land's recent work with solubilization by incipient development (SID),<sup>(70)</sup> the third characteristic is doubtful. Land's alternate hypothesis is that development is essentially a physical process requiring silver ions in solution, the concentration of which is lowered by PMT.

#### 7.6.7 Dye-Coupled Development and Rehalogenation

Experiments have been conducted with the objective of forming different dye and/or silver images for irradiated and light latent images.<sup>(67)(81)</sup> Placing two couplers of different coupling rate characteristics in a developer resulted in the appearance of one color in high silver areas and the other color in the low silver areas.<sup>(67)</sup> Another approach consisted of 1) processing in a high-contrast, slow-speed black and white developer, 2) processing the remaining image in a color forming developer, and 3) bleaching out the silver images. This method seemed most promising but required increased suppression of dye fog to attain image separation.<sup>(67)</sup>

Plumadore<sup>(99)</sup> suggests that dye rehalogenation development might increase control over the slope of irradiated film. Feigenbaum<sup>(81)</sup> found no evidence for improved recovery with this technique, however.

#### 7.6.8 Low-Contrast Development

Wyckoff<sup>(98)</sup> reports some success in recovering images with the low-contrast developer PDK-50, which is prepared by adding Phenidone B to standard DK-50. The amount of Phenidone B to be added is uncertain, however, since both 2.5 gm/L and 0.75 gm/L additions are designated PDK-50. <sup>(100, 101)</sup>

Miller<sup>(102)</sup> has compared the low-contrast developer Tech/Ops XR-514 with Kodak DK-60A for recovering images subjected to a mixture of 1.25-MeV and 0 to 1.25-MeV broad-spectrum x- and gamma rays with exposures of 10 to 800 R. Films investigated were Royal-X Pan recording sheet, 2475 recording sheet, Tri-X Ortho sheet, Tri-X Pan sheet, and Panatomic-X sheet. The XR-514 developer yielded a significant improvement over DK-60A, particularly at higher exposure levels using Royal-X Pan. A 50-R fogging exposure resulted in a 25X decrease in white light speed for XR-514-developed Royal-X Pan and a 90X decrease for RXP developed in DK-60A. However, the DK-60A was found to be superior to XR-514 at low radiation levels. The break-even point seemed approximately proportional to the inherent gamma ray sensitivity of a given film, 10 R for Royal-X Pan and 50 R for Panatomic-X. Significant reductions in background density were obtained with all films and all radiation levels with the XR-514 developer. It may be significant that Tri-X Pan had a higher white light speed than Royal-X Pan for a 10-R post-fogging exposure. Representative results are shown in Figures 7-3 and 7-4. <sup>(102)</sup>

Miller's graphs seem to use different speed point criteria for different curves, and light source quality and duration are not specified. Where actual scope traces are given, there is some uncertainty about the f-number used, in that f-number and numerical aperture do not measure the same characteristic at finite object distances. The formula for the XR-514 developer is not specified; however, the approximate composition of the XR-5 series developers is: <sup>(103)</sup>

$K_2SO_3$	25 g
Metol	1/2-1 g
Hydroquinone	1/2-1 g
$K_2CO_3$ (optional) up to	10 g
$H_2O$ to make	1 L

Miller's approach appears to be an attempt to discriminate between surface and internal latent images by development rate (versus complete development); however, solvent action is only moderate.

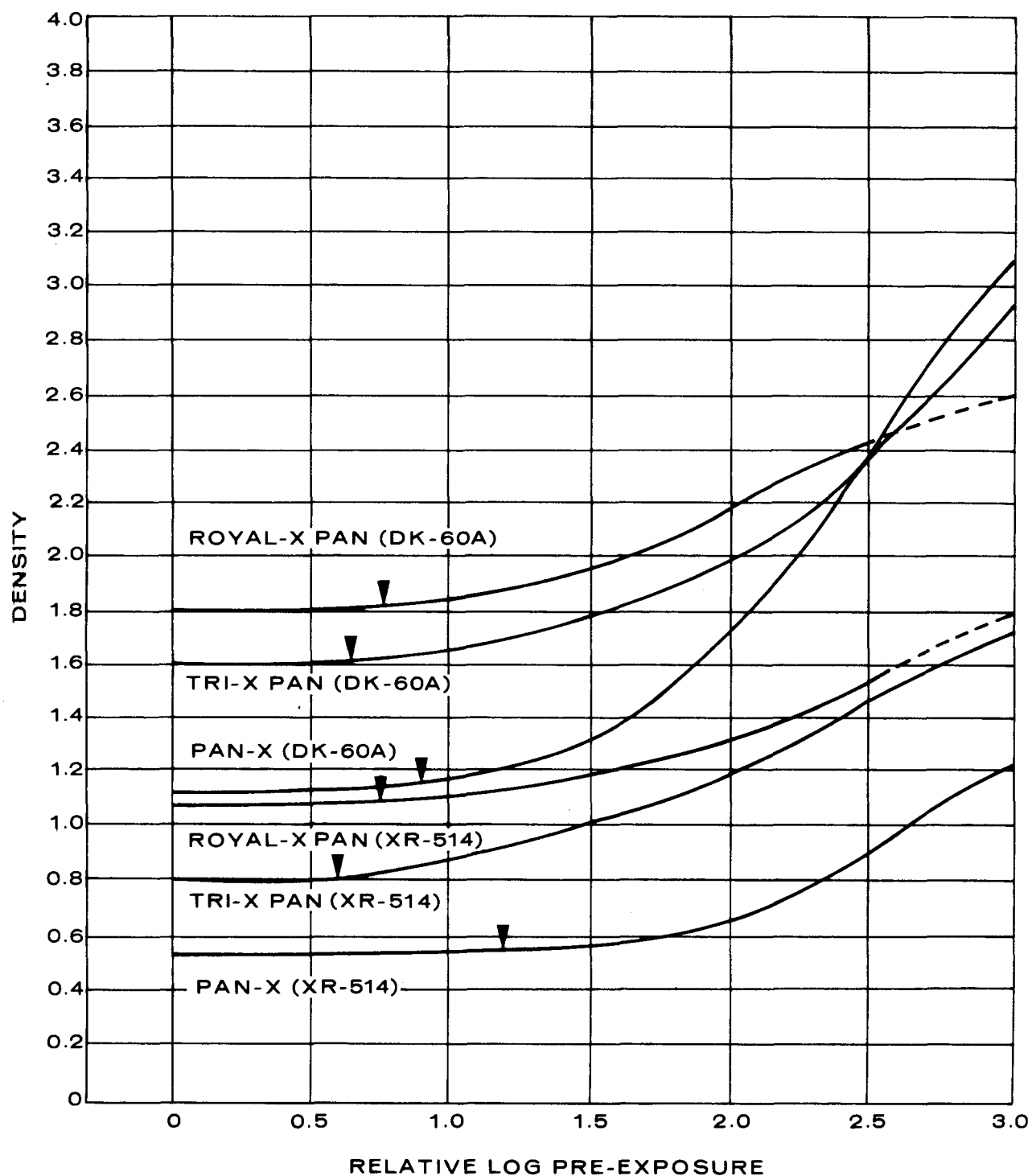


Figure 7-3. Comparison of absolute speeds at 10 R of three films processed in DK-60A and extended range developers.<sup>(102)</sup>

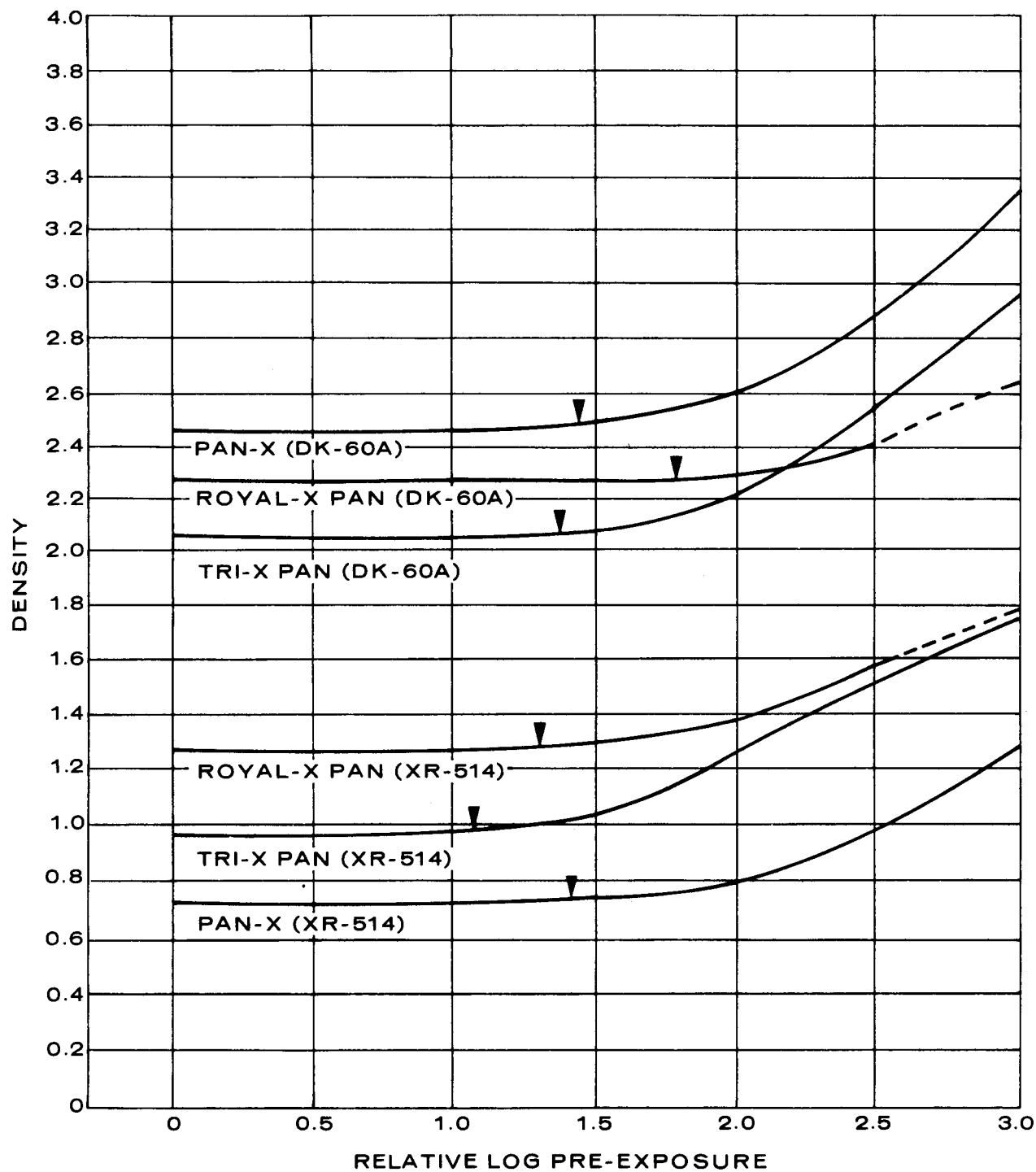


Figure 7-4. Comparison of absolute speeds at 50 R of three films processed in DK-60A and extended range developers. ( $10^2$ )

## 8. PHOTOGRAPHIC IMAGE ENHANCEMENT

Available methods of enhancing existing film images make use of techniques that either increase signal modulation or decrease noise modulation; i. e., they increase the image signal-to-noise ratio (SNR). Because noise is the limiting factor in any image-enhancement or discrimination judgment, a substantial difference in the signal and noise frequency spectra promotes improvement of the image if a filtering technique is used.

Even though noise limits enhancement, a filter can only improve the SNR, not add valid information. A film's information capacity (packing density) is a function of density, range, and granularity, and consequently is severely sacrificed at high radiation fogging levels due to saturation and the statistical properties involved in exposing a finite number of grains and inherent in granularity. Still, it may be possible under less than saturation conditions to obtain improvements with filtering. These procedures may be implemented either by digital computer techniques or analog optical techniques.

### 8.1 HIGH-CONTRAST PRINTING

One problem in interpreting radiation-fogged records is that the fogging exposure acts as a d-c bias, distorting image intensity. Complete speed and contrast recovery are theoretically possible for images printed on appropriate materials, and a desired or corrective characteristic curve for a printing material can be charted through tone reproduction calculations.

Nepela and Nitka,<sup>(81)</sup> experimenting with such a gamma correction scheme, improved radiation-fogged film. High-contrast printing, sometimes used at NTS to enhance fogged oscilloscopes, frequently has resulted in noticeable improvement. However, the enhancement of contrast through high-contrast printing has limited usefulness, because without some type of spatial filtering the image signal-to-noise ratio remains constant.

Figure 8-1 illustrates calculations dealing with one possible tone reproduction problem. The gamma correction curve in the upper left quadrant was calculated based on the radiated response in the lower right quadrant. The resultant tone reproduction response (linear) is shown in the upper right quadrant.

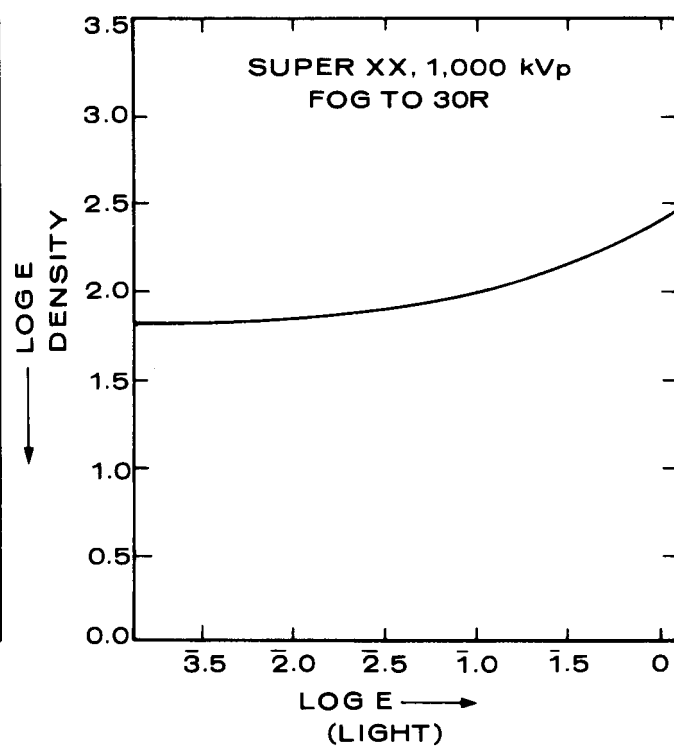
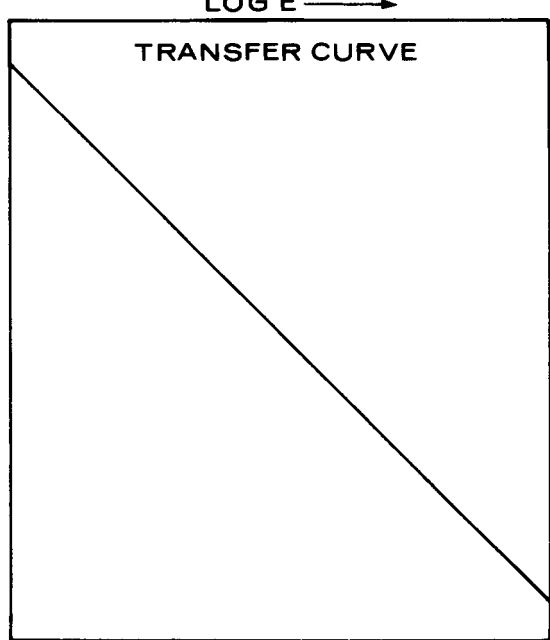
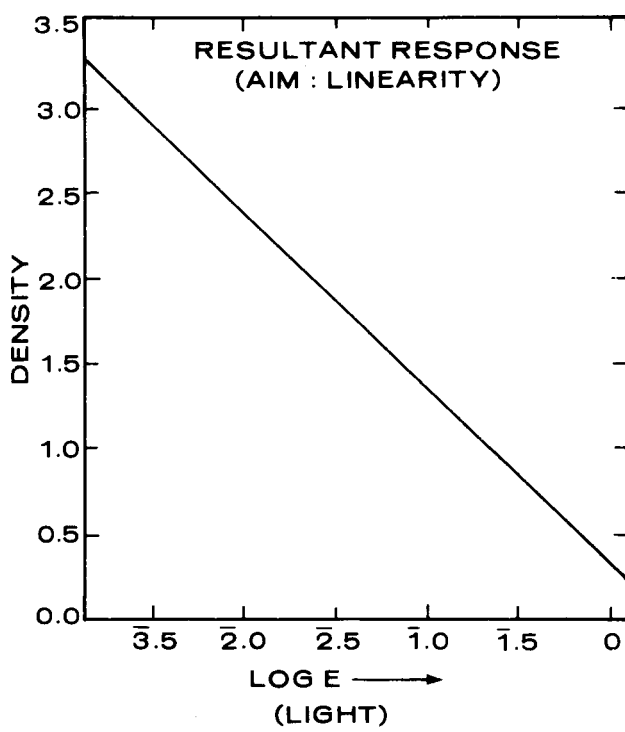
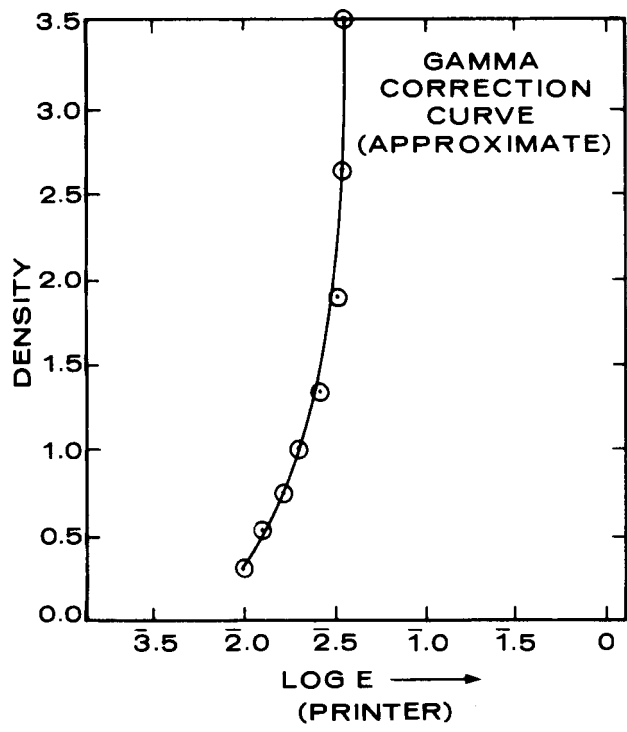


Figure 8-1. Calculating a gamma correction curve.

## NOTE

Figure 2-3 illustrated that the slope of the light  $D \log E$  curve in the toe region reduces sharply as fogging exposure increases. As the slope approaches zero, the necessary corrective slope approaches infinity. This limitation applies to all enhancement techniques.

### 8.2 AN OPTICAL APPROACH

An optical spatial filter is a two-dimensional space equivalent to an electronic filter. In a coherent optical system (see Figure 8-2), a Fourier transform relationship exists between the amplitude and phase of the wave-fronts located in planes  $P_1$  and  $P_2$  and  $P_2$  and  $P_3$ .<sup>(104a)</sup>

As shown in Figure 8-2, the essential components of one possible arrangement of optical spatial filtering are: a quasi-monochromatic point source; a collimating lens ( $L_1$ ); a pattern inserted in the object plane ( $P_1$ ) one focal length in front of transform lens ( $L_2$ ); the transform or filter plane ( $P_2$ ) lying one focal length behind  $L_2$  and one focal length in front of the inverse transform lens ( $L_3$ ); and the image plane ( $P_3$ ). The reconstructed filtered image lies one focal length behind  $L_3$ . A photograph of this spatial filtering system is shown in Figure 8-3.<sup>(104b)</sup>

If a photograph  $s(x, y)$  is inserted in Plane  $P_1$ , the amplitude and phase of the light in plane  $P_2$  will be proportional to  $S(\omega_x, \omega_y)$  or the transform of  $s(x, y)$ . The input signal is a two-dimensional wavefront the diffraction pattern of which (as imaged by the lens) is its two-dimensional transform less some degradation by the spread function of the lens. The coordinates in the transform plane are related to  $\omega$  by the formula  $x = \lambda f \omega / 2\pi$ , where  $\lambda$  is the wavelength of the light and  $f$  is the focal length of  $L_2$ . This transform is multiplied by the amplitude transmittance of the filter located in plane  $P_2$ . The output, located in plane  $P_3$ , is the convolution of  $s(x, y)$  and the inverse transform of the filter.

By inserting appropriate filter functions in filter plane  $P_2$ , it is possible to construct optical filters to pass or attenuate any desired specific spatial frequencies or band of frequencies, including dc. Filtering with respect to orientation is also possible. Figure 8-4 shows four of the many possible configurations.<sup>(105)</sup>

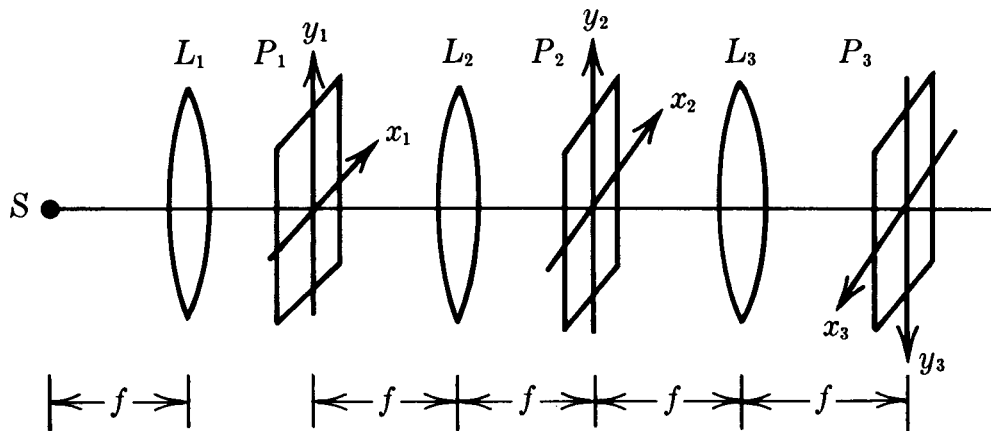
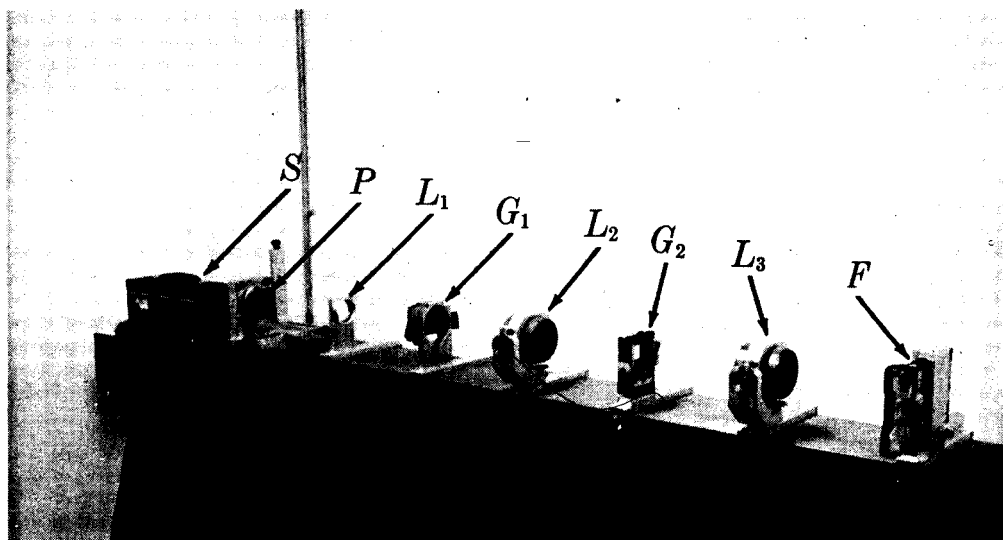


Figure 8-2. An optical spatial filter. (104a)



S LASER SOURCE

L<sub>2</sub> TRANSFORMING LENS

P PINHOLE FILTER

G<sub>2</sub> LIQUID GATE (FREQUENCY PLANE)

L<sub>1</sub> COLLIMATING LENS

L<sub>3</sub> TRANSFORMING LENS

G<sub>1</sub> LIQUID GATE (INPUT PLANE)

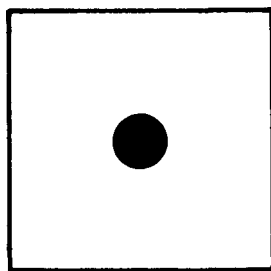
F FILM HOLDER (OUTPUT PLANE)

Figure 8-3. A coherent processing system. (104 b)

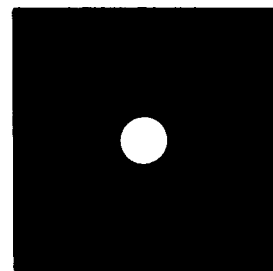
If as in Figure 8-4 total attenuation or transmission is not desired, a filter with the desired amplitude transmission is included; e.g., for a 50% transfer characteristic, a filter density of about 0.15 -- or for a 6% transfer characteristic, a filter density of about 0.60.

Traditionally, spatial filtering involves edge enhancement via high-pass filtering, which increases high-frequency modulation only relative to the lower frequencies. To achieve an absolute increase in modulation for a frequency band, a film with an intensity response or gamma greater than unity must be used in image plane  $P_3$ . In this case, the contrast transfer function of the optical spatial filter is the transfer function of the system; i.e., the filter inserted multiplied by the filter function multiplied by the film gamma.

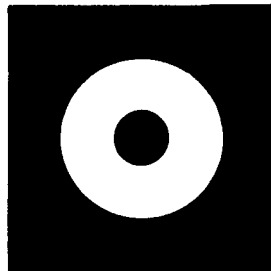
Goodman and Shulman discuss spatial filtering and optical data processing in depth. <sup>(104)</sup> <sup>(105)</sup>



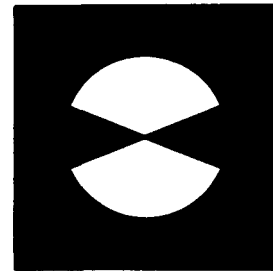
HIGH PASS FILTER



LOW PASS FILTER



BAND PASS FILTER



LOW PASS - DIRECTIONAL FILTER

Figure 8-4. Typical spatial filter functions. <sup>(105)</sup>

### 8.3 A COMPUTER APPROACH

The essential components of a digital approach to photographic image enhancement are shown in Figure 8-5.

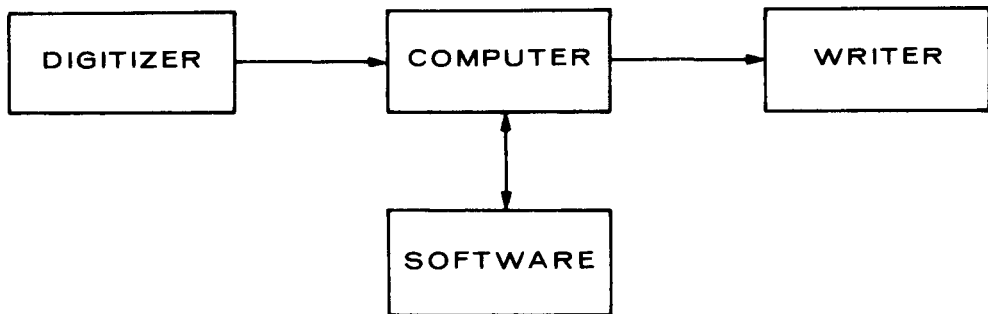


Figure 8-5. Essential components of a digital enhancement system.

A device such as a scanner or microdensitometer samples and digitizes the density values over an array of points to produce computer input. Data processing is done by digital computer software. Using a modulated writer-scanner, the processed array can be recorded as an image on film.

Geometric corrections can be made by shifting video elements to a corresponding calibration position. Stationary photometric nonlinearities can be removed by playing each element through a calibrated response function. With radiation-fogged film, it is of primary importance to enhance detail and suppress noise, which can be accomplished by linear operations and interactions with the real domain.

Linear operations affect the frequency spectrum of image distribution. Linear operations can be performed either by using convolution methods on the spatial distribution or by operating on the distribution's frequency spectrum. The second approach requires that the distribution be transformed from the spatial to the frequency domain and that the transform be multiplied by the filter function and then retransformed to the spatial domain. Nathan has indicated that although filters are easier to describe mathematically in the frequency domain, the convolution approach is much more practical.<sup>(107)</sup> Also, in practice a totally digitized image would tax the storage capacity of the largest computer; therefore, the image is broken down into subsections

of a size governed by the dimensions of the spread function. It is these subsections that are operated on.<sup>(108)</sup> As in optical data processing, it is possible to build filters that vary with position over the image.

Interactions with the real domain or second order logic can be developed to aid in enhancement of details having a spatial frequency distribution similar to that of the noise or the noise filter. In this approach, the filter is turned off in the sensitive region by comparing the difference between the origin and the surrounding region against some chosen threshold.<sup>(108, 109)</sup> When surrounding elements are greater in difference than the threshold, their average is used to replace the origin point. Roetling has discussed a test for edge identification that makes use of subtests repeated in successive rings around the point of origin.<sup>(110)</sup> Levine indicates that edges and corners are the image characteristics bearing the most information.<sup>(111)</sup> This would seem particularly true for NTS alpha oscilloscopes.

#### 8.4 APPLICATIONS OF IMAGE ENHANCEMENT TO RADIATION-FOGGED FILM

Miller<sup>(102)</sup> has compared spatial filtering and high-contrast printing for irradiated oscilloscope traces. In the spatial filtering experiments, the image was amplitude-modulated by a ruling and the optical spatial filtering apparatus used to separate the modulated signal from the dc. (The radiation-produced fog had been expected to produce a signal similar to an unmodulated d-c background.) Unmodulated counterparts were subjected to high-contrast printing. The results of these experiments were not encouraging for small images; while the technique did improve contrast, it failed to recover images that originally were visually undetectable. When the modulated portion occupied a major part of the image, the signal-to-noise ratio was sufficiently high to recover images below the threshold of visual detectability. Miller apparently did not attempt to filter the unmodulated images; in any case, image modulation is not a prerequisite of spatial filtering.

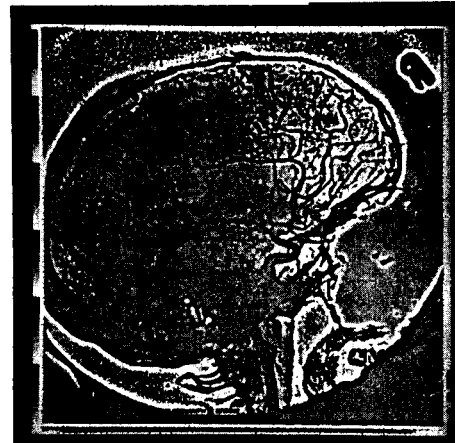
Use of spatial filtering in recovery should consist of d-c filtering and low-frequency attenuation. Figure 2-3 shows that fogging can be treated as a d-c bias, and Figure 2-7 illustrates that the frequency spectrum of granularity caused by ionizing radiation has a distinct low-frequency bias.

Interviews with Shulman<sup>(112)</sup> and Lorber<sup>(113)</sup> were conducive to the conclusion that spatial filtering will aid greatly in the recovery of radiation-fogged film.

Examples of unenhanced and enhanced images are shown in Figure 8-6. The enhanced record was prepared from the original using high-frequency boosting and low-frequency attenuation. The enhanced image is definitely superior, particularly in the areas of greatest exposure.



(A) Unenhanced Original



(B) Enhanced Duplicate

Figure 8-6. Comparison of unenhanced and enhanced x-ray images of a skull. <sup>(107)</sup>

## 9. OPERATIONAL HANDLING OF POTENTIALLY RADIATION-FOGGED FILMS<sup>(114)</sup>

This section discusses pre- and post-event procedures for optimizing, handling, and processing film emulsions potentially exposed to ionizing radiations.

Exposure of films by radiation may result in an increase in background (base plus fog) density to a level where degradation of the data recorded on the film is a problem. Techniques are available for minimizing potential data losses, but their effectiveness is dependent on accurate assessment of this problem. Unfortunately, no chemical or optical process for universal treatment of these fogged films is currently available. The procedures and precautions for handling potentially irradiated film are summarized below.

### 9.1 PRE-EVENT

Pre-event considerations include selection of film and chemical process, shielding, processing and exposure techniques, and use of radiation check films.

#### 9.1.1 Selection of Film and Chemical Process

Although fogging may not be expected, it must be considered a possibility when selecting films. In the case of the fastest displays, it may be necessary to ignore this possibility and use the most light-sensitive film appropriate to the application. Otherwise, it may be more desirable with some level of radiation fogging to use a film/developer combination with high light sensitivity. In the presence of some level of radiation fogging, the following procedure may be used:

1. Expose a variety of prospective films to a calibration photographic step tablet and a sample trace, then fog the films by some standard amount by exposing them to a source.
2. Process the films in their respective developer combinations.
3. Determine which film/developer combinations result in the greatest film speed or the largest difference between background and trace.
4. Repeat the foregoing steps across a range of different fogging exposure levels.

## NOTE

Filtered 250-kVp x-rays are apparently more representative of the actual fogging exposure than the 1.17- and 1.33-MeV gammas of  $\gamma$ Co<sup>60</sup>.

Obviously, successful selection is dependent on an accurate understanding of the problem. Tradeoffs must be made, because what is best in one set of circumstances will not be best in another. Factors to be considered before arriving at a film selection should include the nature and exposure distribution of the display, the spectral distribution of the display, and whether concurrent intensification is to be used.

### 9.1.2 Shielding

Limited shielding (such as that provided by a few millimeters of lead) could be very effective, depending on the wavelength of radiation encountered. Shielding will filter out those wavelengths to which films are most sensitive.

### 9.1.3 Processing and Exposure Techniques

The concurrent intensification processing technique consists of a non-image-forming pre-, concurrent, and post-exposure to low-intensity light. In some cases, this results in an increase in light film speed accompanied by a slight increase in background fog. However, concurrent intensification will not aggravate gamma fogging if, as is now the case, the low-intensity exposure is suspended before the gamma radiation exposure commences. In fact, CI may increase the differentiation between the irradiation fog and the light image.

In the absence of fogging, some correct exposure would produce the optimum image. However, if fogging occurs overexposure may give better results. If fogging does not occur, speed-reducing methods can be applied during processing to compensate for overexposure.

### 9.1.4 Radiation Check Films

Sensitometrically exposed films placed in the recording station or in the cut film holder backs can be used post-recovery in determining background density and may provide a supply of representative fogged film with which to experiment.

## 9.2 POST-EVENT

Recommended post-event procedures are as follows:

1. Isolate film from contamination by removing film from holder or cassette, taking care to preserve film identification.

### NOTE

Unless exposed to high-neutron flux, the film itself will not be radioactive.

2. Store film in a cool, dry place.
3. Determine film fog background density by processing some of the radiation check film (see Paragraph 9.1.4) using the dry run film processing procedure. Measure background density; i. e., the combined radiation fogging exposure and normal base plus fog.
4. Estimate trace or image densities, consulting with the physicist and inspecting dry run film as necessary.

The next step is to evaluate the severity of fogging and to select a processing procedure; however, there is no standard procedure for satisfactorily processing the most severely fogged films. In many cases the films are not severely fogged and may be processed as planned before a fog problem was apparent. Selecting a technique among those available for increasing the density differences between fog and trace is contingent on the severity of the problem (see above Steps 3 and 4). Additional evaluations, if necessary, may be made as follows:

1. Obtain a supply of simulated fogged film or make use of additional radiation check films.
2. Attempt a variety of processing techniques, selecting the technique that results in the largest difference between the background and step wedge or trace densities.
3. Process a sample only of the event film, using the selected technique.
4. If Step 3 results are satisfactory, process the remainder of the event film.

## NOTE

Process control procedures are important when processing radiated film because developers will be depleted at many times their normal rates.

### 9.3 IMAGE ENHANCEMENT

Post-processing techniques, such as printing on high-contrast duplicating film or spatial filtering, may improve the visibility of the trace or image. Experiments using different types of spatial filters may be conducted to determine which filter provides maximum differentiation between trace or image and background.

If supplemental optical systems are used to enhance event film, a small amount of geometric distortion may occur; therefore, calibration film should be run through the same optical system before critical analysis begins.

## REFERENCES

1. Baltz, D. W., and Lorber, H. W., "PFR-2 Development Study Final Progress Report," Tech Report No. L-966, p. 21, EG&G, Inc., Las Vegas, Nevada, 25 November 1969.
2. Corney, G. M., "The Effect of Gamma-Ray Exposure on Camera Films," Photogr. Sci. Eng., 4:291, 1960.
3. Dutton, D. M., "The Definition and Measurement of Granularity," Tech Report No. L-998, EG&G, Inc., Las Vegas, Nevada, 31 July 1970.
4. Shaffer, R. M., and Dutton, D. M., "Wide Latitude Processing of Tri-X Ortho Oscillographic Film," Tech Report No. L-974, p.31, EG&G, Inc., Las Vegas, Nevada, 15 January 1970 (Rev 5 May 1971).
5. Frieser, H., "Noise Spectrum of Developed Photographic Layers Exposed by Light, X-Rays, and Electrons," Photogr. Sci. Eng., 3:164, 1959.
6. Hoerlin, H., "The Photographic Action of X-Rays in the 1.3 to 0.01 Å Range," J. Opt. Soc. Am., 39:894, 1949.
7. Herz, R. H., The Photographic Action of Ionizing Radiations, Wiley, New York, 1969.
  - a. pp. 150, 615
  - b. p. 23
  - c. p. 97
  - d. pp. 96, 159
  - e. pp. 117-121
  - f. p. 106
  - g. pp. 98-100
  - h. pp. 144-148
8. "Underground Nuclear Testing," AEC TID-25180, September 1969.
  - a. p. 6
  - b. p. 15
  - c. p. 13
  - d. p. 16
  - e. pp. 6, 13-16, 58, 59
9. "Safety of Underground Nuclear Testing," AEC TID-24996, April 1969.
  - a. p. 7
  - b. p. 1
  - c. p. 8
  - d. pp. 1, 7, 8

10. "Technical Discussions of Offsite Safety Procedures for Underground Nuclear Detonations," AEC NVO-40 Rev 2, May 1969.
  - a. p. 261
  - b. p. 265
  - c. pp. 7, 15, 39, 40, 261-265
11. Smith, M. E., and Carnahan, C. L., "The Movement of Gaseous Radionuclides through Geologic Media," Report No. AEC NVO-1229-85, Isotopes Co., February 1968.
  - a. p. 14
  - b. p. 8
  - c. p. 3
  - d. p. 4
  - e. p. 9
  - f. pp. 3-14
12. Glasstone, S., Ed., "The Effects of Nuclear Weapons," AEC, April 1962.
  - a. p. 705
  - b. p. 402
  - c. p. 371
13. Weaver, L. E., Strom, P. O., and Killeen, P. A., "Estimated Total Chain and Independent Fission Yields for Several Neutron-Induced Fission Processes," USNRDL-TR-633, 1963.
14. Bolles, R. C., and Ballou, N. E., "Calculated Activities and Abundances of U<sup>236</sup> Fission Products," USNRDL-456, 1956.
15. Fleming, E. H., "The Fission Product Decay Chains (Pu<sup>239</sup> with Fission Spectrum Neutrons)," UCRL-50243, Vols I, II, and III, 1967.
16. Conversation among D. M. Dutton and O. W. Mullen, B. P. Smith, L. S. Sygitowicz, and I. J. Wells of REECO Rad-Safe, NTS, June 1970.
17. Johnson, G. W., Higgins, G. H., and Violet, C. E., "Underground Nuclear Detonations," AEC UCRL-5626, 1959.
18. Lynch, J., and Cullimore, C., "Spatial Distribution of Radioactive Materials Around the Cavity of an Underground Nuclear Detonation," AEC HNS-1229-47, 1964.
19. Izrael, U. A., Ed., "Radioactive Contamination of the Environment by Underground Nuclear Explosions, and Methods of Forecasting It, Moscow, 1969," AEC-tr-7122, March 1970.
  - a. p. 5
  - b. p. 10
  - c. p. 13
  - d. p. 7
  - e. p. 25
  - f. pp. 3, 7-10, 25

20. Conversation between D. M. Dutton and A. Peterson of the Borden Chemical Co., Northfield, Illinois, September 1970.

21. Conversation between D. M. Dutton and G. K. Iverson of EG&G LVD, July 1970.

22. Izrael, Y. A., "Radioactivity in Contained Underground Nuclear Explosions," UCRL-Trans-10475, July 1970, 1-9.

23. Mees, C. E. K., and James, T. H., The Theory of the Photographic Process, Macmillan, New York, 1966.

a. p. 181	g. p. 135
b. p. 93	h. p. 133
c. p. 192	i. p. 140
d. p. 101	j. p. 84
e. p. 189	k. pp. 344-346
f. pp. 193-195	

24. Nepela, D. A., and Nitka, H. F., "Effect of Chemical Ripening on the Photographic Response to Light, X- and Gamma Radiation," Photogr. Sci. Eng., 4:12, 1960.

25. Hoerlin, H., Ed., "Development of a Wavelength-Independent Radiation Monitoring Film," Final Report ANL-5168, 1 August 1953.

26. Yamakawa, K. A., Phys. Rev., 82:522, 1951.

27. Hamm, F. A., and Comer, J. J., "The Electron Microscopy of Photographic Grains, Specimen Preparation Techniques and Applications," J. App. Phys., 24:1495, 1953.

28. Hoerlin, H., and Hamm, F. A., "Electron Microscopical Studies of the Latent Image Obtained by Exposures to Alpha Particles, X-Rays, and Light," J. App. Phys., 24:1514, 1953.

29. Kornfeld, G., "Latent-Image Distribution by X-Ray Exposures," J. Opt. Soc. Am., 39:1020, 1949.

30. Berg, W. F., Marriage, A., and Stevens, G. W. W., Photogr. J., 81:413, 1941.

31. Ehrlich, M., and McLaughlin, W. L., J. Opt. Soc. Am., 46:797, 1956.

32. Tellez-Plasencia, H., Sci. Ind. Photogr., (2) 28:144, 1957.
33. Larson, E. T., PSA J. (Photogr. Sci. Tech.), 17B:19, 1951.
34. Malinowski, J., Z. Phys. Chem. (Leipzig), 204:276, 1955.
35. Tomoda, Y., "Hypersensitization of X-Ray Films," Photogr. Sci. Eng., 3:122, 1959.
36. Yagoda, H., Radioactive Measurements with Nuclear Emulsions, Wiley, New York, 1949.
  - a. p. 14
  - b. pp. 14, 15
  - c. pp. 103-105
  - d. pp. 13, 109
37. Nam, B., "Preparation of Radiation Resistant Emulsions and Processing Techniques," Report CR-66769 to NASA, Technical Operations Research, Burlington, Mass.
38. Ehrlich, M., and McLaughlin, W. L., "Photographic Response to Successive Exposures of Different Types of Radiation," J. Opt. Soc. Am., 51:1172, 1967.
39. Seemann, H. E., "Spectral Sensitivity of Two Commercial X-Ray Films Between 0.2 and 2.5 Angstroms," Rev. Sci. Instr., 21:314, 1950.
40. Gunther, P., and Tittel, H., Z. Electrochem., 39:646, 1933.
41. Smith, H. L., "X-Ray Film Detector Calibration Progress Report, July-December 1970," Report No. L-1025, EG&G, Inc., Las Vegas, Nevada, 25 January 1971.
42. Conversation between D. M. Dutton and H. L. Smith, EG&G LVD, March 1971.
43. Greening, J. R., "The Photographic Action of X-Rays," Proc. Phys. Soc., 64B:977, 1957.
44. Feigenbaum, S. A., "Boston and Rochester Trip Report," EG&G LVD Memo to D. Daly, 7 December 1960.
45. Chhabra, A. S., "Effect of Silver Halide Content on the Film Dosimetry of a Sr<sup>90</sup> -  $\gamma$ <sup>90</sup> Applicator."

46. Shaffer, R. M., "A Sensitometric Investigation of the Mechanisms of Photosolubilization of Silver Halides and Their Potential Applications in Oscillography," Tech Report No. L-995, EG&G, Inc., Las Vegas Nevada, 15 June 1970.
47. James, T. H., "Some Effects of Environment on Latent Image Formation by Light," Photogr. Sci. Eng., 14:84, 1970.
48. Faraggi, H., and Albouy, G., Sci. Ind. Photogr., (2) 20:336, 1949.
49. Berg, W. F., and Mendelssohn, K., "Photography, Sensitivity and the Reciprocity Law at Low Temperatures," Proc. Roy. Soc., 168A:168, 1938.
50. Falla, L., Sci. Ind. Photogr., (2) 23A:46 (1953) and (2) 26:81 (1955).
51. Brodsky, A., and Kathren, R. L., "Accuracy and Sensitivity of Film Measurements of Gamma Radiation - Part III - Effects of Humidity and Temperature During Gamma Irradiation," Health Phys., 9:769, 1963.
52. McLaughlin, W. L., and Ehrlich, M., "Film Badge Dosimetry: How Much Fading Occurs?," Nucleonics, 12:34, 1954.
53. Tomoda, Y., and Nakamura, N., J. Soc. Sci. Photogr., Japan, 21:16, 1958.
54. Yoshitada, T., and Nobuya, N., Rept. Govt. Chem. Ind. Res. Inst., Tokyo, 53:146, 1958.
55. Tomoda, Y., J. Soc. Sci. Photogr., Japan, 22:12, 1959.
56. Tomoda, Y., and Kawasaki, M., Rept. Govt. Chem. Ind. Res. Inst., Tokyo, 54:37, 1959.
57. Hansen, D. F., McCue, J. L., and Wyckoff, C. W., "Alpha Oscillographic Film Program, 1 July 1964 - 1 July 1965," Report No. 65/36U, EG&G, Inc., Las Vegas, Nevada, 9 July 1965.
58. Adams, R. R., "Briefing on Contract for Preparation of Radiation Resistant Emulsions and Processing Techniques," Memo to Distribution, NASA Langley Research Center, 23 May 1969.

59. Anderson, A. C., "Proposed Methods to Reduce Background Radiation in Photographic Films," Chrysler Corp. Space Div. Eng. Dept. Tech. Note TN-AE-68-183, 25 October 1968.
60. Hansen, P. P., "Unconventional Photographic Systems - A Bibliography of Reviews," Photogr. Sci. Eng., 14:438, 1970.
61. Kosar, J., Light-Sensitive Systems, Wiley-Interscience, New York, 1967.
62. Robillard, J. J., "New Approaches in Photography," Photogr. Sci. Eng., 8:18, 1964.
63. James, T. H., and Higgins, G. C., Fundamentals of Photographic Theory, Morgan and Morgan, Hastings-on-Hudson, New York, 1968.
64. Zelikman, V. L., and Levi, S. M., Making and Coating Photographic Emulsions, Focal Press, London, 1965.
65. Croome, R. J., and Clegg, F. G., Photographic Gelatin, Focal Press, London, 1965.
66. Duffin, G. F., Photographic Emulsion Chemistry, Focal Press, London, 1967.
67. Francis, R., "Alpha Film Studies 1 January - 30 June 1968," pp. 33-35, Report No. B-530, EG&G, Inc., Boston, Mass., 5 August 1968.
68. Conversations between D. M. Dutton and J. D. Plumadore, August 1969.
69. Land, E. H., Annual Conference of Society of Photographic Scientists and Engineers, Boston, Mass., 12 June 1968.
70. Land, E. H., Farney, L. C., and Morris, M. M., "Solubilization by Incipient Development," Photogr. Sci. Eng., 15:4, 1971.
71. Kalashnikova, V. I., and Samoilovich, D. M., Zhurn. Nauchnoi i Prikladnoi Fotograffii i Kinematogr., 9:464, 1964.
72. Kolyubin, A. A., Pevchev, Yu, F., and Finogenov, K. G., Zhurn. Nauchnoi i Prikladnoi Fotograffii i Kinematogr., 12:42, 1967.
73. Samoilovich, D. M., and Ardashev, I. V., "The Destruction of the Latent Photographic Image in an Electric Field," Soviet Phys., 13:211, 1968.

74. Lockwood, H. E., "The Armored Film Back as a Radiation Attenuator," EG&G LVD Memo SDED-6069-70, 1 September 1970.
75. Hoerlin, H., "Preliminary Report - Erasing of Gamma Ray Background on Fast Photographic Emulsions," 1 May 1954.
76. Goldstein, A. M., and Sherman, C. H., "The Herschel Effect and Selective Erasing of Nuclear Emulsion," Rev. Sci. Instr., 23:267, 1952.
77. Urbach, F., and Wolinsky, A., Sitzungber. der Acad. der Wissenschaften in Wien, Abt. IIa, 147:29, 1938.
78. Falla, L., Bull. Soc. Roy. des Sciences Liege, 10:276, 1941.
79. Kornfeld, G. J., "The Herschel Effect and the Structure and Stability of the Photographic Latent Image," J. Opt. Soc. Am., 39:490, 1949.
80. Strome, F. C., "Measurement of Very Rapid Changes in Latent-Image Stability Against Herschel Bleaching with Lasers," Photogr. Sci. Eng., 10:81, 1966.
81. Feigenbaum, S. A., "A Study of Data Recovery Techniques for Gamma Irradiated Photographic Film," Tech Memo No. L-62, EG&G, Inc., Las Vegas, Nevada, 27 September 1963.
82. Hansen, D. F., McCue, J. C., and Wyckoff, C. W., "Alpha Oscillographic Film Program, 1 January 1965 - 31 March 1965," Report No. 65/27U, EG&G, Inc., Las Vegas, Nevada, 12 May 1965.
  - a. pp. 41, 42
  - b. pp. 41-47
  - c. pp. 38-40, 44
83. Ackerman, H., and Faissner, H., "Fading in Nuclear Emulsion Induced by Acid Agents," Nuc. Instr. Meth., 10:339, 1961.
84. Johnson, A. C., "Trip Report," EG&G LVD Memo to B. L. Hanson, 5 January 1963.
85. Johnson, A. C., Laboratory Notebook entry (EG&G LVD), 13 December 1962.
86. Smith, H. L., "In-Camera Processing System for Dynafax Camera," Tech Memo No. L-59, EG&G, Inc., Las Vegas, Nevada, 2 August 1963.

87. Ebeltoft, W., and Hatch, M. A., "Operation and Maintenance Manual - Automatic Polaroid Film Processor (Model N-PH27 Remote Camera Actuator)," Tech Memo No. L-152, EG&G, Inc., Las Vegas, Nevada, 2 May 1966.
88. Meibaum, R. A., and McKellar, J. Y., "Results of Preliminary Tests of the Rapid Processing Module for Oscilloscope Cameras," Report No. L-929, EG&G, Inc., Las Vegas, Nevada, 4 March 1969.
89. "Alpha Film Studies Monthly Progress Reports," February 1965 (9 March 1965) and April 1965 (24 May 1965), EG&G, Inc., Advanced Research Department, Bedford, Mass.
90. Barnes, J. C., Bahler, W. H., and Johnston, G. J., "Rapid Processing of a Panchromatic Negative Film by the Application of a Viscous Monobath," J. Soc. Mot. Pic. Tel. Eng., 74:242, 1965.
91. Nepela, D. A., and Nitka, H. F., "Gamma-Ray Insensitive Emulsions," Quarterly Report No. 6, 1 July 1957 - September 1957, AD 154596.
92. Spear, V. D., Prog. Mgr., "Radiation Protection Study for Photographic Space Film," Final Report (NASA-CR-100016), Chrysler Corp., 17 January 1969.
93. Feigenbaum, S. A., "Preliminary Consideration in Minimizing the Effects of Radiation Induced Fog on Films," Tech Memo No. L-42, EG&G, Inc., Las Vegas, Nevada, 7 July 1962.
94. James, T. H., and Vanselow, W., "The Role of Silver Halide Solvents in Practical Development," Photogr. Eng., Vol 7, No. 2, 1956.
95. Shaffer, R. M., and Dutton, D. M., "Additive 'C' for TEA-12 Low Contrast Oscillographic Film Developers," EG&G LVD Memo NTSED-004-70, 16 January 1970.
96. Dutton, D. M., "Additive 'C' for TEA-12 with Improved Royal-X Pan," EG&G LVD Memo SDDED-6033-70, 26 June 1970.
97. Wilson, D., "Recovery of Gamma-Irradiated Royal-X Pan and 2479 Film - Project Door Mist," EG&G LVD Memo SOD 865, 17 October 1967.
98. Conversation between D. M. Dutton and C. W. Wyckoff, September 1969.

99. Conversation between D. M. Dutton and J. D. Plumadore, September 1969.
100. Paulsen, P., "Alpha Film Study Input," EG&G Bedford Memo to R. Francis, 19 December 1968.
101. Paulsen, P., "Compilation of 'Wide-Latitude' Film Processing Techniques," EG&G Bedford Memo to R. Francis, 11 March 1969.
102. Miller, C. S., "Recovery of Radiation-Fogged Oscilloscope Traces by Spatial Filtering and Extended Range Development," Final Report TO-B 66-99, Technical Operations Research, December 1966.
103. Conversation between D. M. Dutton and A. Shepp of Technical Operations Research, 10 October 1969.
104. Goodman, J. W., Introduction to Fourier Optics, McGraw-Hill, New York, 1968.
  - a. p. 167
  - b. p. 168
105. Shulman, A. R., "Principles of Optical Data Processing for Engineers," NASA Tech Brief 68-10069 (p. 68), August 1966.
106. Shulman, A. R., Optical Data Processing, Wiley, New York, 1970.
107. Nathan, R., "Digital Video-Data Handling," preprint of paper presented at SPSE Symposium on Photo-Electronic Imaging, Washington, D. C., 31 October - 2 November 1968.
108. Helstrom, C. W., "Image Restoration by the Method of Least Squares," J. Opt. Soc. Am., 57:297, 1967.
109. Graham, D. N., "Image Transmission by Two-Dimensional Contour Coding," Proc. IEEE, 55:336, 1967.
110. Roetling, P. G., "Image Enhancement by Noise Suppression," Letters to Editor, J. Opt. Soc. Am., 60:867, 1970.
111. Levine, M. D., "Feature Extraction - A Survey," Proc. IEEE, 57:1391, 1969.
112. Conversation between D. M. Dutton and A. R. Shulman, November 1970.

113. Conversation between D. M. Dutton and H. W. Lorber, EG&G LVD, January 1971.
114. Lockwood, H. E., "Handling Potentially Radiation Fogged Films," EG&G LVD Memo SDED-6021-70, 12 May 1970.

## DISTRIBUTION

### AEC/DTIE

P. Rosser (2)

### AEC/NVOO

J. Koch  
R. Loux  
R. Purcell

### DASA

W. Isengard

### LASL

W. Biggers  
B. Carpenter  
R. Crook  
H. Hoerlin  
M. Koffman  
A. Koonce  
M. Peek  
S. Stone  
D. Westervelt

### LRL

D. Buchla  
V. Denton  
C. Dittmore  
D. Dixon  
R. Gathers  
R. Geil  
W. Gieri  
T. Hamm

### EG&G-Albuquerque

R. Johnson  
Library

### EG&G-Bedford

Library (2)

### EG&G-Las Vegas

W. Barak  
G. Bull  
D. Dutton (15)  
P. Hawkins  
V. Hedges  
D. Hunt  
W. Kitchen  
P. Leibold  
H. Lockwood  
R. Meibaum  
B. Murphy  
L. Perez  
F. Pointer  
T. Rottunda  
J. Sedlmeyer

H. Smith  
E. Story  
A. Tarr  
J. Trabert  
J. Tsitouras  
A. Villaire  
D. Wallace  
B. Warner  
D. Wilson  
C. Young (2)  
Library

### EG&G-Los Alamos

F. Bunker  
A. Johnson  
P. Zavataarro  
Library

### EG&G-San Ramon

S. Sternick  
Library